Olfactory Ensheathing Cell Phenotype after Implantation into the Lesioned Spinal Cord

Emma Woodhall BSc. Hons.

Submitted in fulfilment of the requirements for the degree of

Doctor of Philosophy

University of Tasmania

April 2004

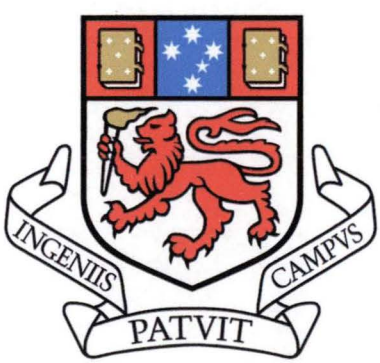

STATEMENT

This thesis contains no material which has been accepted for a degree or diploma by the University of Tasmania or any other institution, except by way of background information duly acknowledged in the text. To the best of my knowledge and belief this thesis contains no material previously published or written by another person except where due acknowledgment is made.

Emma Woodhall

STATEMENT OF AUTHORITY OF ACCESS

This thesis may be made available for loan and limited copying in accordance with the *Copyright Act 1968.*

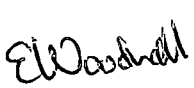

EmmaWoodhall

ACKNOWLEGEMENTS

Many thanks to my supervisors Dr Inn Chuah and Dr Adrian West (for all their help and support), Julie Harris, Dr Adele Holloway, Dr Lisa Foa and Dr Niels Anderson (for all the encouragement), Dr Derek Choi-Lundberg (for help with the surgery), each of my office mates Lee-Lee, Liz, Meredith, and Adele W (for entertainment, conversation and lots of mocha coffee), Gerry Nash (for expert technical assistance with the electron microscope), to the animal house staff (without whom this project would not have been possible), Roger (just for being himself), Adele V (for loads of excellent tech tips), Jill Aschman (for being the chief distraction), all of the MBUites (your wonderful), the Anatomy and Physiology crew, the Biochemistry Department and Pete (for being such a sweetie). Thankyou all for making my time at UTAS most enjoyable!!.

ABSTRACT

Although olfactory ensheathing cells (OECs) are used to promote repair in the injured spinal cord, little is known of their phenotype in this environment. This study examined the effect of the injured spinal cord on OEC morphology and gene expression. For *in situ* experiments OECs were encapsulated in porous polymer tubes and implanted into the lesioned rat spinal cord. Adult male hooded Wistar rats (300-350g) were anaesthetised with isoflurane maintained at 2.5% with 100% O_2 (0.5L/min). Lesions were made to the corticospinal tract at the level of T7-T8 and OEC-filled capsules were inserted under the dura above the lesion. After one week animals were sacrificed and the capsules retrieved. Procedures were performed in accordance with NHMRC guidelines approved by the University of Tasmania Animal Ethics Committee. Morphological characteristics were examined using scanning electron microscopy (SEM) for which implanted and un-implanted capsules were cut into halves so as the inner surfaces could be viewed. Implanted capsules were filled with rounded OECs and extracellular matrix (ECM)-like matter. Although no cells with the morphology of cultured OECs were observed these may have been obscured by the abundant ECM. In the un-implanted capsules cells with morphology typical of cultured OECs were predominant and although some rounded cells were detected. Real-time reverse transcriptase-polymerase chain reaction (RT-PCR) was used to analyse expression of Neuregulin-1 (Nrg-1) and Nogo in cultured OECs and encapsulated OECs both in culture and after implantation. Neuregulins are known mitogens and survival factors for central nervous system (CNS) cells whilst Nogo is an axonal growth regulator. For comparison transcripts were also examined in a number of other glial cell types. Similar to astrocytes (ASTs) and fibroblasts (FBs), OECs expressed various Nrg-1 subtypes

including *neu* Differentiation Factor (NDF), Glial Growth Factor (GGF) and Sensory and Motorneuron-derived Factor (SMDF) along with other splice variants including those containing the epidermal growth factor (EGF), α-EGF, β-EGF and secreted domains. After implantation, OECs increased expression of NDF and secreted Neuregulin and decreased expression of the other variants. Olfactory ensheathing cells, oligodendrocytes (OLGs) Schwann cells (SCs) and ASTs all expressed Nogo-A, -B and -ABC. OECs and OLGs were also immunopositive for Nogo-A protein. Unlike OLGs, OECs, SCs and ASTs expressed mRNA for the Nogo-66 receptor (NgR) although the protein could not be detected by immunocytochemistry in OECs. Implantation of OECs resulted in an increase in Nogo-A and -B and a decrease in Nogo-ABC and the NgR. Taken together these results show that OEC phenotype in the lesion environment is different from their characteristic profile in culture.

TABLE OF CONTENTS

LIST OF TABLES

LIST OF FIGURES

CHAPTER ONE

Introduction

1.1. Injury in the Central Nervous System

In contrast to the peripheral nervous system (PNS), neurons in the central nervous system (CNS) fail to regenerate after injury despite an initial sprouting response. After injury the segment of the axon distal to the injury degenerates via a process termed Wallerian degeneration and the debris is phagocytosed by activated macrophages and microglia (Stichel and Muller, 1998). Provided that the cell body survives, the proximal segment retracts and sprouts neurites that advance toward the lesion site (Guth, 1974). These newly formed neurites are usually transient and extend for only short distances before they arrest and degenerate or persist at the lesion site (David and Aguayo, 1981). This initial sprouting response suggests that the failure of CNS neurons to regenerate is not intrinsic to the neurons themselves but is more likely to be a function of the inhospitable CNS environment. In fact this phenomenon was clearly demonstrated by Aguayo and colleagues who showed that CNS axons could extend neurites over long distances when exposed to peripheral nervous tissue but when in contact with CNS tissue their growth terminated abruptly (Richardson et al., 1980; David and Aguayo, 1981).

1.2. Inhibitors of Neurite Regeneration in the Central Nervous System

It is now known that the CNS environment is hostile to axonal growth due to the presence of a variety of factors that actively inhibit neuronal growth. Some of these are considered below.

1.2.1. The Glial Scar

One of the major barriers to successful regeneration in the CNS is the inhibitory nature of the glial environment. Injury to the CNS results in the rapid activation of non-neuronal cells at the lesion site resulting in what is known as a glial scar. A large proportion of the glial scar is composed of tightly interwoven astrocyte processes which are surrounded by extracellular matrix (Reier and Houle, 1988). Reactive astrocytes (ASTs) are characterised by rapid proliferation, hypertrophy and upregulation of glial fibrillary acidic protein (GFAP) (Latov et al., 1979; Mathewson and Berry, 1985; Vijayan et al., 1990). Several *in vivo* studies have highlighted the extremely inhibitory nature of the glial scar (McKeon et al., 1991; Bahr et al., 1995; Davies et al., 1996). Whether the glial scar is inhibitory because it creates a physical or chemical barrier to neuronal growth is being investigated. However it is known is that reactive ASTs express molecules such as tenascin-C, neurocan, brevican, NG2 and chondroitin sulphate proteoglycans (CSPGs) which are inhibitory to axonal growth (Levine, 1994; McKeon et al., 1995; Yamada et al., 1997; Asher et al., 2000).

1.2.2. Nogo

CNS myelin and the surfaces of differentiated oligodendrocytes (OLGs) have long been associated with inhibition of neurite growth (Schwab and Caroni, 1988). CNS myelin contains two membrane bound proteins NI-35 and NI-250 (or Nogo) that are potent inhibitors of neurite outgrowth and fibroblast spreading *in vitro* (Caroni and Schwab, 1988b). A monoclonal antibody termed IN-1 raised against NI-250, was subsequently shown to neutralise the inhibitory action of NI-35/250 *in vitro* (Caroni and Schwab, 1988a). More importantly the same antibody also neutralized the inhibitory effects of NI-35/250 *in vivo* (Schnell and Schwab, 1990). Not surprisingly the inhibitory nature of differentiated OLG surfaces could also be neutralized by IN-1 (Bandtlow et al., 1990). Although it was clear from these early studies that IN-1 application could enhance neurite outgrowth no improvements in functional recovery were shown. Since then several reports have demonstrated varying degrees of functional recovery after application of IN-1 to various lesioned CNS tracts in the rat (Bregman et al., 1995; Thallmair et al., 1998; Blochlinger et al., 2001; Merkler et al., 2001; Raineteau et al., 2001; Raineteau and Schwab, 2001; Bareyre et al., 2002), see Table 1.1 for a review. In addition, IN-1 promotes the growth of spared projections (Wenk et al., 1999) and sprouting of uninjured axons in the intact cerebellum (Buffo et al., 2000), suggesting a role for Nogo as a regulator of neuronal plasticity.

The discovery of the bovine homologue of NI-250 termed bNI-220 (Spillmann et al., 1998) whose potent inhibitory action could also be neutralized by IN-1 led to the initial cloning of the IN-1 antigen, Nogo (Chen et al., 2000; GrandPre et al., 2000; Prinjha et al., 2000). The *nogo* gene encodes three major protein products, Nogo-A the

largest at 1163 amino acids, Nogo-B an intermediate splice variant at 360 amino acids and Nogo-C the smallest splice variant at 199 amino acids (Fig. 1.1). The three variants have a common C-terminal domain 188 amino acids long, Nogo-A and -B also have a common 172 amino acid N-terminal domain whilst Nogo-C has a truncated N-terminus (Chen et al., 2000). All three variants have two long hydrophobic membrane-spanning regions and an endoplasmic reticulum (ER) retention motif at their C-terminus.

Nogo was also identified as a member of the reticulon (Rtn) protein family (Rtn-4A) owing to its sequence homology with other Rtn family members (GrandPre et al., 2000). Nogo has a 66 amino acid residue lumenal/extracellular domain similar to that found in Rtn 1, 2 and 3. The Nogo-66 domain was found to inhibit axon extension and induce growth cone collapse in dorsal root ganglion (DRG) neurons. In contrast the 66-residue domains of Rtn 1, 2 and 3 do not inhibit neuronal regeneration (GrandPre et al., 2000). Although the Nogo-66 domain was found to have inhibitory properties this did not discount the possibility that other domains may contribute to the inhibitory nature of Nogo. In a recent study of the Nogo-A protein, inhibitory activity was localized to three distinct sites including a region within the N-terminal domain, a Nogo-A specific region and the Nogo-66 C-terminal domain (Oertle et al., 2003b).

Of the major isoforms, Nogo-A is expressed mostly in the CNS where it has been localised to OLGs and some neurons (Chen et al., 2000), Nogo-B is expressed in neuronal and non-neuronal tissues (Chen et al., 2000; GrandPre et al., 2000; Huber et al., 2002) and Nogo-C is largely expressed in muscle and to some extent in brain, kidney and liver (Chen et al., 2000; GrandPre et al., 2000; Huber et al., 2002). Restricted expression of Nogo-A in contrast to the ubiquitous expression of Nogo-B is thought to be due to

tissue-specific differential splicing (Oertle et al., 2003a). A complete overview of Nogo expression is given in Table 1.2.

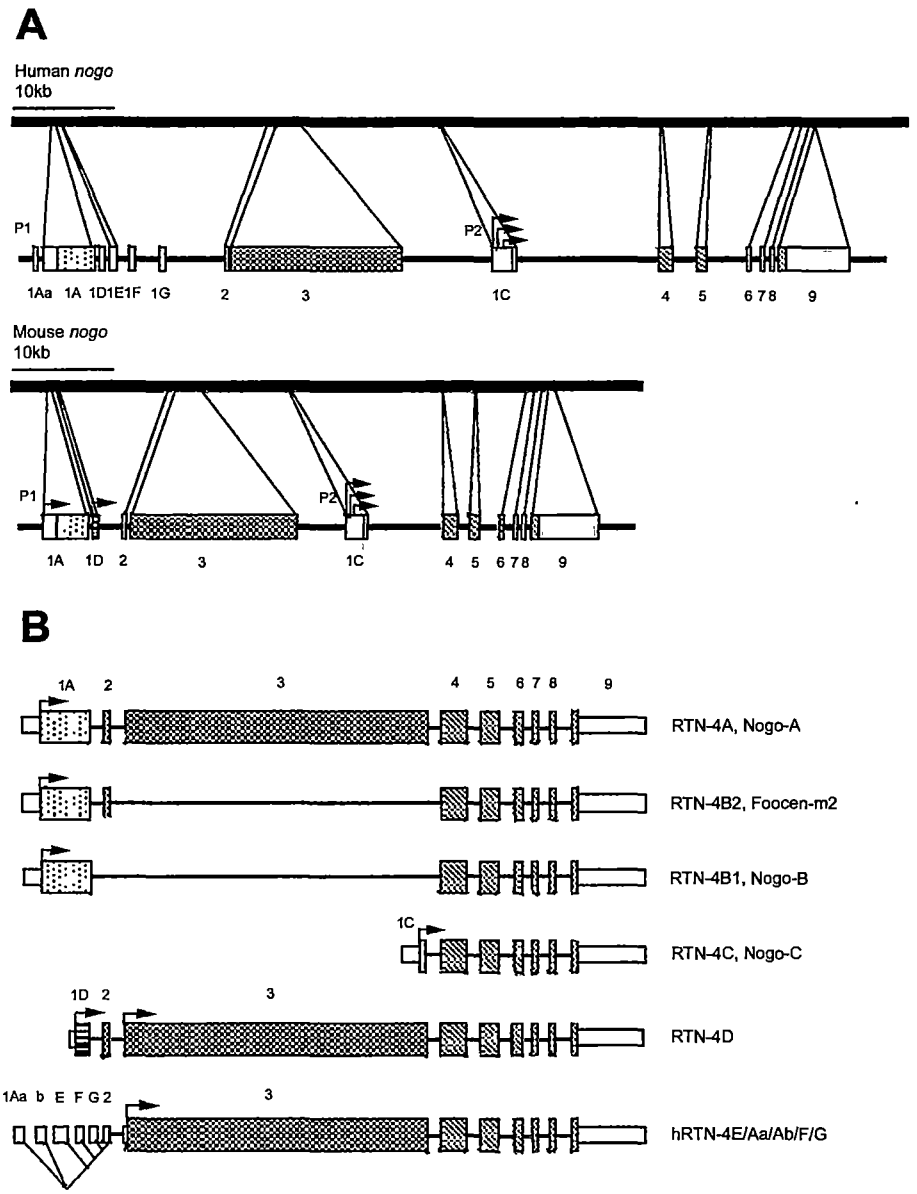
A
Human nogo
10kb
P1
P2
1Aa 1A 1D1E1F 1G
2
3
1C
4
5
6 7 8
9
Mouse nogo
10kb
P1
P2
1A 1D 2
3
1C
4 5 6 7 8 9
B
1A 2
3
4 5 6 7 8 9
RTN-4A, Nogo-A
RTN-4B2, Foocen-m2
RTN-4B1, Nogo-B
1C
RTN-4C, Nogo-C
1D 2
3
RTN-4D
1Aa b E F G 2
3
hRTN-4E/Aa/Ab/F/G

FIGURE 1.1. Gene structure of human and mouse *nogo*/Rtn4.

(A) The human *nogo* gene has 9 known exons and eight start sites (arrow heads) under the control of two separate promoters (P1 and P2). The mouse gene is comprised of 9 exons with 5 start sites under the control of the P1 and P2 promoters (Oertle et al., 2003a). Nogo-A/B transcription is regulated by the P1 promoter while Nogo-C is regulated by P2 (Oertle et al., 2003a). Exons 1 and 3 have been shown to be inhibitory for 3T3 fibroblast spreading in vitro and the middle part of exon 3 (found only in Nogo-A) potently inhibits neurite outgrowth from retinal ganglion cells, cerebellar granule cells, dorsal root ganglion (DRG) cells and PC12 cells. Exons 4 and 5 code for the loop-region termed Nogo-66, involved in DRG growth cone collapse (Oertle et al., 2003a). The second hydrophobic domain has a leucine-zipper like motif and has been implicated in apoptosis induction in some cancer cells (Li et al., 2001). (B) There are ten known splice variants of *nogo* including the major variants Nogo-A, -B and -C, the minor variant RTN4-B2 and the testis specific variants RTN4-D, -E, -Aa, -Ab, -F and -G. Modified from (Oertle et al., 2003a).

TABLE 1.1. IN-1 antibody treatment in models of CNS injury.

Reference	Model	Results
(Schnell and Schwab, 1990)	Intracerebral IN-1 application 7-10 days prior to complete transection of CST.	Induced sprouting and long distance (ie. 7-11mm) elongation of CST neurites after 2-3 weeks of injury.
(Bregman et al., 1995)	Mid-thoracic bilateral dorsal column hemisection and injection of IN-1 secreting hybridoma cells into parietal cortex.	Increased growth of CST axons which persisted at the lesion site for 12 weeks after injury, accompanied by functional recovery in exercises dependant upon the CST.
(Schulz et al., 1998)	Unilateral sensorimotor aspiration lesions of cortex plus grafts of embryonic neocortical tissue and IN-1 secreting hybridoma cells implanted	Increased cholinergic fibre growth into the grafts and increased density of grafts after 12 weeks.
(von Meyenburg et al., 1998)	Bilateral spinal cord hemisection, 2 or 8 weeks after injury IN-1 secreting hybridoma cells injected and NT-3 soaked gelfoam inserted into lesion site.	IN-1 treatment 2 weeks after injury produced regenerating CST fibres reaching 2-11.4mm in length whereas IN-1 treatment 8 weeks after injury resulted in sprouting up to 2mm in length.
(Z'Graggen et al., 1998)	uPT and injection of IN-1 secreting hybridoma cells	Complete restoration of forelimb use in treated animals, increase in corticopontine and corticorubral midline crossing sprouts.
(Thallmair et al., 1998)	Unilateral CST lesion in brainstem and IN-1 secreting hybridoma cells injected into cortex.	Increased sprouting of intact CST fibres was paralleled by functional improvements.
(Raineteau et al., 1999)	uPT and injection of IN-1 secreting hybridoma cells.	Increased sprouting of lesioned CST fibres and collaterals and improved elongation of sprouts.
(Wenk et al., 1999)	Unilateral motor cortex ablation and injection of IN-1 secreting hybridoma cells.	Increased sprouting of spared projections into the unlesioned hemisphere.
(Oudega et al., 2000)	Dorsolateral hemisection at T8 and sub-dural infusion of a recombinant IN-1 antibody fragment.	Increased growth of lesioned CST axons and collaterals, regenerating fibres reached lengths of 1.4 -9mm.
(Buffo et al., 2000)	Recombinant IN-1 fragment injected into intact cerebellum.	Induced sprouting of uninjured Purkinje cell axons the effect of which was reversible.
(Blochlinger et al., 2001)	uPT and injection of IN-1 secreting hybridoma cells into contralateral cortex.	Increased sprouting and fibre rearrangement, sprouts formed synaptic contacts in ipsilateral and contralateral pontine nuclei.
(Raineteau et al., 2001)	bPT and injection of IN-1 secreting hybridoma cells into left hippocampus.	Increased collateral sprouting of rubrospinal tract and recovery of forelimb movement including a rapid EMG response.
(Merkler et al., 2001)	Dorsal hemisection and injection of IN-1 secreting hybridoma cells into hippocampus.	Improved locomotor recovery in a range of exercises.
(Papadopoulos et al., 2002)	Middle cerebral artery occlusion and injection of IN-1 secreting hybridoma cells posterior to lesion	8 weeks after injury forelimb reaching task performance reached 80% of pre-lesion levels, collateral sprouting found in unlesioned hemisphere.
(Bareyre et al., 2002)	uPT and injection of IN-1 secreting hybridoma cells into hippocampus.	Increased midline crossing collateral sprouts from intact CST, gene expression changes including upregulation of growth associated proteins, growth factors and receptors, guidance molecules and transcription factors and downregulation of immune response molecules.
(Raineteau et al., 2002)	bPT and injection of IN-1 secreting hybridoma cells into left side of the hippocampus.	Reorganisation of uninjured RST, collateral sprouts innervated ventral horn of spinal cord where they contacted motoneurons.
(Emerick et al., 2003)	Sensorimotor aspiration lesion on left side and injection of IN-1 secreting hybridoma cells into hippocampus.	Intracortical microstimulation mapping of the uninjured cortical hemisphere revealed an increase in movement of the lesion-impaired forelimb suggesting motor cortex reorganisation.

[1] Abbreviations include unilateral pyramidotomy (uPT), bilateral pyramidotomy (bPT), corticospinal tract (CST), rubrospinal tract (RST), electromyography (EMG).

TABLE 1.2. Distribution of Nogo and Nogo-66 receptor (NgR) expression.

Location	Nogo-A	Nogo-B	Nogo-C	NgR
Spinal Cord	+[a]+	+[a]	+[a]	
White matter	++		-	--
Grey Matter	+			+
Intermediate Grey	+			
Dorsal horn	+			
Ventral horn	++			
Dorsal root ganglion	+* ++	++	--	+
Cortex (neocortex)	+[a]+	+[a]	+[a]	
Layer I molecular layer	-		-	-
Layer II external granular layer	++		+	+
Layer III external pyramidal layer	++		+	+
Layer IV internal granular layer	++		+	+
Layer V internal pyramidal layer	++		+	+
Layer VI multiform layer	++		+	+
Hippocampal formation				
Subiculum	+		+	
Ammon's horn (pyramidal cell layer)	-+		+	+
Hippocampus	+ ++		+	+
Dentate gyrus (granule cell layer)	+		+	++
Brainstem				
Habenular nucleus	+++		+	++
Red nucleus	+			+
Pontine nuclei				+
Hypoglossal nuclei	+			+
Reticular formation				+
Vestibular nuclei				+
Amygdala	++			++
Piriform cortex	++			++
Thalamus	+			
Hypothalamus	+			
Cerebellar Cortex	+[a]+			
Purkinje cell layer	-++		-	-
Granular cell layer	++		+	++
Molecular layer	++		+	
Olfactory Bulb	+*[a]+			
Mitral cell layer				+
Eye				
Optic nerve	+++	+++	+++	
Retina	+		+	
Peripheral Nerves				
Sciatic nerve	+++	+++	++	
Non-neuronal Cells				
Schwann cells	-			-
Astrocytes	---	-	-	-
Oligodendrocytes	++++++		+	-
Ependymal cells	-			
Microglia	-			
Adipocytes			+	
Other Tissues				
Skeletal muscle	+* -	-	+++	
Testis	+	+	-	
Heart	+	+	+	+
Lung	-	++	++	
Liver	-	+	+	
Spleen	-	++	++	
Kidney	-	++	++	
Cartilage		+	+	
Skin		+	+	

All data presented within this table represent rat and mouse tissues only. The (+) or (–) signs indicate positive or negative expression respectively. Absence of a sign indicates that the authors either did not investigate that region, tissue and/or cell type, or that no data were reported. The presence of (*) indicates that the isoform was detected in fetal tissue and ([a]) is where the specific location of the isoform within the given region was unspecified. Each sign is colour-coded as follows depending on the reference from which the data were sourced; (Chen et al., 2000), (GrandPre et al., 2000), (Huber et al., 2002), (Hunt et al., 2002), (Jin et al., 2003), (Josephson et al., 2001), (Josephson et al., 2002) and (Liu et al., 2002b). The occasional discrepancies in expression data shown here may have resulted from the differences in detection techniques used in these studies.

1.2.2.1. The Nogo-66 Receptor

To elicit its inhibitory effects the Nogo-66 domain interacts with a cell surface receptor termed the Nogo-66 receptor (NgR) (Fournier et al., 2001). The NgR is a high affinity glycophosphatidylinositol (GPI)-linked protein that contains a signal sequence, eight leucine-rich repeat (LRR) motifs and a cysteine rich LRR carboxy-terminal (LRRCT) flanking domain. The NgR has been localized to the surfaces of axons but is not found in OLGs. Cleavage of this receptor from the axonal surface renders neurons insensitive to Nogo-66 inhibition. Furthermore induction of NgR expression is sufficient to impart Nogo-66 responsiveness to previously unresponsive neurons (Fournier et al., 2001).

The NgR is largely expressed in brain and spinal cord although it has been detected in the olfactory bulb and heart (Hunt et al., 2002; Josephson et al., 2002) (refer to Table 1.2 for an overview of NgR expression). Recently two proteins structurally and biochemically similar to the NgR termed NgRH1 and NgRH2 were identified (Pignot et al., 2003). Together with NgR these molecules may represent members of a novel receptor protein family. NgRH1 and NgRH2 could also potentially bind uncharacterised inhibitors of neurite outgrowth.

1.2.2.2. OMgp and MAG Signaling via the NgR

Oligodendrocyte-myelin glycoprotein (OMgp) is another CNS myelin protein that inhibits neurite outgrowth. OMgp is a GPI-linked protein containing a leucine rich repeat (LRR) domain which is sufficient to bind the NgR (Wang et al., 2002b). Evidence for this came from the demonstration that cleavage of the NgR from the surfaces of DRG axons

renders them insensitive to OMgp whilst addition of exogenous NgR confers OMgp responsiveness to insensitive neurons (Wang et al., 2002b).

Myelin-associated glycoprotein (MAG) was also found to bind with high affinity to the NgR suggesting that NgR is necessary for MAG inhibition of neurite outgrowth. Hence cleavage of GPI-linked proteins from the axonal surface protects growth cones from MAG-induced collapse. Similarly MAG-resistant embryonic neurons are rendered MAG-sensitive by expression of NgR (Liu et al., 2002a).

Although Nogo-66, MAG and OMpg share no sequence similarities their apparent ability to compete for binding sites on the same receptor suggested that they may share structural similarities. Competition for the same receptor may also explain the redundancy observed when the action of a single inhibitory component is blocked *in vivo* (e.g. only moderate improvements in neurite outgrowth are achieved by blocking MAG, Nogo-66 or OMgp individually). Hence the effects of these three neurite growth inhibitors could potentially be blocked by developing an effective antagonist of the NgR derived from any one of the three NgR ligands already identified (Domeniconi et al., 2002).

1.2.2.3. Mechanisms of NgR Function

To elucidate the mechanisms involved in NgR function each domain was investigated for its involvement in Nogo binding and inhibition (Fournier et al., 2002). Deletions in any individual LRR region resulted in a lack of binding perhaps due to disruption of tertiary structure. The NgR C-terminal (NgRCT) domain appeared not to be required for Nogo binding but was necessary for inhibitory signaling. Therefore the CT domain could facilitate NgR conformational changes leading to axon inhibition by the LRR domain. The NgR GPI domain was also found not to be directly involved in NgR signaling but alternatively could play a modulatory role. It has also been proposed that the GPI domain provides a cleavage site for the NgR. A truncated NgR protein termed NgREcto, lacking the NgRCT and GPI linkage domain antagonizes Nogo and a significant proportion of myelin-dependant inhibition both as a bound substrate and a soluble protein. However NgREcto was unable to overcome the inhibitory activity of CSPG/aggrecan suggesting that the protein acts specifically on the NgR pathway (Fournier et al., 2002).

1.2.2.4. The $p75^{NTR}$ as a Co-receptor for the NgR

Since the NgR is GPI-linked to the cell surface by analogy with other similarly anchored receptors it is likely that it associates with a transmembrane signal-transducing peptide. In fact the co-receptor for NgR was recently shown to be the p75 neurotrophin receptor ($p75^{NTR}$) (Wong et al., 2002). Evidence for this came from a study in which an antibody raised against the $p75^{NTR}$ abolished the repulsive turning of growth cones

induced by a MAG gradient (Wong et al., 2002). In a later study a truncated $p75^{NTR}$ protein lacking the signal transducing intracellular domain was shown to block the inhibitory properties of Nogo-66, MAG, OMgP and CNS myelin suggesting that $p75^{NTR}$ mediates inhibitory signals through its interaction with the NgR (Wang et al., 2002a). Furthermore immunostaining revealed extensive co-expression of the NgR and $p75^{NTR}$ in the developing nervous system of the rat providing further evidence for a functional interaction between these two receptors.

1.2.3. Myelin-Associated Glycoprotein

Myelin-associated glycoprotein (MAG or siglec 4a) is a well known myelin-derived inhibitor of neurite outgrowth (McKerracher et al., 1994; Mukhopadhyay et al., 1994). However its inhibitory activity was discovered long after it was initially cloned (Arquint et al., 1987). Interestingly MAGs inhibitory activity is mediated by a developmental switch in the neuronal response. For example MAG promotes the growth of embryonic neurons but inhibits the growth of postnatal and adult neurons (DeBellard et al., 1996). Moreover increasing the endogenous cAMP levels in adult neurons has been shown to override the growth inhibitory response to MAG (Cai et al., 2001). This may suggest that embryonic neurons have higher endogenous cAMP levels than adult neurons hence their ability to grow in the presence of MAG.

MAG binds sialic acid residues on sialylated glycans and gangliosides (Kelm et al., 1994; Vinson et al., 1996; Tang et al., 1997). MAG interacts directly with the sialylated gangliosides GT1b and GD1a present on the surfaces of responsive neurons (Vinson et al., 2001; Vyas et al., 2002). Neuraminidase treatment which removes sialic acid from the

surfaces of neurons was therefore shown to block MAG inhibition, as were antibodies against GT1b and GD1a (Vyas et al., 2002). Similarly a mutation in the sialic acid binding domain of MAG reduced the potency of its inhibitory activity (Vinson et al., 2001). Taken together these results suggest that GT1b and GD1a act as functional MAG receptors.

It was later found that multivalent clustering of GT1b and GD1a on the surfaces of neurons was sufficient for inhibition of neurite outgrowth on permissive substrates in the absence of inhibitory molecules (Vyas et al., 2002). This led to the theory that multivalent ganglioside clustering was perhaps an important first step in MAG associated neurite outgrowth inhibition, especially since GT1b and GD1a lack an intracellular signaling domain. However GT1b was then shown to interact with $p75^{NTR}$ forming a receptor complex that transmits the inhibitory signal from MAG to neurons (Yamashita et al., 2002). Reports also suggest that MAG can signal via the NgR which requires $p75^{NTR}$ as a co-receptor (Domeniconi et al., 2002; Liu et al., 2002a). Recently MAG, GT1b, $p75^{NTR}$ and the NgR were localized to lipid rafts on the surfaces of neurons (Vinson et al., 2003). Therefore raft-raft interactions on the surfaces of opposing cells could facilitate the interaction between MAG, its multiple receptors and downstream signaling components (Fig. 1.2).

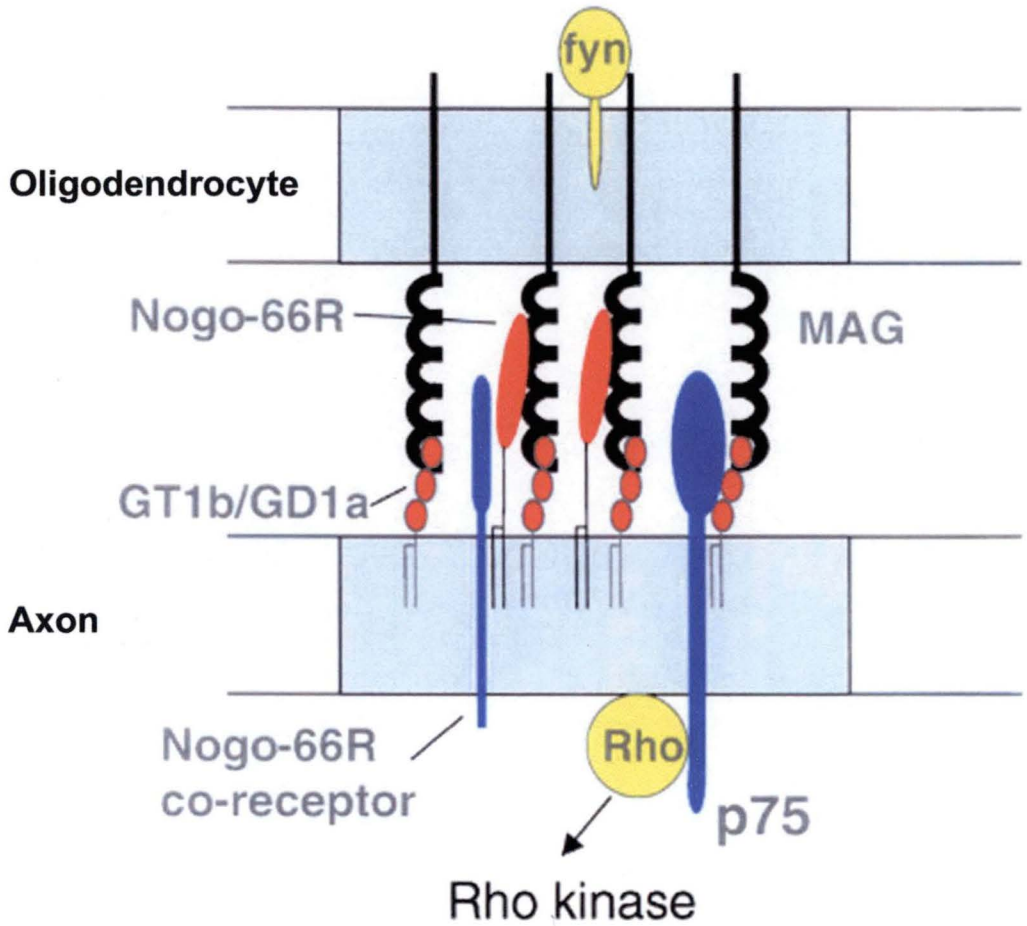

FIGURE 1.2. Lipid-raft model of MAG and Nogo-66 signaling.

Schematic representation of raft-raft interactions between axons and myelin-forming oligodendrocytes. Rafts are represented by blue/grey shading, MAG molecules in black, MAG receptors GT1b/GD1a in red, p75 and NgR co-receptors in blue and associated signaling molecules in yellow. The localisation of MAG and its binding partners GT1b, GD1a and the Nogo-66 receptor (NgR) within lipid rafts could provide discrete regions of high avidity interactions between the two cell types. Rafts may also provide a platform for multiple interactions involving MAG, its receptors and signaling molecules. Modified from (Vinson et al., 2003).

1.2.4. Rho Signaling by Myelin-Associated Inhibitors of Neurite Regeneration

Intracellular signaling by MAG, Nogo and OMgp is known to involve the small GTPase Rho (Lehmann et al., 1999; Niederost et al., 2002; Yamashita et al., 2002; Fournier et al., 2003). In its active form Rho is bound to GTP but when inactive is bound to GDP. In the GTP-bound active state Rho family members regulate the assembly and stability of the actin cytoskeleton (Hall, 1994). Activation of Rho is therefore known to cause growth cone collapse and neurite inhibition (Kozma et al., 1997; Kranenburg et al., 1999; Lehmann et al., 1999). Rho is maintained in an inactive state by Rho guanine nucleotide dissociation inhibitors (Rho-GDIs). Rho-GDIs are proteins that inhibit Rho activation by binding and sequestering Rho in the cytoplasm away from its targets in the cell membrane and blocking the binding of Rho to its substrates (Olofsson, 1999; Hoffman et al., 2000; Del Pozo et al., 2002). In a recent study it was found that $p75^{NTR}$ binds to Rho-GDI thereby displacing Rho from GDI allowing it to become activated (Yamashita and Tohyama, 2003). The resultant active Rho can then bind to and stimulate the activity of growth inhibitory proteins such as MAG, Nogo-66 and OMgp. Given that inhibitory signaling by these proteins converge on a common signaling pathway involving Rho this molecule could represent an important therapeutic target to overcome the barriers to neurite outgrowth in the CNS.

1.3. Use of Olfactory Ensheathing Cells in Promoting Repair in the Injured CNS

Many strategies have been employed in the past to overcome the inhibitory nature of the CNS. One of the more successful techniques has been the use of cell transplantation therapy to stimulate neuronal survival and growth. Of the myriad of cell and tissue types used in transplantation studies one of the more promising ones in terms of regeneration and functional recovery has been the olfactory ensheathing cell (OEC). Here are described the origin, phenotype, growth promoting properties of these cells and their potential for transplantation mediated regeneration and remyelination.

1.3.1. Origin of Olfactory Ensheathing Cells

Olfactory ensheathing cells are derived from precursor cells in the olfactory epithelium. During development OECs migrate from the epithelium with the axon bundles they ensheath. Olfactory sensory neurons (OSNs) are continuously replaced from progenitor cells located in the olfactory epithelium of the nasal mucosa (Graziadei and Graziadei, 1979; Calof and Chikaraishi, 1989; Chuah and Au, 1991; Caggiano et al., 1994). The axons of newly formed neurons cross from the peripheral to the central nervous system (PNS-CNS) where they form functional synapses with central neurons in specialised structures termed olfactory glomeruli in the olfactory bulb (OB) (Graziadei and Graziadei, 1979; Doucette et al., 1983). Even after transection of the olfactory nerves new neurons grow and form appropriate connections within the OB as demonstrated by structural studies using light microscopy (Graziadei and Graziadei, 1979; Doucette et al., 1983). It is thought that OECs provide the necessary guidance and trophic support

required by OSNs to make the correct connections within the glomeruli after transection (Tennent and Chuah, 1996; Chuah and West, 2002). Some of the growth promoting guidance molecules and neurotrophic factors expressed by OECs include laminin, N-CAM, L1, Galectin-1 HSPG, and semaphorin 3A, FGF-1, FGF-2, PDGF, NGF, BDNF, NT-4/5, GDNF, NTN, CNTF and neuregulins (see review by Chuah and West). In this way OECs are considered to be at least partly responsible for the apparent plasticity of the olfactory system (Doucette, 1990) which has since made them attractive candidates for transplant-mediated CNS repair.

1.3.2. Phenotypic Properties and Plasticity

It is now widely accepted that OECs share phenotypic characteristics in common with related glial cell types namely Schwann cells (SCs) and astrocytes (ASTs) (Doucette, 1990). In fact OECs have in the past been classified into two major groups; those with astrocyte-like properties and those with SC-like properties (Pixley, 1992; Franceschini and Barnett, 1996). Astrocyte-like OECs have a flattened morphology and express fibrous GFAP, embryonic neural cell adhesion molecule (EN-CAM) and low levels of $p75^{NTR}$ (Barber and Lindsay, 1982; Franceschini and Barnett, 1996). Schwann cell-like OECs have a spindle-like morphology, express $p75^{NTR}$, diffuse GFAP and the major peripheral myelin protein P_0 (Pixley, 1992; Franceschini and Barnett, 1996). However OECs can interchange between these two forms as the need arises which has led some authors to believe that OECs belong to a single malleable population that can exhibit a variety of phenotypic characteristics (Barber and Lindsay, 1982; Pixley, 1992; Doucette, 1995; Vincent et al., 2003).

However OECs have some characteristics that distinguish them from their closely related counterparts. Unlike SCs and ASTs, OECs are derived from the olfactory placode (Chuah and Au, 1991; Norgren et al., 1992). They exist almost exclusively in the outer olfactory nerve fibre layer (ONL) of the OB in the CNS and along the olfactory nerve in the PNS (Doucette, 1991, 1993). Olfactory ensheathing cells also contribute to the formation of the *glia limitans* (or glial limiting membrane) at the PNS-CNS boundary at the periphery of the olfactory bulb (Doucette, 1991). In embryonic animals the *glia limitans* is composed mostly of OECs. However after birth astroblasts are thought to migrate from deeper layers of the olfactory bulb into the *glia limitans* and differentiate into interfascicular astrocytes.

1.3.3. Regulation of OEC Proliferation, Differentiation and Survival *In Vitro*

Modulation of OEC biology is an extremely complex process and is only now beginning to be understood. Described below are some of the molecules known to regulator these processes in OECs *in vitro*.

Heregulin (HRG) basic fibroblast growth factor (bFGF or FGF-2), platelet derived growth factor (PDGF) glial growth factor (GGF), insulin-like growth factor 1 (IGF-1) and forskolin (FSK) are known to stimulate OEC proliferation in serum-containing medium (Chuah and Teague, 1999; Chuah et al., 2000; Yan et al., 2001b). However in serum-free medium only FGF-2 and HRG were found to promote OEC proliferation (Yan et al., 2001b).

The mitogenic effects of HRG, FGF-2, PDGF and IGF-1 on OECs in serum-containing medium can be enhanced by addition of the cyclic (cAMP) elevating agent

FSK (Yan et al., 2001b). Similarly in serum-free medium the mitogenic effects of HRG and FGF-2 can be improved by addition of FSK (Yan et al., 2001b). Although FSK increases intracellular cAMP levels the mechanism by which this increase potentiates the effects of various growth factors in OECs is unclear. However FSK induced cAMP elevation enhances the proliferative reponse of Schwann cells (SCs) to PDGF by increasing expression of PDGF receptors (Weinmaster and Lemke, 1990). Therefore this could suggest that the synergistic proliferative effect of FSK and growth factors is related to cAMP-mediated receptor induction.

Hepatocyte growth factor (HGF) was also found to enhance OEC proliferation in serum-free medium (Yan et al., 2001a). The proliferative effect of HGF on OECs was inhibited by FSK suggesting that HGF does not affect intracellular cAMP levels (Yan et al., 2001a). Similarly expression of the HGF receptor c-met remained unchanged after incubation of OECs with FSK (Yan et al., 2001a). Hence it appears that HGF enhanced proliferation in OECs is not associated with intracellular cAMP-mediated receptor induction.

Lysophosphatidic acid (LPA) is a phospholipid that has been shown to enhance the proliferation and migration of OECs *in vitro* (Yan et al., 2003). LPA exerts its effects via the G-protein-coupled receptors LPA_1, LPA_2 and LPA_3, which are expressed by OECs (Yan et al., 2003). These cell surface receptors can mediate the downstream effects of LPA via activation of the; (1) Rho/Rho associated kinase (Rho/ROCK), (2) mitogen activated protein kinase/extracellular signal related kinase (MAPK/ERK) and/or (3) phosphoinositol 3-kinase (PI-3K) pathway. LPA induced proliferation and migration in OECs is blocked by inhibitors of the Rho/ROCK, MAPK/ERK and PI-3K pathways

suggesting involvement of these pathways in mediating the effects of LPA in OECs (Yan et al., 2003). Similarly inhibitors of the Rho/ROCK pathway were found to block LPA associated changes in morphology, F-actin assembly and the formation of focal adhesion complexes in OECs indicating a role for Rho/ROCK in cytoskeletal reorganisation and therefore migration (Yan et al., 2003).

1.3.4. OECs Promote Axonal Growth

Since OECs have the ability to promote growth in a system in which it occurs naturally it was thought that they may have the capacity to support growth in areas of the CNS where successful regeneration does not normally occur. This theory prompted the use of OEC transplants to enhance axonal growth in various regions of the nervous system including: the spinal cord (Ramon-Cueto and Nieto-Sampedro, 1994; Li et al., 1997, 1998; Ramon-Cueto et al., 2000), brainstem (Gudino-Cabrera et al., 2000), fimbria-fornix (Smale et al., 1996), hippocampus (Gudino-Cabrera and Nieto-Sampedro, 1996) and sciatic nerve (Verdu et al., 1999). A summary of studies using OECs to promote regeneration in the nervous system is given in Table 1.3. Many of these studies show improved axonal growth, elongation and sprouting in animals receiving OEC transplants (Ramon-Cueto and Nieto-Sampedro, 1994; Ramon-Cueto et al., 1998; Navarro et al., 1999; Verdu et al., 1999). Similarly varying degrees of functional recovery have also been achieved with OEC implants (Li et al., 1997; Ramon-Cueto et al., 2000; Nash et al., 2002a; Li et al., 2003).

A recent study attempted to enhance the regenerative capacity of OECs by transfecting the cells with growth factor transgenes (Ruitenberg et al., 2002; Ruitenberg

et al., 2003). This study used adenoviral vectors to introduce the neurotrophin genes BDNF and/or NT-3 into OECs prior to implantation into the lesioned spinal cord of adult rats. The engineered cells were shown to reduce lesion volumes, increase sprouting and enhance hindlimb function when compared with normal OEC implants (Ruitenberg et al., 2003). Since the engineered cells only transiently expressed the transfected genes perhaps stable transfection of OECs could further improve the regenerative outcome.

TABLE 1.3. Promoting regeneration in the nervous system using OEC-transplants.

Reference	Lesion and Transplantation Model	Results
(Ramon-Cueto and Nieto-Sampedro, 1994)	Rhizotomy and transplantation of OECs into the dorsal root entry zone (DREZ)	3 wks after injury axons re-entered the spinal cord.
(Li et al., 1997)	Corticopsinal tract transection and injection of OECs	OECs stimulated regeneration of cut CST axons through the lesion site and improved directed forepaw reaching performance.
(Ramon-Cueto et al., 1998)	Removal of a 4mm section of rat spinal cord. SC-filled guidance channel created a bridge between cord stumps. OECs injected into midline of both stumps.	OECs promoted long-distance growth of raphe and propriospinal neurons, axons grew through the graft and into the host tissue. OECs migrated longitudinally and laterally from the injection sites and also entered SC bridges.
(Navarro et al., 1999)	Injection of OECs into the DREZ after lumbar rhizotomy.	No major improvements seen after 14 days. After 60 days there were improvements in regeneration and functional reconnection of sensory fibres.
(Verdu et al., 1999)	Sciatic nerve transection and implantation of collagen-filled tubes containing OECs.	79% of rats receiving collagen filled tubes plus OECs exhibited regeneration compared with 60% of rats with collagen tubes alone.
(Ramon-Cueto et al., 2000)	Stereotaxic injections of OECs into completely transected rat spinal cords	3-7 months post-surgery OEC transplanted animals displayed locomotor recovery and regained sensorimotor reflexes.
(Lu et al., 2002)	Olfactory lamina propria transplanted into transected spinal cord 4 weeks after initial injury.	10 weeks after implantation of lamina propria improved locomotor activity was observed.
(Verdu et al., 2001)	Injection of OECs into photochemical lesion of the rat spinal cord.	OECs reduced astrocytic gliosis and cystic cavitation during the first 15 days post-lesion.
(Nash et al., 2002b)	Methylprenisolone (MP) administered for 24 hours post CST lesion and implantation of OECs	6 weeks after injury rats that received MP in addition to OEC transplants displayed improved axonal regrowth and functional recovery.
(Li et al., 2003)	OEC matrix transplant into hemisection lesions of the upper cervical spinal cord.	2 months after injury improvements in supraspinal control of breathing had occurred. In the first 10-20 days after injury OECs induced a rapid recovery of climbing skill, which remained stable over a period of 6 weeks.
(Verdu et al., 2003)	Injection of purified OECs after photochemical lesion of the spinal cord.	OECs prevented loss of spinal cord parenchyma and improved functional outcome up to 3 months after injury.

1.3.5. OEC Transplant-Mediated Remyelination

Although OECs are normally non-myelinating they have the capacity to remyelinate demyelinated axons *in vitro* (Devon and Doucette, 1992) and *in vivo* (Franklin et al., 1996; Li et al., 1998; Barnett et al., 2000; Kato et al., 2000). Remyelination by OECs was found to be of a peripheral-type similar to that described for Schwann cells (Franklin et al., 1996; Kato et al., 2000). This is consistent with the finding that OECs express the peripheral myelin protein P_0 and the non-compact myelin protein 2'3'-cyclic nucleotide 3'-phosphodiesterase (CNPase) (Lee et al., 2001; Santos-Silva and Cavalcante, 2001). Olfactory ensheathing cells also express transcriptional factors and signalling molecules associated with the myelin formation pathway such as Krox-20, SCIP/Oct-6 and desert hedgehog (Dhh) (Smith et al., 2001). However there are conflicting reports regarding the presence of the major compact myelin component, myelin basic protein (MBP) in OECs (Doucette and Devon, 1994, 1995). This may be due to the fact that MBP expression in cultured OECs is highly dependent upon culture conditions (Doucette and Devon, 1994, 1995).

Several *in vivo* studies have shown that OECs can remyelinate demyelinated axons *in vivo* a summary of which is given in Table 1.4. However remyelinating characteristics appear to be restricted to a distinct subset of cells. In one paticular study a range of OEC morphologies were observed after transplantation (Franklin et al., 1996). While a majority of transplanted cells assumed a SC-like myelinating phenotype there were some cells that associated with axons without forming myelin sheaths, while others did not associate with axons at all. From this study, it was unclear as to whether the non-myelinating cells represented different morphological subsets of OECs or contaminating

cell types. In another study the presence of meningeal cell-like, SC-like and AST-like cells was detected following transplantation of a human OEC suspension (Barnett et al., 2000). This suggested that the transplanted cells could exhibit a range of morphologies reflecting their tendency for phenotypic plasticity in culture. However the authors also stated that the meningeal cell-like population may have been a contaminating cell type which is possible, given that the human OECs used in this study were only 30-45% pure on the basis of $p75^{NTR}$ expression. Taken together these results demonstrate the need to develop a standardised set of characteristics that define OECs or to identify a new marker that is specific for OECs alone.

One question directly emanating from the aforementioned studies was whether the purity of OEC transplants affected the ability of the cells to remyelinate axons. Interestingly one study showed that purified OECs selected by $p75^{NTR}$ expression produced less extensive remyelination than unpurified OEC populations (Lakatos et al., 2003). The authors suggested that this could have been due to the presence of meningeal cells in the unpurified preparations. To determine if the presence of meningeal cells could improve remyelination by OECs a 70:30 mix of OECs and meningeal cells was injected into the demyelinated spinal cord. Indeed the resultant remyelination induced by the OEC/meningeal cell mix was more widespread compared with that produced by purified OECs suggesting that the remyelinating capacity of OECs may be profoundly affected by the purity of the cultures.

TABLE 1.4. OEC transplant-mediated remyelination studies.

Reference	Lesion and Transplantation Model	Results
(Franklin et al., 1996)	OECs injected into sites of X-EB demyelinating lesions in the rat spinal cord.	OECs formed peripheral type myelin sheaths around most demyelinated axons within 21 days.
(Imaizumi et al., 1998)	OECs injected into X-EB lesions of the dorsal columns in the rat 6 days after initial injury.	21-25 days after OEC injection spinal cords were removed and maintained in an *in vitro* recording chamber, remyelinated axons displayed enhanced conduction velocity.
(Li et al., 1998)	Electrolytic CST lesion and injection of OEC suspension.	1 week after injury OECs promoted sprouting of cut CST axons, 3 weeks after injury peripheral type remyelination of CST axons was observed, remyelinated fibres crossed the length of the lesion and re-entered the CST.
(Barnett et al., 2000)	Human OECs injected into X-EB demyelinated lesions in the rat spinal cord.	Limited peripheral type remyelination occurred 3 weeks after transplantation whilst at 6 weeks remyelination was more widespread.
(Kato et al., 2000)	Compared human and rat OECs injected into X-EB demyelinated lesions in the rat spinal cord.	3 weeks after transplantation of human or rat OECs extensive peripheral-type remyelination occurred.
(Lakatos et al., 2003)	Injection of pure OECs, unpure OECs or OEC/meningeal cell suspension (70:30) after X-EB lesion of rat spinal cord.	After 3 weeks 3-fold greater remyelination occurred with unpurified OECs compared with pure OECs. Similarly OEC/meningeal cell suspensions produced 3-fold greater remyelination compared with pure OECs.

[1] Abbreviations X-irradiated ethidium bromide (X-EB) lesion, corticospinal tract (CST).

1.3.6. The Effect of the Injured Spinal Cord on OECs

The multitude of cytokines, proteoglycans and guidance factors upregulated after CNS injury, have the potential to modulate the biology of implanted OECs. Especially considering the degree of phenotypic plastiscity seen in OECs both *in vitro* and *in vivo*. Some of the more well characterised molecules found in the injured CNS and what is currently known of their effects on OEC biology are discussed here.

The cytokines interferon γ (IFNγ) and basic fibroblast growth factor (FGF-2) play a major role after CNS injury in the induction of the glial scar. IFNγ produced by activated T-lymphocytes increases the proliferation of astrocytes (ASTs) thereby enhancing formation of the glial scar (Yong et al., 1991). The effect of IFNγ on OECs is unknown although its role as a mitogen for ASTs suggests that it may also have the potential to induce OEC proliferation.

After injury to the brain and spinal cord FGF-2 is rapidly upregulated perhaps to initiate wound repair (Logan et al., 1992; Mocchetti et al., 1996). This increase in expression has been localised to neurons, macrophages, ASTs and endothelial cells (Logan et al., 1992). FGF-2 is a known mitogen for OECs *in vitro* (Chuah and Teague, 1999) hence its upregulation in the injured spinal cord could promote proliferation of implanted OECs.

Expression of transforming growth factor β (TGFβ) has been shown to increase around the glial scar after spinal cord injury (Lagord et al., 2002). Upregulation of TGFβ1 expression occurs in the acute phase of injury where its presence is associated largely with neurons (Lagord et al., 2002). In contrast upregulation of TGFβ2 expression occurs during the subacute phase and is localised to the vicinity of the wound in ASTs

and endothelial cells (Lagord et al., 2002). This pattern of expression may suggest that TGFβ1 modulates the inflammatory and neuronal response whilst TGFβ2 regulates glial scarring. The effects elicited by TGFβ appear to depend on cell type. In ASTs TGFβ1 upregulates expression of glial fibrillary acidic protein (GFAP) a key indicator of reactive AST phenotype (Reilly et al., 1998), in SCs TGFβ1 and 2 enhance proliferation (Watabe et al., 1994), whilst in OLGs TGFβ induces apoptosis (Schuster et al., 2002). However the effect of TGFβ in modulating OEC biology has not yet been investigated.

Tumor necrosis factor α (TNFα) is upregulated immediately after CNS injury. Its expression has been attributed to neurons, glial cells (including astrocytes, oligodendrocytes and microglia) and endothelial cells in the injured spinal cord (Yan et al., 2001c). Again the effect of this molecule on OECs is not known, yet these cells have recently been shown to express TROY a member of the TNF receptor superfamily (Hisaoka et al., 2004). Expression of this receptor could confer upon OECs the ability to respond to the TNF family of proteins.

Lack of neurite growth in the injured CNS is also associated with increased levels of chondroitan sulphate proteoglycans (CSPG). These proteins are produced by reactive ASTs, OLGs and macrophages at the injury site (McKeon et al., 1991; Jones et al., 2002; Moon et al., 2002). The effects of these molecules on OECs are unknown and perhaps should be investigated.

Breakdown of damaged oligodendrocytes and myelin at the injury site releases neurite growth inhibitors such as oligodendrocyte myelin glycoprotein (OMgp), myelin-associated glycoprotein (MAG) and Nogo. Whilst the inhibitory effects of these molecules on neurite growth at the injury site have been characterised their effects on

glial cells have not been reported. The potential for these factors to modulate OEC behaviour has not been investigated despite the fact that OECs posses the p75 neurotrophin receptor ($p75^{NTR}$), a co-receptor with the Nogo receptor (NgR) in OMgp, MAG and Nogo signalling (Wang et al., 2002a). It is possible since OECs express $p75^{NTR}$ that they also express the NgR, which could imply that they respond to OMgp, MAG and Nogo. Alternatively NgR could be used by OECs as a means of presenting inhibitory antigens to neurons as negative guidance cues.

1.4. Properties of OECs that Promote Central Nervous Tissue Repair

The regeneration promoting characteristics of OECs are thought to include their ability to successfully integrate into the host environment, the production of growth-promoting soluble factors and the expression of membrane-associated proteins involved in cellular migration and guidance. Indeed each of these factors may be important for promoting CNS repair although perhaps not in isolation but in combination.

1.4.1. Integration Within the Host Environment

Although transplanted SCs have the ability to promote CNS regeneration and remyelination their capacity to do so is impeded by the presence of ASTs. In fact transplanted SCs migrate and survive poorly in the presence of ASTs resulting in limited remyelination capability (Iwashita et al., 2000). Since astrocytosis is a common feature of the CNS injury site the efficacy of SC transplants for promoting repair in these environments is questionable. In contrast several studies have shown that OECs not only survive transplantation into the injured spinal cord but that they can migrate unimpeded

through the host tissue unlike their SC counterparts (Ramon-Cueto and Nieto-Sampedro, 1994; Ramon-Cueto et al., 1998; Ramon-Cueto et al., 2000). In one study OECs were transplanted into the lesion site in combination with SC-filled PAN/PVC guidance channels (Xu et al., 1997). Olfactory ensheathing cells moved freely through the glial scar, entered the SC-channel and invaded both spinal cord stumps. In contrast the SCs remained inside the channels and did not migrate. This may be partly due to the unique interactions between OECs and reactive ASTs. Several *in vitro* studies have demonstrated that OECs unlike SCs freely intermingle with ASTs, migrate into astrocytic areas and do not induce AST hypertrophy (Lakatos et al., 2000; Boruch et al., 2001; Van Den Pol, 2003). Indeed OECs implanted into the photochemically damaged spinal cord can reduce astrocytic gliosis and cystic cavitation (Verdu et al., 2001). Taken together these results suggest that OECs may be capable of modifying the injury induced response of other glial cell types thereby counteracting the upregulation and/or release of growth restrictive molecules.

1.4.2. Neurotrophic Factors

Olfactory ensheathing cells produce a variety of neurotrophic factors that may enhance neuronal proliferation, differentiation and survival after transplantation. These factors belong to several distinct families some of which are described below.

1.4.2.1. Neurotrophin Family

The neurotrophin family consists of four members including nerve growth factor (NGF), brain-derived neurotrophic factor (BDNF), neurotrophin-3 (NT-3) and

neurotrophin-4/5 (NT-4/5). These factors have been shown to act as survival and differentiation factors for various neuronal populations. For example NGF (the neurotrophin family prototype) is a survival factor for cholinergic neurons *in vitro* (Hartikka and Hefti, 1988; Hatanaka et al., 1988) and *in vivo* (Hefti, 1986; Williams et al., 1986; Kromer, 1987; Gage et al., 1988) whilst BDNF, NT-3 and NT-4/5 enhance the survival and differentiation of striatal neurons (Mizuno et al., 1994; Ventimiglia et al., 1995; Perez-Navarro et al., 1999). Olfactory ensheathing cells express several members of the neurotrophin family including; NGF, BDNF, and NT-4/5 (Boruch et al., 2001; Woodhall et al., 2001). Of these only NGF and BDNF are known to be secreted.

The neurotrophin proteins interact with two classes of receptor; the high affinity tyrosine kinase (Trk) receptors and the low affinity $p75^{NTR}$. The Trk receptors, TrkA, TrkB and TrkC confer ligand specificity for NGF, BDNF/NT-4/5 and NT-3 respectively (Klein et al., 1991a; Klein et al., 1991b; Lamballe et al., 1991; Klein et al., 1992). The $p75^{NTR}$ receptor belongs to the tumor necrosis factor (TNF) family and lacks intrinsic catalytic activity (Chao, 1994). Although $p75^{NTR}$ is a common receptor for each of the neurotrophins (Rodriguez-Tebar et al., 1990; Dechant et al., 1997) NGF binding can uniquely activate a programmed cell death pathway (Dechant and Barde, 1997). The $p75^{NTR}$ is also an accepted marker for OECs *in vitro* and *in vivo* despite the fact that it is expressed by SCs. To date the only the high affinity neurotrophin receptor that has been localised to OECs is TrkB (Woodhall et al., 2001).

1.4.2.2. Neurotrophin-Related Factors

Another closely related group of neurotrophic factors is the glial cell-line derived neurotrophic factor (GDNF) family of ligands (GFL) which form a subgroup within the transforming growth factor beta (TGF-β) superfamily (Kingsley, 1994). The members of this family include GDNF, artemin (ART), neurturin (NTN) and persephin (PSP) (Lin et al., 1993; Kotzbauer et al., 1996; Milbrandt et al., 1998; Airaksinen et al., 1999). GDNF is a known survival factor for dopaminergic neurons both *in vivo* (Lin et al., 1993) and *in vitro* (Lin et al., 1994; Meyer et al., 2000). Artemin is primarily a survival factor for sympathetic neurons but can also promote proliferation and act as a guidance factor (Baloh et al., 1998; Andres et al., 2001; Honma et al., 2002). Neurturin and PSP both promote survival of dopaminergic neurons (Horger et al., 1998; Milbrandt et al., 1998). Both GDNF and NTN mRNA have been detected in OECs (Woodhall et al., 2001). The GDNF protein is produced but it is not secreted by OECs, whilst the presence of NTN protein has not yet been investigated.

The actions of the GFLs are mediated via members of the GDNF family receptor alpha (GFRα) group. GDNF, NTN, ART and PSP bind to GFRα-1 GFRα-2, GFRα-3 and GFRα-4 respectively. Although these receptors confer ligand specificity they require the presence of the co-receptor RET for signal transduction (Trupp et al., 1996). Since OECs seemingly lack RET expression it is unlikely that GDNF and NTN could elicit intracellular signals within OECs (Woodhall et al., 2001). Nevertheless GFRα-1 and 2 found in OECs could function to bind and present GDNF and NTN to growing neurons (Woodhall et al., 2001). GFRα-3 is also known to be expressed in embryonic but not adult olfactory epithelium and OECs (Widenfalk et al., 1998). The presence of its ligand

ART has recently been detected in embryonic and early postnatal OECs (Lipson et al., 2003).

1.4.2.3. Neuregulins

In addition to the neurotrophins and related factors some neuregulin-1 (nrg-1) family members are expressed by OECs. The *nrg-1* gene is located on the long arm of chromosome 8 and gives rise to multiple mRNA variants by way of alternative splicing and promoter usage (Orr-Urtreger et al., 1993) (Fig. 1.3). The nrg-1 proteins are derived from different combinations of the same structural domains and have been classified into 3 major groups. Type I includes neu differentiation factor (NDF) or heregulin (HRG) and acetyl-choline receptor inducing activity (ARIA). These factors contain an immunoglobulin (Ig)-like domain, epidermal growth factor (EGF)-like domain (α and β), a hydrophobic domain and an internal signal sequence for secretion (Falls et al., 1993). Type II or glial growth factors (GGF) contain a signal peptide, an Ig-like domain an EGF-like domain (β) and a kringle-like sequence (Marchionni et al., 1993). Type III sensory and motor neuron derived factors (SMDF) have only a hydrophobic domain and an EGF-like domain (β) in common with other nrg-1 isoforms (Ho et al., 1995). The neuregulins are potent glial cell mitogens and survival factors (Pinkas-Kramarski et al., 1994; Vartanian et al., 1994; Dong et al., 1995; Canoll et al., 1996; Grinspan et al., 1996). They are also crucial for PNS and CNS development (Lee et al., 1995; Gassmann and Lemke, 1997) and are important for neuromuscular synapse formation during cardiac development (Gassmann et al., 1995; Lee et al., 1995; Meyer and Birchmeier, 1995).

In a recent study OECs were shown to express mRNA for NDF, GGF and SMDF (Thompson et al., 2000). Whilst mRNA encoding both membrane bound and secreted transcripts were detected the protein could not be located on the surface of the cells nor in concentrated conditioned medium. However the protein was detected in the nucleus or cytoplasm depending on the isoform suggesting a possible intracellular role for nrg-1 proteins in OECs.

The Nrg-1 receptors belong to the class 1 family of tryosine kinases termed erbB or epidermal growth factor (EGF) receptors. Members of this family (erbB2, erbB3 and erbB4) form various homo- and hetero-dimeric complexes which can induce different biological responses depending on the activation of specific intracellular signal transduction pathways (Muthuswamy et al., 1999; Olayioye et al., 1999). Some studies suggest that OECs express erbB2 and erbB3 (Salehi-Ashtiani and Farbman, 1996; Perroteau et al., 1998), while others showed that OECs express erbB2 and erbB4, but not erbB3 (Pollock et al., 1999; Thompson et al., 2000). The apparent inconsistencies between these reports could either be due to culture conditions or differences in detection methods.

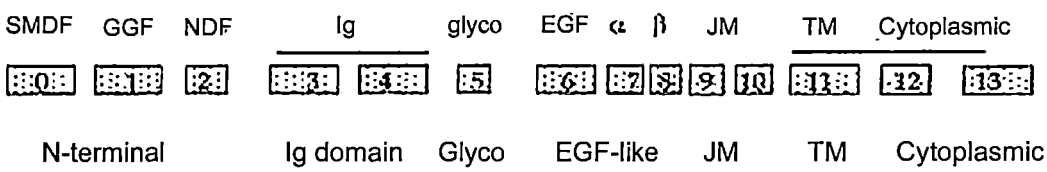

FIGURE 1.3. Putative representation of the *neuregulin-1* (*nrg-1*) gene.

The *nrg-1* gene has fourteen exons (0-13), the structural domains that each exon represents is shown above (Ig = immunoglobulin domain, glyco = glycosylation domain, EGF = epidermal growth factor α or β domain, JM = juxtamembrane domain and TM = transmembrane domain). Alternative splicing at the N-terminal region of the gene produces Type I (NDF), Type II (GGF) and Type III (SMDF) nrg-1 subtypes. Further alternative splicing can occur in the EGF domain to produce α and β variants of each of the three subtypes. Other known splice variants include secreted and transmembrane variants. Modified from (Thompson et al., 2000).

1.4.2.4. Other Growth Factors

Ciliary neurotrophic factor (CNTF) is a member of the interleukin-6 neuropoietic cytokine (IL-6) family along with leukemia inhibitory factor (LIF), oncostatin-M (OSM), IL-11 and cardiotrophin-1 (Patterson, 1992; Ip and Yancopoulos, 1996; Murphy et al., 1997). Each of these cytokines activates a different signalling protein that is anchored to the cell membrane via a GPI linkage. The lack of a transmembrane domain means that signal transduction requires a second receptor component, which is provided by gp130 (or IL-6 signal transducing glycoprotein 130). In the case of LIF and OSM the receptor complex is composed of the binding protein LIF receptor β (LIFRβ or gp190) bound to the signal transducer gp130 (Gearing et al., 1991; Gearing and Bruce, 1992; Gearing et al., 1992). The IL-6 and IL-11 receptors are composed of the IL-6 receptor α (IL-6Rα or gp80) or IL-11 receptor α (IL-11Rα) subunits similarly bound to gp130 (Yamasaki et al., 1988; Murakami et al., 1993; Hilton et al., 1994; Yamasaki et al., 2001). However CNTF signalling involves the formation of a heterotrimeric complex initiated by binding of CNTF to its α receptor subunit (CNTFRα). The resultant CNTF/CNTFRα complex recruits the signal transducing binding partners gp130 and LIFRβ (Davis et al., 1991).

Both CNTF and CNTFRα mRNA have been detected in OECs (Wewetzer et al., 2001; Lipson et al., 2003). However another study failed to detect CNTF mRNA in OECs although this may have been due to the fact that their OECs were derived from a clonal cell line rather than primary culture (Boruch et al., 2001).

LIF is thought to be a key mediator of injury-induced neurogenesis in the olfactory epithelium. Evidence for this comes from the observation that LIF and LIF receptor (LIFR) expression is upregulated after olfactory bulbectomy (Nan et al., 2001; Getchell et

al., 2002; Bauer et al., 2003). This increase appears to coincide with the peak time for macrophage recruitment and the onset of progenitor cell proliferation after injury. Furthermore LIF has been localised to infiltrating macrophages and injured OSNs, whilst the LIFR has been detected in globose basal cells (GBCs) the immediate precursors of OSNs (Nan et al., 2001; Getchell et al., 2002; Bauer et al., 2003). Taken together these data suggest that LIF derived from infiltrating macrophages may function as a mitogen that stimulates proliferation of GBCs and that LIF produced by injured OSNs could act as an intracellular survival factor. Interestingly LIFR, IL-6 and IL-6R are upregulated in OECs after bulbectomy perhaps suggesting that these cells may play a role in OSN survival or repair after injury (Nan et al., 2001).

The fibroblast growth factor (FGF) family consists of 18 known members (FGF-1 to -18) (Ohbayashi et al., 1998). Acidic and basic fibroblast growth factor, FGF-1 and FGF-2 respectively were the first of these to be identified (Baird, 1994). The FGFs bind to the high affinity tyrosine kinase receptors FGFR1-4 of which there are seven known splice variants, including FGFR-1b, FGFR-1c, FGFR-2b, FGFR-2c, FGFR-3b, FGFR-3c and FGFR-4 (Ornitz et al., 1996). However to elicit their biological actions FGFs must also bind to a low affinity proteoglycan receptor on the cell surface (Yayon et al., 1991).

Of the FGF ligands only FGF-1 and FGF-2 have been located in OECs and the olfactory nerve (Gall et al., 1994; Key et al., 1996; Chuah and Teague, 1999) although both ligands were also detected in distinct regions of the OB (Ernfors et al., 1990; Matsuyama et al., 1992; Key et al., 1996). In addition FGF-5 and -9 were detected in various regions of the OB but not in OECs (Gomez-Pinilla and Cotman, 1993; Tagashira et al., 1995). The receptors FGFR1-3 but not FGFR-4 were detected in the OB (Yazaki et

al., 1994). Olfactory ensheathing cells have also been shown to express FGFR-1 and perlecan (Chuah and Teague, 1999) a heparin sulphate proteoglycan known to be crucial for FGF binding and subsequent signalling events (Yayon et al., 1991). The presence of FGF-1 and -2 along with the FGFR-1 receptor and perlecan in OECs suggests that these cells could respond to FGFs in an autocrine manner. In fact FGF-1 and FGF-2 have been shown to stimulate proliferation of OECs *in vitro* (Key et al., 1996; Chuah and Teague, 1999).

1.4.3. Cell Adhesion Molecules and Guidance Cues

In addition to neurotrophic factors OECs express an array of adhesion and extracellular matrix (ECM) molecules that provide a permissive substrate for neurite extension, growth and migration. Many of these molecules play essential roles in development and may therefore be important in promoting CNS repair after injury. Described below are some of the various guidance factors expressed by OECs.

Laminin has been localised to the axons of the olfactory nerve layer of the OB and to OECs (Liesi, 1985; Treloar et al., 1996). The spatiotemporal distribution pattern of laminin within the developing olfactory system suggests that it may function as a growth promoting molecule. In addition laminin appears to promote migration of olfactory axons from explant cultures of olfactory epithelium (Calof and Lander, 1991). Futhermore laminin facilitates the *in vivo* migration of OECs and increases their axon outgrowth promoting activity (Tisay and Key, 1999). Olfactory ensheathing cells also express neural cell adhesion molecule (N-CAM) and the L1 glycoprotein which are similarly expressed

by olfactory axons (Miragall et al., 1989; Gong and Shipley, 1996). Both N-CAM and L1 mediate extension and fasciculation of olfactory axons during development.

Galectin-1 is a carbohydrate binding protein expressed by OECs residing in the nerve fibre layer of the OB and in the olfactory nerve (St John and Key, 1999). This protein is thought to mediate sorting of olfactory axon subpopulations during development and to maintain specific glomerular connections postnatally.

Neuroligin-3 is a homologue of the glial specific transmembrane adhesion molecule gliotactin which is crucial for the formation of the glial sheath in the PNS of *Drosophila melanogaster* (Gilbert et al., 2001). Neuroligin-3 is expressed by OECs, ASTs and SCs during development but is also found in mature OECs (Gilbert et al., 2001). By analogy with the function of gliotactin Neuroligin-3 in OECs could mediate the formation of cellular contacts or junctions between OECs and axons during ensheathment of olfactory nerve fascicles. The finding that mature OECs retain expression of Neuroligin-3 could reflect their capacity to retain some of their developmental characteristics, which aid neurite growth.

Semaphorin 3A (Sema 3A) is a negative guidance cue that is differentially expressed by $p75^{NTR}$ positive OECs in the ONL of the OB (Schwarting et al., 2000). Sema 3A (or collapsin-1) is chemorepulsive for neuropilin-1 (npn-1) a receptor molecule found on the surfaces of some olfactory axons. In knockout mice lacking Sema 3A, npn-1 positive axons entering the ONL are misrouted forming inappropriate connections within the glomeruli (Schwarting et al., 2000). Hence Sema 3A expressing OECs may help to guide subsets of npn-1 positive olfactory axons to their appropriate targets within the OB.

Given the roles of these proteins in guidance and elongation of axons and their presence in OECs it is conceivable that they may play an important role in the capacity of OECs to promote neurite growth in the CNS.

1.5. Summary

In summary OECs are a versatile cell type that can change morphology and antigenic profile as required. Since OECs share many characteristics in common with other glial cell types the search for a specific marker that will unequivocally distinguish these cells from their glial counterparts continues. It is well known that OECs promote axonal growth both in their natural environment and when transplanted into sites of CNS injury. Results of transplantation studies infer that the array of neurotrophic factors and cell adhesion molecules expressed by OECs *in vitro* and *in vivo* continue to be expressed by OECs when implanted into the injured CNS. However direct evidence supporting this characteristic is limited. Therefore the likelihood that OEC phenotype is altered by CNS injury associated molecules is an issue that should be addressed. As a result my hypotheses are:

- Because OECs exhibit such diverse phenotypic characteristics depending upon culture conditions their morphology and antigenic profile will be affected by implantation into the injured CNS.
- Specific isoforms of nrg-1 act as mitogens and survival factors for OECs *in vitro* and are known to change after olfactory nerve injury hence the profile of nrg-1 expression in OECs will change after implantation into sites of CNS

injury, reflecting the antigenic plasticity of OECs and their potential to assume a regeneration specific phenotype.

- Because Nogo and the NgR are commonly associated with axonal growth inhibition it is hypothesised that OECs *in vitro* and implanted into the injured spinal cord will express low levels of Nogo and NgR.

1.6. Aims

Hence the purpose of this study was to:

- To investigate the morphology of encapsulated OECs *in vitro* and after implantation into the injured spinal cord by scanning electron microscopy.
- To investigate Nrg-1 mRNA expression in cultured OECs compared with other cell types, and to determine if Nrg-1 mRNA expression in OECs is affected by the injured spinal cord.
- To determine if cultured OECs express Nogo and NgR mRNA and the corresponding proteins, and to investigate whether Nogo expression is influenced by the injured spinal cord.

CHAPTER TWO

General Materials and Methods

All procedures involving animals were approved by the Animal Experimentation Ethics Committee of the University of Tasmania and are consistent with the Australian Code of Practice for the Care and Use of Animals for Scientific Purposes.

2.1. Cell Cultures

2.1.1. OEC Culture

Primary OEC cultures were prepared as described previously (Chuah and Teague, 1999; Woodhall et al., 2001). Briefly ten 1-2 day old hooded Wistar rat pups were anaesthetised and their olfactory bulbs dissected out. The ONL of each bulb was removed and digested in 0.09% trypsin and 0.25% collagenase diluted 1:2 with Minimum Essential Eagle Medium Hepes modification (MEM-H) (3 × 15 minutes at 37°C) then filtered through nylon mesh (80μm pore size). After centrifugation for 10 minutes at 500×g the cells were resuspended and plated into a 25cm^2 flask. Cells were maintained in Minimum Essential Eagle Medium D-valine modification (MEM D-valine) (Life Technologies), containing 10% dialysed fetal calf serum (dFCS) and 1% penicillin-streptomycin-fungizone solution (Life Technologies) at 37°C, 5% CO_2. Contaminating fibroblasts were removed by addition of cytosine arabinofuranoside (2.5 × 10^{-7}M) (Sigma). To enhance the proliferation of OECs, 125μg/ml bovine pituitary extract (BPE) (Sigma) was added to the cultures. Once sufficient confluency was obtained cells were passaged to a new flask by trypsinisation with 0.25% trypsin in Hank's Balanced Salt

Solution (HBSS). Cells were then grown for 3 days or until they reached confluency. To determine purity of the cultures cells were grown on 13mm diameter coverslips at a density of 1×10^4 per coverslip and immunostained with monoclonal anti-$p75^{NTR}$ (Chemicon) and monoclonal anti-glial fibrillary acidic protein (GFAP) diluted 1:100. Cells were also counterstained with 0.01% Nuclear Yellow (Sigma Cat. No. N-2137). OECs were estimated to be 91% $p75^{NTR}$ and 93% GFAP positive in serum containing medium (Fig. 2.1).

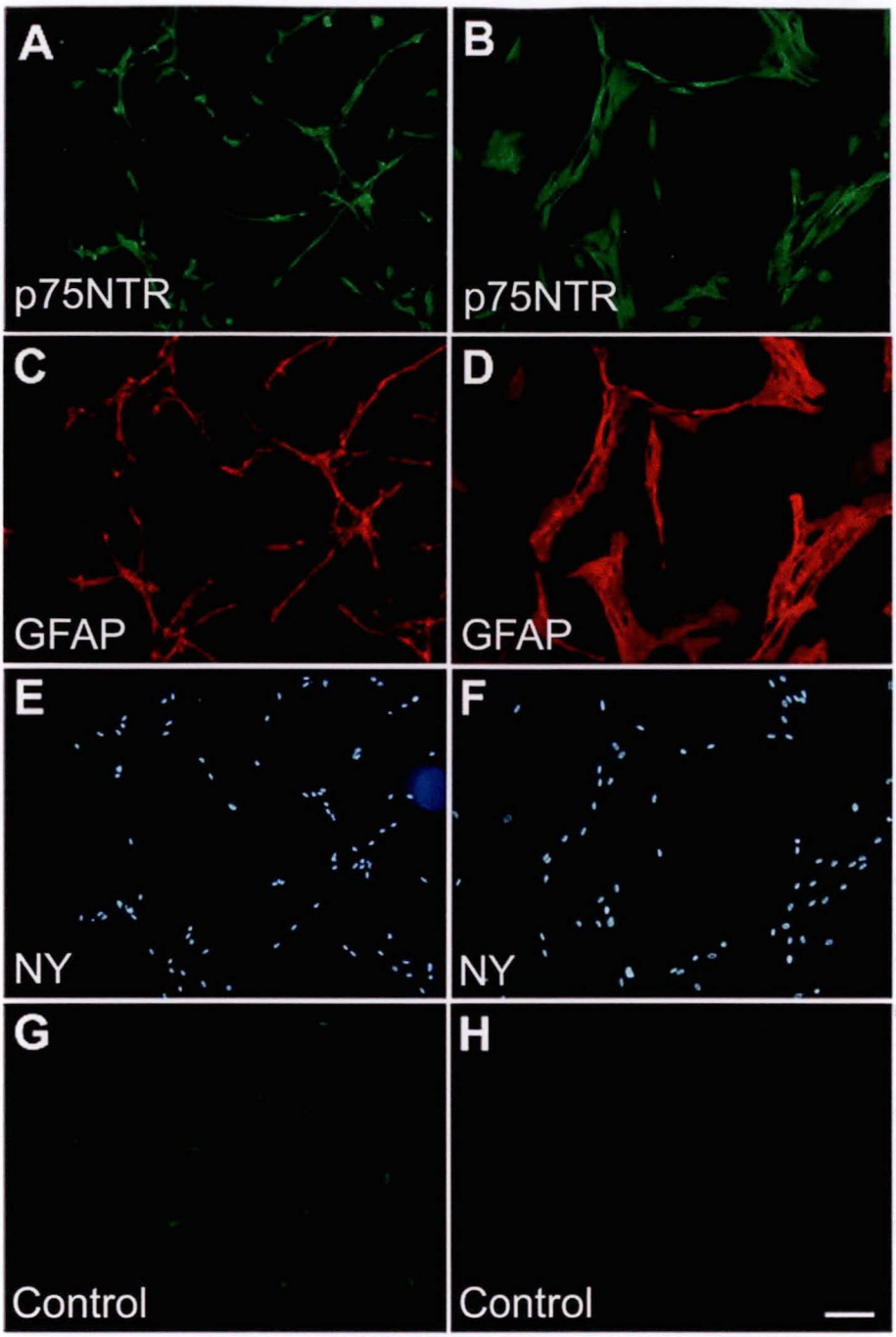

FIGURE 2.1. Immunofluorescence of $p75^{NTR}$ in olfactory ensheathing cells (OECs).

Immunostaining of OECs maintained in MEM D-valine with G-5 supplement (left) and MEM D-valine with 10% dFCS (right). Cultures were estimated to be 91% $p75^{NTR}$ positive (A, B) and 93% GFAP positive (C, D). Cells were counterstained with Nuclear Yellow (E, F). Controls in which the primary antibodies were omitted were negative (G, H). Scale bar, 100μm.

2.1.2. Astrocyte and Oligodendrocyte Culture

2.1.2.1. Mixed Culture

Primary AST and oligodendrocyte (OLG) cultures were prepared from the cortices of 2 day old hooded Wistar rat pups and purified using a modification of a previously described method (McCarthy and De Vellis, 1980). Whole brain was dissected out and the meninges, cerebellum and brainstem removed. The tissue was placed in Minimum Essential Eagle Medium Hepes modification (MEM-H) (Sigma) then minced and triturated through a flame polished pasteur pipette and filtered through nylon mesh (80μm pore size). Cells were centrifuged at 500×g for 5 minutes and plated at a density of 1-2 × 10^7 cells per 75cm^2 flask. Cultures were maintained in Dulbecco's Modified Eagle Medium/F-12 modification (DMEM/F-12) (Life Technologies) with 10% FCS and 1% penicillin-streptomycin-fungizone solution at 37°C and 5% CO_2. Medium was changed every 3 days until confluency was reached (7-9 days). The length of the initial culture period was held between 7 and 9 days as periods shorter than this are insufficient to obtain stratification of ASTs and OLGs whilst periods longer than this can result in the clustering of ASTs above the normal bedlayer (McCarthy and De Vellis, 1980). Due to the nature of the separation procedure these AST clusters can break up and contaminate the OLG preparation (McCarthy and De Vellis, 1980). Microglia were removed mechanically by shaking the flasks on a rotary shaker for 1 hour at 200 rpm. Medium was then replaced and the cultures were shaken for a further 18 hours at 180rpm to isolate the OLG precursors that grow on top of the AST bedlayer.

2.1.2.2. Purification of Astrocytes

After the OLGs were removed ASTs were passaged by trypsinisation with 2.5% trypsin in 10ml EDTA solution. Cells were centrifuged at 500×g for 5 minutes and resuspended in Dulbecco's Modified Eagle Medium (DMEM) (Sigma) with 10% FCS and 1% penicillin-streptomycin-fungizone solution (Life Technologies). The cell suspension was plated into three 75cm^2 flasks and grown to confluence at 37°C and 5% CO_2. For immunostaining cells were plated at a density of 1×10^4 per 13mm diameter coverslip. To determine the purity of AST cultures, cells were stained with mouse monoclonal anti-GFAP (Sigma) diluted 1:100 and polyclonal rabbit anti-cow S-100 (DAKO) diluted 1:100. Cells were also counterstained with 0.01% Nuclear Yellow (Sigma, Cat. No. N-2137). Astrocytes purified by this technique were estimated to be 92% GFAP positive and 97% S-100 positive in serum-containing medium (Fig. 2.2).

2.1.2.3. Purification of Oligodendrocytes

The supernatant containing the OLGs was pelleted at 500×g for 10 minutes resuspended in DMEM containing 10% FCS and transferred to a 25cm^2 flask. Oligodendrocytes were further purified by transferring the supernatant to a new 25cm^2 flask 45 minutes after initial plating. Since serum contains inducers and repressors of OLG differentiation, their maturation is favoured by low serum-containing medium. After an initial 24 hours in serum-containing medium the cells were rinsed three times with DMEM and fed with DMEM containing G-5 supplement and 50 ng/ml tri-iodothyronine (T3). T3 was added to increase proliferation and differentiation of OLG progenitors. Cells were maintained at 37°C with 5% CO_2 until they reached confluency

(~10 days). For immunostaining cells were plated onto 13 mm diameter coverslips at a density of ~1 × 10^4 cells per coverslip in DMEM with 10% FCS. After 24 hours the cells were rinsed three times with DMEM and the medium was changed to DMEM containing G-5 supplement and 50ng/ml tri-iodothyronine (T3). To determine the purity of OLG cultures cells were immunostained with monoclonal mouse anti-myelin/oligodendrocyte specific protein (MAB328) diluted 1:100 (Chemicon). Cells were counterstained with 0.01% Nuclear Yellow (Sigma, Cat. No. N-2137). Oligodendrocytes were estimated to be 98% pure on the basis of MAB328 staining (Fig. 2.3).

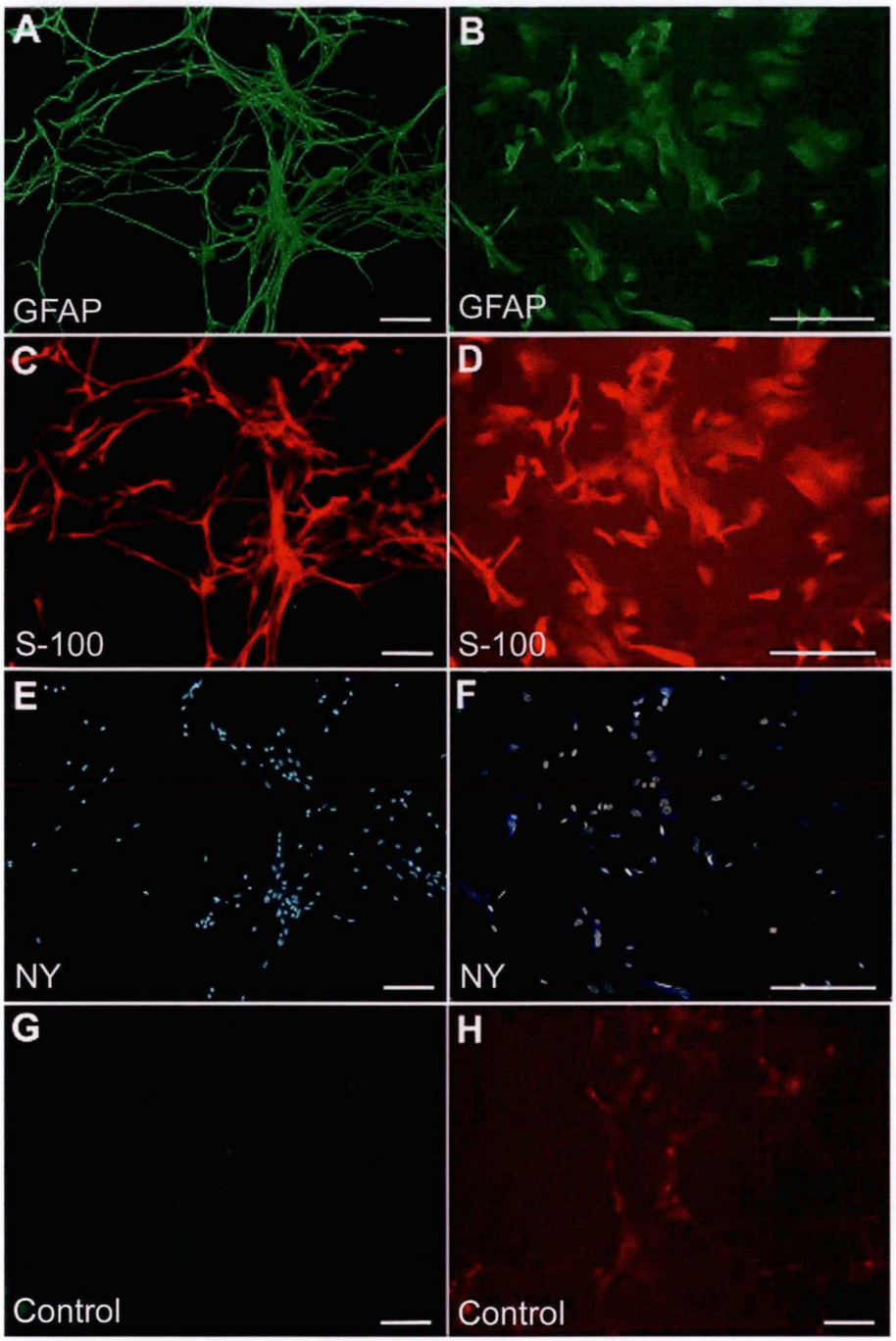

FIGURE 2.2. Immunofluorescence for GFAP in astrocytes (ASTs).

Immunostaining of ASTs maintained in DMEM with G-5 supplement (left) and DMEM with 10% FCS (right). Cultures were estimated to be 92% GFAP positive (A, B) and 97% S-100 positive (C, D). Cells were counterstained with Nuclear Yellow (E, F). Controls in which the primary antibody was omitted were negative (G, H). Scale bars, 100μm.

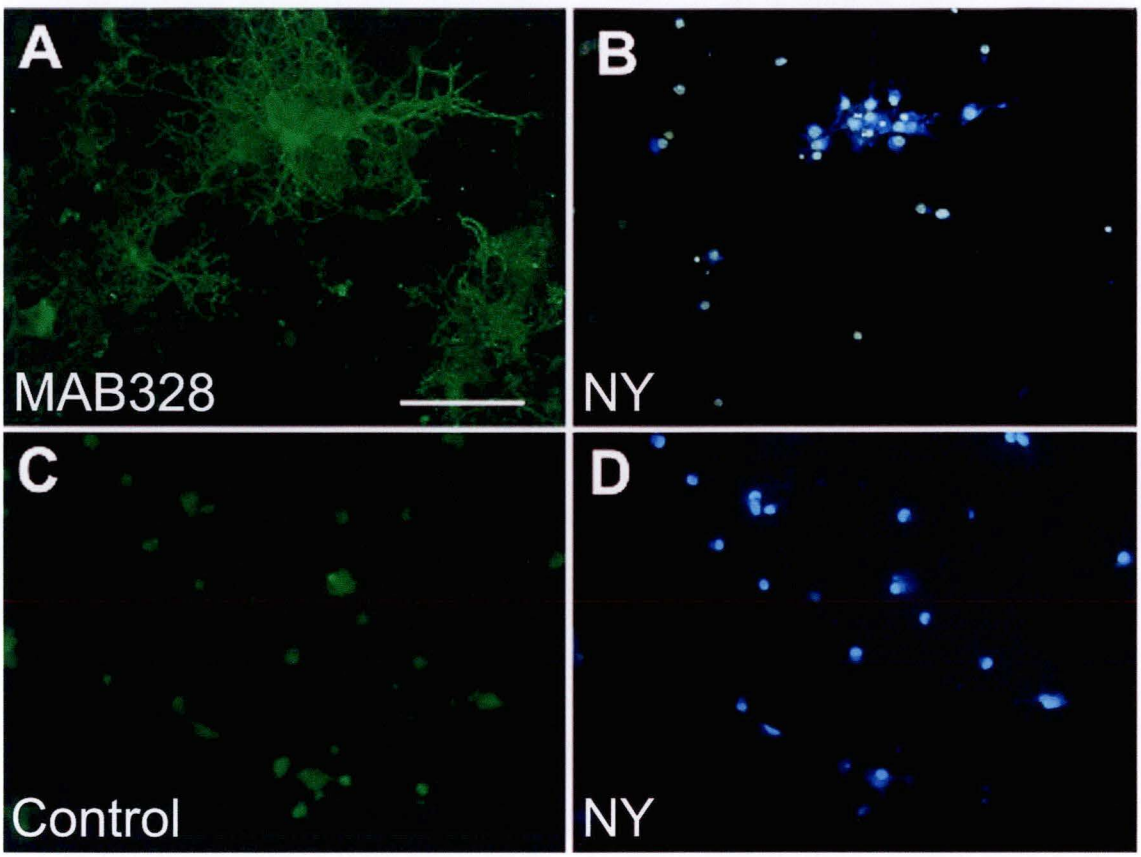

FIGURE 2.3. Immunofluorescence for MAB328 in cultured oligodendrocytes (OLGs).

Immunostaining of OLGs maintained in DMEM with G-5 supplement and 50ng/ml T3 for the myelin associated marker MAB328. Cultures were estimated to be 98% MAB328 positive (A). Cells were counterstained with Nuclear Yellow (B). Controls where the primary antibody was omitted showed negative staining (C, D). Scale bars, 100μm.

2.1.3. Fibroblast Culture

Explant cultures of fibroblasts were prepared using skin dissected from the back of two day-old hooded Wistar rat pups. A $1cm^2$ slice of skin was placed into a petri dish containing warmed 0.1M phosphate buffered saline pH7.4 (PBS) and cut into small pieces. Explants of approximately $2mm^2$ were placed into a $50cm^2$ dish and maintained in DMEM (Sigma) containing 10% FCS, 200mM L-glutamine and 1% penicillin-streptomycin-fungizone solution. After about 7 days cells were passaged using 0.25% trypsin/EDTA solution and centrifuged at 250×g for 10 minutes. The pellet was resuspended in 20ml medium and distributed into two $75cm^2$ flasks. Cells were incubated at 37°C with 5% CO_2 and grown to-confluency.

2.2. Immunohistochemistry and Cell Purity

2.2.1. Immunostaining Procedure

Cells on 13mm diameter coverslips were fixed with 4% paraformaldehyde for 15 minutes at room temperature. After washing three times in PBS the cells were incubated with the appropriate primary antibodies diluted 1:100 in PBS containing 1% normal goat serum (NGS) overnight at 4°C. To provide negative controls cells were incubated with 1% NGS without primary antibody. Cells were rinsed three times and incubated with the appropriate secondary antibodies diluted 1:1000 in PBS containing 1% NGS for 1 hour at room temperature. Cells were counterstained with 0.01% Nuclear Yellow and mounted with DAKO® Fluorescent Mounting Medium. Staining was then examined by fluorescent microscopy using an Olympus BX50 microscope with the appropriate filters for the

fluorochromes conjugated to the secondary antibodies. Cells were imaged using the Olympus DP50 digital camera.

2.2.2. Cell Counts

All positive cells were scored at 200× magnification using the appropriate fluorescent filter for the fluorochromes conjugated to the secondary antibodies. The total number of cells per field of view was determined by counting the Nuclear Yellow positive cells. Coverslips were scanned and ten adjacent fields per coverslip were counted. The cell-labelling index was determined using the following equation:

$$\text{Cell-labelling index (\%)} = (\#\text{ Specific antigen positive cells} \div \#\text{ Nuclear yellow positive cells}) \times 100\%$$

2.3. Rat Brain Tissue Procurement

Neonatal 1-2 day-old Hooded Wistar rat pups were sacrificed and their heads were removed. The cranium was dissected so as the whole brain could be retrieved. The meninges, olfactory bulbs and brainstem were removed and the remaining tissue was snap frozen in liquid nitrogen and stored at -80°C to be used for RNA extraction.

2.4. Total RNA Isolation and Quantitation

2.4.1. RNA Isolation

2.4.1.1. Monolayered Cells

Total RNA was isolated from all cultured cells using TRIzol Reagent according to the manufacturer's instructions (Life Technologies, Cat. No. 15596-026). To each culture flask, 10ml of TRIzol per 10cm^2 of flask area was added. Cells were detached from the flask using a cell scraper and allowed to sit for 2-3 minutes. The supernatant was then pipetted over the surface of the flask several times before being transferred to a corex tube. The sample was then incubated for 5 minutes at room temperature. To each sample 0.2ml of chloroform per 1ml of TRIzol was added. Tubes were then shaken vigorously for 15 seconds and incubated at room temperature for a further 2-3 minutes. Samples were centrifuged at 12 000×g for 15 minutes at 4°C in a Sorvall RC5C (DuPont). The aqueous phase was then transferred to a new corex tube. To precipitate the RNA 0.5ml of isopropyl alcohol was added per 1ml of initial TRIzol volume. Samples were incubated at room temperature for 10 minutes and centrifuged at 12 000×g for 10 minutes at 4°C. The pellet was rinsed with 75% ethanol and centrifuged at 7 500×g for 5 minutes at 4°C. RNA samples were vacuum-dried for 5 minutes and redissolved in 20µl RNase-free water.

2.4.1.2. Encapsulated Cells

RNA was extracted from encapsulated cells by a modification of the TRIzol technique described in section 2.4.1.1. Capsules were placed in an eppendorf tube containing 800µl of TRIzol reagent. To ensure that the cells were adequately exposed to the reagent capsules were minced and the solution triturated. Following 5 minutes incubation at room temperature 160µl of chloroform was added to each sample. The samples were shaken vigorously for 15 seconds and centrifuged at 12 000×g for 15 minutes at 4°C. The supernatant was removed and placed into another eppendorf tube. To improve the yield of RNA from the capsules 10µg of RNase-free glycogen (Life Technologies, Cat. No. 10814-010) was added to each sample to carry the RNA to the aqueous phase. To precipitate the RNA 400µl of isopropylalcohol was added to the supernatant and samples were incubated for 10 minutes at room temperature. Samples were then centrifuged at 7 500×g for 5 minutes at 4°C, vacuum-dried for 5 minutes and redissolved in 10µl of RNase-free water.

2.4.1.3. Rat Brain Tissue

Total RNA from whole rat brain tissue was extracted using the RNeasy maxi kit (Qiagen). Approximately 0.25g of tissue per extraction was crushed in liquid nitrogen and homogenized in extraction buffer using an ultra-turrax. The homogenate was then applied to an RNeasy maxi-column and processed according to the manufacturer's protocol. RNA was eluted from the column in 100µl of RNase-free water and stored at -80°C.

2.4.2. DNase-1 Treatment

RNA samples were pretreated with DNase-1 (Sigma) to remove any genomic DNA contamination. For each sample a separate tube containing the following reaction components was prepared.

- 1µg RNA sample
- 8µl RNase-free water
- 1µl 10× Reaction buffer
- 1µl Amplification grade DNase-1 (1U/µl)

After 15 minutes incubation at room temperature 1µl of stop solution was added to each sample and tubes were heated to 70°C for 10 minutes. Treated samples were stored at -80°C.

2.4.3. RNA Quantitation and Purity

A 1µl aliquot of each total RNA sample was resuspended in 40µl of water, mixed and quantified spectrophotometrically at A_{260}. Measurements of RNA purity were determined in TE buffer in the same manner using the A_{260}/A_{280} ratio. Samples with ratios of 1.8-2.1 were considered pure.

2.5. Media and Solutions

All media and solutions for tissue culture were sterilised via a 0.22µm bottle top filtration system (Millipore).

2.5.1. Cell Culture

Dulbecco's Modified Eagle Medium (DMEM)

Contents of sachet 13.4g (Sigma, Cat. No. 12100-046) plus 3.7g $NaHCO_3$ (Sigma, Cat.No. 5-5761) made up to one litre with distilled water (pH 7.2).

DMEM with G-5 Supplement

1ml G-5 supplement (Life Technologies, Cat. No. 17503-012)

1ml penicillin-streptomycin-fungizone solution (CSL, Cat. No. 09291501)

Made up to 100ml with DMEM (Sigma, Cat. No. 12100-046).

Minimum Essential Eagle Medium D-valine Modification (MEM D-valine)

Contents of one vial 9.6g (Sigma, Cat. No. M7395) plus 2.2g $NaHCO_3$ (Sigma, Cat. No. 5-5761) made up to one litre with distilled water (pH 7.2) and filtered.

MEM D-valine with 10% dialysed Fetal Calf Serum (dFCS)

1ml of penicillin-streptomycin-fungizone solution (CSL, Cat. No. 09291501)

10ml dFCS (Sigma, Cat. No.)

Made up to 100ml with MEM D-valine (Sigma, Cat. No. M7395).

Hanks Balanced Salt Solution (HBSS)

Contents of one vial 9.5g (Sigma, Cat. No. H-2387) plus 0.35g $NaHCO_3$ (Sigma, Cat. No. 5-5761) made up to one litre with distilled water (pH 7.2).

Minimum Essential Eagle Medium Hepes modification (MEM-H)

Contents of one vial (Sigma, Cat. No. M-2645) plus 2.2g $NaHCO_3$ (Sigma, Cat. No. 5-5761) made up to one litre with distilled water (pH 7.2).

Dulbeccos Modfied Eagle Medium/F-12 Modification (DMEM/F-12)

Contents of one sachet 15.6g (Life Technologies, Cat. No. 12400-024) plus 1.2g $NaHCO_3$ (Sigma, Cat. No. 5-5761) made up to one litre with distilled water (pH 7.2).

DMEM/F-12 with 10% FCS

10ml FCS (Life Technologies, Cat No.)

1ml penicillin-streptomycin-fungizone solution (CSL, Cat. No. 09291501)

Made up to 100ml with DMEM/F-12 (Life Technologies, Cat. No. 12400-024).

Neurobasal with B-27 Supplement

0.1ml B-27 supplement (Life Technologies, Cat. No. 1704-044) made up to 10ml in Neurobasal medium (Life Technologies, Cat. No. 21103-049).

0.09% Trypsin and 0.25% Collagenase Solution

0.009g trypsin (Life Technologies, Cat. No. 27250-042)

0.025g collagenase (Sigma, Cat. No. C-9891)

Made up to 10ml with MEM-H (Sigma, Cat. No. M-2645)

0.25% Trypsin Solution

0.025g trypsin (Life Technologies, Cat. No. 27250-042) in 10ml MEM-H (Sigma, Cat. No. M-2645).

2.5% Trypsin Solution

0.25g trypsin (Life Technologies, Cat. No. 27250-042) in 10ml PBS

Bovine Pituitary Extract (BPE)

Contents of one vial 5mg (Sigma) in 1ml HBSS (Sigma, Cat. No. H-2387) to give a concentration of 5mg/ml divided into 10× aliquots of 100µl and frozen at -20°C.

2.5.2. Solutions

2.5.2.1. RNA Extraction and RT-PCR

TE Buffer (10mM Tris-HCl; 1mM EDTA)

1ml tris-HCl (pH7.4) (Sigma, Cat. No. T-3253)

0.2ml 0.5M EDTA (BDH Analar)

Made up to 100ml in distilled water and filtered.

10× TBE Buffer (1M Tris-base; 1M boric acid; 20mM EDTA)

Dissolve 121g Tris-base (Sigma, Cat. No. T-6791), 61.7g boric acid (Sigma, Cat. No. B-6768) and 7.44g EDTA (BDH Analar) in 800ml of distilled water (pH 8.0) and make up to one litre.

1.5% Agarose

1.5g agarose powder (Life Technologies, Cat. No. 15510-027) in 100ml 1× TBE buffer.

2.5.2.2. Scanning Electron Microscopy

0.1M Phosphate Buffer (pH 7.2)

68.4ml 1M Na_2HPO_4 (Univar)

31.6ml 1M $NaH_2PO_4.2H_2O$ (Univar)

Made up to one litre with distilled water.

1M Na_2HPO_4

14.2g Na_2HPO_4 (Univar) in 100ml distilled water

1M $NaH_2PO_4.2H_2O$

15.6g $NaH_2PO4.2H_2O$ (Univar) in 100ml distilled water

2.5% Phosphate Buffered Glutaraldehyde

1.0ml of 25% glutaraldehyde diluted in 9ml of 0.1M phosphate buffer (pH 7.2).

0.1% Phosphate Buffered Osmium Tetroxide

0.5ml of 2.0% osmium tetroxide diluted in 9.5ml of 0.1M phosphate buffer (pH 7.2).

2.5.2.3. Immunocytochemistry

10× Saline

90g NaCl (BDH Analar) in one litre of distilled water.

0.1M $NaH_2PO_4.2H_2O$

31.2g $NaH_2PO_4.2H_2O$ (Univar) in one litre of distilled water.

0.1M Na_2HPO_4

28.4g Na_2HPO_4 (Univar) in one litre of distilled water.

0.01M Phosphate Buffered Saline (PBS)

100ml saline (10×)

10ml $NaH_2PO_4.2H_2O$ (Univar)

10ml Na_2HPO_4 (Univar)

Made up to one litre with distilled water.

4% Paraformaldehyde in PBS

4.0g paraformaldehyde (Sigma, Cat. No. P6148) in 100ml of 0.01M PBS.

CHAPTER THREE

Characterisation of Encapsulated Olfactory Ensheathing Cells

3.1. Introduction

Olfactory ensheathing cells are an extremely plastic cell type both in terms of their morphology and antigenic profile. *In vitro* OECs exist as flattened or spindly forms that closely resemble central ASTs and peripheral SCs respectively. Some authors regard these morphologically distinct groups as two sub-populations, those with AST-like properties and those with SC-like properties (Barber and Lindsay, 1982; Pixley, 1992; Franceschini and Barnett, 1996). Astrocyte-like OECs are identified by their flat angular appearance and fibrous GFAP expression while the SC-like OECs are spindly process-bearing cells that are immunopositive for $p75^{NTR}$, S-100 and diffusely positive for GFAP (Barber and Lindsay, 1982; Pixley, 1992; Franceschini and Barnett, 1996; Li et al., 1998; Sonigra et al., 1999; Alexander et al., 2002). Yet a definitive distinction between these two groups is difficult to make since cells with characteristics of both populations are not uncommon. In fact OECs have the capacity to switch between the two morphological profiles depending upon the composition of the media they are grown in (Pixley, 1992; Chuah and Teague, 1999; Vincent et al., 2003). A recent report also suggests that this morphological switch is regulated by cAMP and endothelin-1 (a serum component) *in vitro* (Vincent et al., 2003). Taken together these results strongly suggest that OECs belong to a single phenotypically plastic population rather than two distinct sub-populations.

It appears that phenotypic heterogeneity is not restricted to OECs *in vitro*. For example OECs of the OB were found to differentially express Sema3A whereby only $p75^{NTR}$ positive OECs in the outer ONL not the inner ONL were Sema3A positive (Schwarting et al., 2000). Similarly $p75^{NTR}$ positive OECs were found to be restricted to the outer ONL, neuropeptide Y positive OECs were located in the inner ONL and GFAP positive OECs were restricted to the inner ONL (Au et al., 2002). Ultrastructural studies have also demonstrated a degree of heterogeneity in OECs *in vivo*. Rather than being uniformly distributed throughout the ONL the association of OECs with axon bundles was orderly in the outer ONL but less so in the inner ONL.

In recent years many studies have shown that OECs can promote the growth of injured axons (Ramon-Cueto et al., 1998), enhance remyelination (Franklin et al., 1996; Kato et al., 2000; Lakatos et al., 2003) and help restore functional connections between injured axons and their targets (Ramon-Cueto et al., 2000; Verdu et al., 2003). Although it is clear that OECs produce many neurotrophic factors (Boruch et al., 2001; Wewetzer et al., 2001; Woodhall et al., 2001) and cell adhesion molecules (Miragall et al., 1988; Pixley, 1992; Ramon-Cueto and Nieto-Sampedro, 1992; Doucette, 1996; Franceschini and Barnett, 1996; Kafitz and Greer, 1999; Barnett et al., 2000) that may play a role in their growth promoting activity there has been little progress toward our understanding of regenerative OEC biology. Since OECs exhibit different phenotypic characteristics depending upon culture conditions (Franceschini and Barnett, 1996) it is possible that the lesion environment induces OECs to exhibit characteristics associated with their role in regeneration. Similarly any changes in OEC phenotype brought about by exposure to the injury site could affect cell behaviour.

Olfactory ensheathing cells are migratory and can travel substantial distances from the lesion site after implantation into the injured spinal cord (Ramon-Cueto and Avila, 1998; Ramon-Cueto et al., 1998; Ramon-Cueto et al., 2000). In these studies *in vivo* migration of OECs was examined by light microscopy of cells tagged with a fluorescent label. However the disadvantage of this technique is that the fluorescent label can be picked up by surrounding cells if the labelled cells die and/or can be diluted if the cells undergo proliferation (Chuah et al., 2004). OECs have been reported to enhance regeneration by migrating toward the injury site *in vivo*, suggesting that they can respond to signals from injured neurons (Boruch et al., 2001). In contrast after transection of the medial longitudinal fasciculus OECs were shown to migrate away from the lesion site and therefore failed to promote axon regeneration (Gudino-Cabrera et al., 2000). Hence migration could play a role in the growth promoting activity of OECs.

In this study OECs were immobilized within semi-permeable polymer tubes prior to implantation into the injured spinal cord. Since the direct cellular contacts normally established by implanted OECs are abolished by encapsulation this technique examines the potential impact of soluble factors generated by the injured spinal cord on the phenotypic heterogeneity of OECs. It is hypothesised that (1) encapsulated cells will adopt a different morphological phenotype in the presence of injured spinal cord tissue and (2) encapsulated OECs will survive in the injured spinal cord environment.

3.2. Materials and Methods

3.2.1. Cell Culture

Olfactory ensheathing cell cultures were prepared and characterised as described in section 2.1.1.

3.2.2. Preparation of OECs for Implantation

Preliminary experiments were peformed to investigate the behaviour of OECs plated onto matrigel *in vitro*. Observations made over the course of one week showed that OECs differentiate and elaborate processes on matrigel in a similar way to that normally seen *in vitro*.

Upon reaching confluency OEC cultures were encapsulated into porous polymer tubing prior to implantation into the injured spinal cord. Cells to be placed in capsules were removed from the culture flasks by trypsinisation. Flasks were rinsed with HBSS three times before 0.25% trypsin was added. The reaction was stopped by addition of MEM D-valine containing 10% dFCS. The cell suspension was then centrifuged at 500×g for 10 minutes. Supernatant was removed and the cell pellet containing ~2 × 10^5 cells ~5µl was resuspended 1:1 with 5µl of growth factor reduced MATRIGEL® Matrix (Becton Dickenson). An aliquot of suspension containing ~3 × 10^4 cells on average was injected into each open-ended polymer tube (Bio/Por® Type F PVDF Hollow Fibre, molecular weight cut off or MWCO of 300 000) 6-8mm in length (Becton Dickenson). Tubes were heat sealed at both ends to create closed capsules. OEC-filled capsules were then implanted into the injured spinal cords of adult male hooded Wistar rats. Control

OEC-filled capsules were placed in a petri-dish containing MEM D-valine supplemented with 10% dFCS and incubated at 37°C for one week in a 5% CO_2/air incubator during which time three media changes were performed.

3.2.3. Spinal Surgery

Lesions to the corticospinal tracts (CST) of 18 adult male hooded Wistar rats (300-350g) were performed under isoflurane anaesthesia maintained at 1.5-2.5% with 100% O_2 (flow rate of 0.5L/min). The skin overlying the spinous processes of T5-T10 was incised and the underlying muscles were dissected and retracted. The spinous processes T7 and T8 were removed along with the lamina to expose the dorsal surface of the spinal cord. Fine micro-dissection scissors were used to make a transverse cut across one half of the dorsum of the spinal cord (unilateral). After lesioning the cord a capsule containing OECs was placed on top of the lesion under the dura (Fig. 3.1). The overlying muscle was sutured and the skin closed with wound clips. After surgery animals were returned to their cages and kept under a heat lamp until they were fully awake. The analgesic Carprofen (Pfizer) (5mg/kg) was given intraperitonealy for the following two days. One week after surgery rats were sacrificed by CO_2 inhalation and the capsules removed. Capsules were rinsed in 0.1M phosphate buffer pH 7.2 and snap frozen in liquid nitrogen and stored at -80°C or processed immediately for SEM analysis.

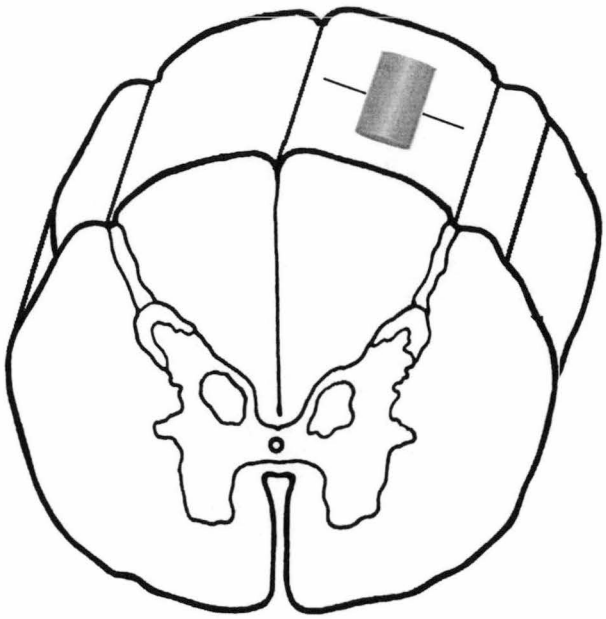

FIGURE 3.1. Schematic representation of capsule placement in the lesioned rat spinal cord.

Diagram showing a section of thoracic spinal cord with an OEC-filled capsule (grey) lying parallel to the length of the spinal cord above the lesion site.

3.2.4. Scanning Electron Microscopy

Capsules (three implanted and three unimplanted) were fixed in 2.5% phosphate buffered glutaraldehyde for 20 minutes at room temperature. They were then rinsed three times for 5 minutes each in PBS and post-fixed in 0.1% phosphate buffered osmium tetroxide (OsO_4) for 15 minutes at room temperature. The capsules were rinsed again in PBS for 3 × 5 minutes before being dehydrated in 50% and 70% ethanol for 5 minutes respectively. At this point the sealed ends of the capsules were removed and the remaining cylinder was cut in half longitudinally using the point of a 25G needle. The capsule halves were dehydrated through an ascending series of ethanol baths (80, 90, 95 and 100%) 10 minutes per incubation with three incubations in 100% ethanol. They were then critically point dried, sputter coated with gold (Balzers) and examined using a JEOL JSM-840 Scanning Electron Microscope.

3.2.6. Total Cell Number Assay

Quantitation of total cell number in each capsule was achieved using the CytoTox 96® Non-Radioactive Cytotoxicity Assay kit (Promega) to measure lactate dehydrogenase (LDH) activity. A linear standard curve was produced in which the absorbance generated by known numbers of free OECs was measured spectrophotometrically and plotted against cell number. To create the standard curve a dilution series of free OECs ranging from 0 - 3 × 10^4 cells per well (increasing in increments of 5000 cells) was prepared. As LDH is present in FCS the cells were maintained in 200µl of Neurobasal medium containing B-27 supplement (Life Technologies). Culture medium without cells was included as a background control for the standard curve. After overnight incubation at 37°C the cells were frozen at -80°C.

Eight capsules were loaded with matrigel containing 2.5×10^4 cells as described in section 3.2.2. As a background control some capsules were loaded with matrigel alone. All capsules were maintained in MEM D-valine containing 10% dFCS until the day of analysis when they were transferred into 200µl of Neurobasal (Life Technologies) containing B-27 supplement. The capsules (two per time-point) were analysed on day zero, four and seven post encapsulation, where day zero was the day the capsules were prepared. To analyse LDH activity cells were lysed by freeze/thaw treatment and by incubation with lysis buffer for 30 minutes at 37°C. Capsules were minced with vannas scissors to ensure that the lysis buffer could penetrate the cells. LDH activity in the supernatant collected from the lysed cells was performed using the assay kit described above, in accordance with the manufacturer's instructions. The amount of reaction product was measured at 492nm using a Titertek®Plus MS212 plate reader. Absorbance readings of the background controls were subtracted from the sample absorbance readings and the total cell number in each capsule was calculated using the equation ($y = 1.18341(x) + 0.2646$) to the standard curve line (Fig. 3.4A).

3.3. Results

3.3.3. Morphological Changes in OECs after Implantation into the Lesioned Spinal Cord

3.3.3.1. Implanted OEC-filled Capsules

To determine if there were any morphological changes in OECs following implantation into the injured spinal cord OEC-filled capsules were examined using SEM (Fig. 3.2). Capsules were cut into halves so as the inner surfaces could be viewed although this released some of the contents of the capsules (Fig. 3.2A). Observations of the cut edge of the capsule revealed the presence of a thick extracellular matrix (ECM) like layer deposited on the inner surface of the capsules (Fig. 3.2B). Higher magnification of the capsule contents indicated the presence of small (less than 1μm) round depositions or secretory droplets (Fig. 3.2C). There was also evidence of what appeared to be clotting factors such as fibrin threads and red blood cells (Fig. 3.2D). No cells were seen lodged in the pores of the capsules. A number of larger cells with a rounded morphology were also observed. These were presumed to be OECs - despite their uncharacteristic morphology - on the basis of their size (~10μm) and the similarity between these cells and some of their *in vitro* counterparts (Fig. 3.2E and F). In some cases the rounded cells were surrounded and therefore obscured by the heavy ECM making it difficult to examine their morphology.

3.3.3.2. OEC-filled Capsules In Vitro

In contrast to the implanted capsules the inner surface of the capsules maintained *in vitro* appeared to be devoid of cells (Fig. 3.3A). Similarly the cut edge of the control capsules lacked the abundant ECM observed in the implanted capsules (Fig. 3.3B). Close inspection of the inner surface of the cultured capsules revealed the presence of a small number of cells with characteristic OEC-like morphology (Fig. 3.3C, D, E and F). These cells were ~10μm in diameter and were flattened bipolar or multipolar in shape. However there were also some rounded cells (as described in section 3.3.3.1), secretory depositions (Fig. 3.3D, E and F) and a small amount of ECM (Fig. 3.3E and F). In comparison to the implanted capsules there appeared to be fewer cells.

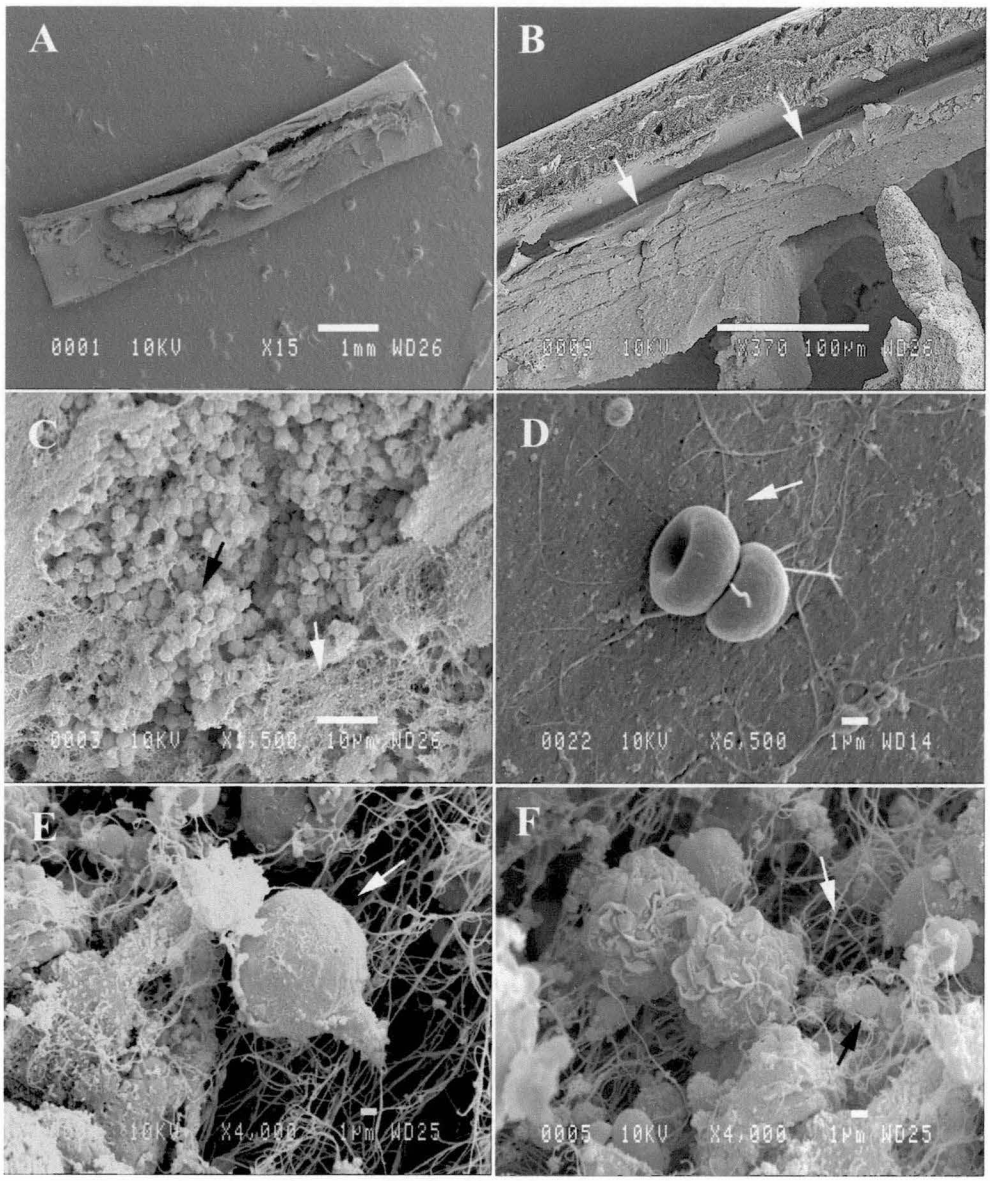

FIGURE 3.2. Scanning electron micrographs of implanted encapsulated olfactory ensheathing cells (OECs).

Encapsulated OECs were implanted into the injured rat spinal cord for one week. (A) Capsules were removed from the animals, cut into halves and examined by scanning electron microscopy. (B) The cut edge showed a thick layer of extracellular matrix deposited on the inner surface of the capsule. (C) Higher magnification of the capsule contents showed evidence of secretory droplets (black arrow) and fibrin threads (white arrow). (D) Red blood cells were also present. (E) OECs with rounded morphology were frequently surrounded by (F) fibrin threads (white arrow) and secretory depositions (black arrow).

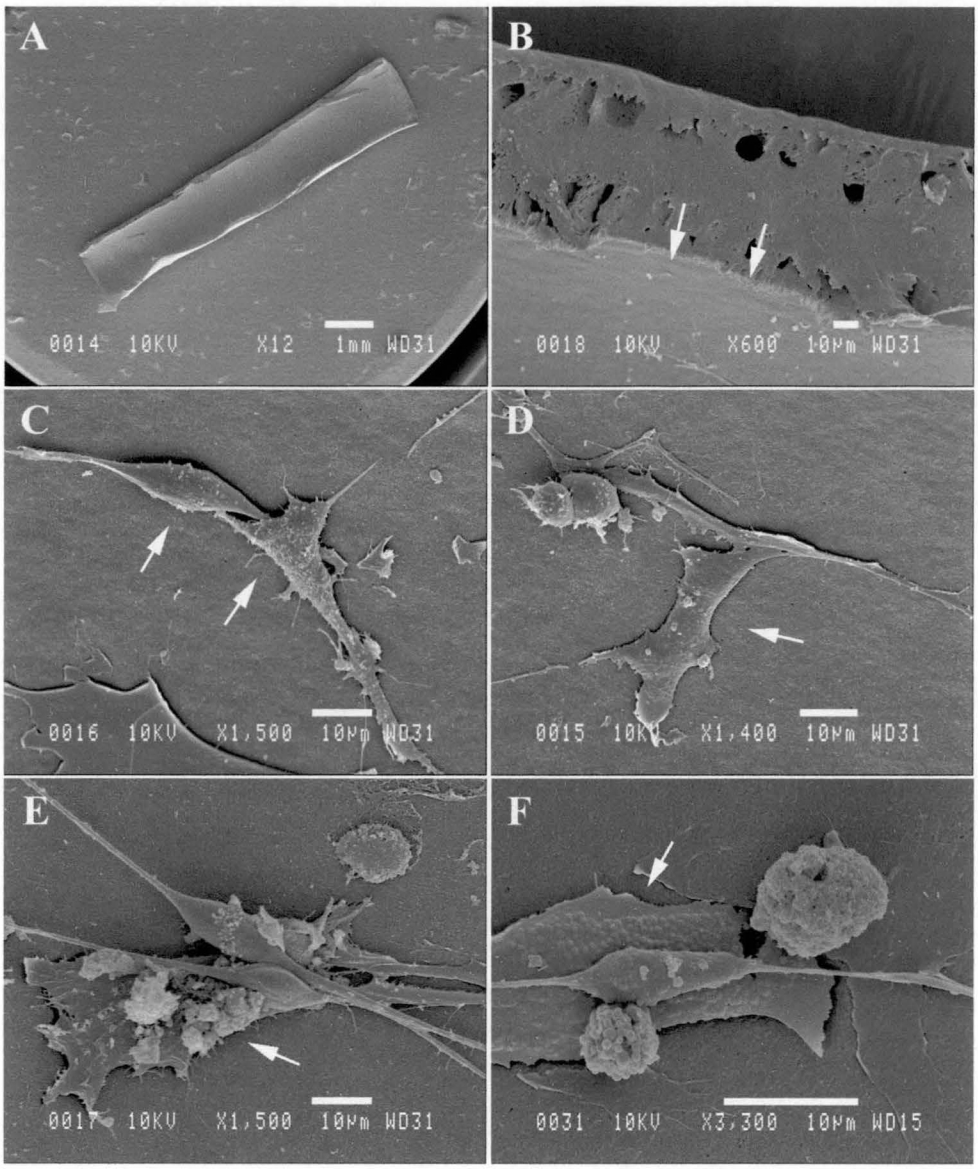

FIGURE 3.3. Scanning electron micrographs of cultured encapsulated olfactory ensheathing cells (OECs).

Encapsulated OECs were maintained in MEM D-valine with 10% FCS at 37°C, 5% CO_2 for one week. (A) Capsules were cut into halves and examined by scanning electron microscopy. (B) The cut edge of the capsule showed a lack of robust extracellular matrix deposition. (C, D) High magnification of the inner capsule surface showed evidence of OECs with tissue culture-like morphology (arrows), (E) secretory droplets (arrows) and a small amount of (F) extracellular matrix (arrows).

3.3.5. OEC Survival after Encapsulation

To determine if encapsulation affected the viability of OECs the total number of viable cells present per capsule was measured over time. In this assay cell number was determined at day zero (or the point of encapsulation), then at four and seven days *in vitro*. On day zero $1.14 \times 10^4 \pm 3.15 \times 10^2$ cells were present in the capsules. After four days within the capsules 41% of these cells remained viable (ie. $4.71 \times 10^3 \pm 1.27 \times 10^2$ cells) (Fig. 3.4B). At day seven the decline in cell number had ceased and the population remained stable (ie. $4.97 \times 10^3 \pm 1.67 \times 10^2$ cells remaining).

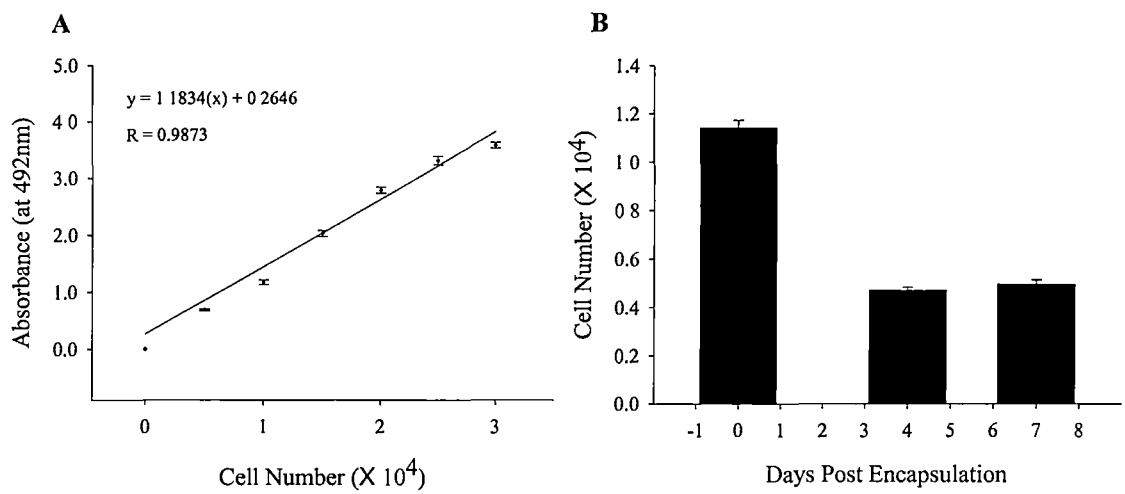

FIGURE 3.4. The effect of encapsulation on olfactory ensheathing cell (OEC) survival over time in culture.

OEC survival was determined by measuring the total viable cell number at the time of encapsulation (day zero) and then after four and seven days in culture at 37°C, 5% CO_2 in serum-free medium. (A) The standard curve from which the total viable cell number was extrapolated for each time-point. (B) Graph showing the number of viable cells per capsule over time in culture.

3.4. Discussion

This study investigated the response of OECs to soluble factors present within the injured spinal cord. The results of this report suggest that OEC morphology may change after implantation into the injured spinal cord with respect to that seen *in vitro*. After implantation most encapsulated OECs displayed what appeared to be a rounded morphology and produced abundant ECM. A small number of cells with tissue culture-like morphology may also have been present. In fact such cells would have been attached to the inner surface of the capsules and were potentially obscured by the ECM. Similarly the rounded cells may also have had processes that were obscured by debris.

In contrast, a majority of encapsulated OECs maintained *in vitro* displayed a bipolar or multipolar morphology and secreted moderate amounts of ECM. Yet there were also a small number of rounded cells in the *in vitro* capsules similar to those seen after implantation. It was also noteworthy that very few cells remained adherent to the walls of capsules maintained *in vitro*. The low numbers of cells combined with the fact that large cell clusters were seen floating in solution after the capsules were dissected for processing could indicate that they were loosely attached to the capsule due to a lack of ECM to bind them.

It was also notable that the debris within the implanted OEC-filled capsules contained red blood cells although white blood cells and other inflammatory cells may have been present but not identified. A possible explanation for this could be that the cells migrated through the pores in the polymer capsule. But the fact that no cells were seen lodged in the pores of the capsules could indicate that only a limited number of cells migrated in.

To determine whether cells from the spinal cord were migrating into the capsules real-time RT-PCR for the housekeeping gene GAPDH was performed on three empty capsules that were implanted into the injured spinal cord. Approximately 200pg of GAPDH was detected per capsule on average. Since an average of ~4000pg of GAPDH was detected per implanted OEC-filled capsule contaminating cells could have contributed to ~5% of the total GAPDH levels in the implanted OEC-filled capsules. Therefore the fact that only a small amount of GAPDH mRNA was detected supports the notion that only a small number of cells migrated into the capsules. In addition when OEC-filled capsules were maintained *in vitro* no cells were found to migrate out of the capsules into the culture dish. Therefore any loss of OECs from the capsules may be more likely to have occurred during processing as described earlier.

Since it was difficult to positively identify OECs in the implanted capsules by SEM alone attempts were made to pre-label the cells with Hoescht dye prior to encapsulation and to immunostain for specific antigens after implantation. However these techniques were unsuccessful mainly due to the difficulties experienced in sectioning the capsules for microscopy. More specifically the capsule polymer was difficult to cut using conventional techniques and the cells inside the capsules were not attached to the polymer firmly enough to withstand the rigors of processing. If sectioning were possible OECs could have been identified by immunostaining for $p75^{NTR}$, GFAP and S-100 or by pre-labeling as mentioned. The fact that the antigenic profile of OECs is variable suggests that a battery of antigens may be required. Furthermore it would also have been possible to confirm the presence or absence of contaminating cells such as lymphocytes, macrophages and fibroblasts by immunostaining for specific antigens such as CD3 on T-

lymphocytes, CD21 on B-lymphocytes, ED-1 on macrophages and Thy 1.1 on fibroblasts.

If in fact injury-associated soluble factors in the spinal cord do induce morphological change in OECs the mechanism for this change is unclear. However a recent study proposed that morphological plasticity in OECs is regulated by a RhoA dependent mechanism (Vincent et al., 2003). The authors theorise that the RhoA signalling cascade regulates organization of the actin cytoskeleton in OECs in a similar manner to that described for ASTs (Suidan et al., 1997; Safavi-Abbasi et al., 2001). By analogy it is possible that factors intrinsic to the CNS injury environment trigger RhoA and induce morphological plasticity in implanted OECs. Since the CNS lesion environment is extremely complex there could be an array of inflammatory molecules that influence the state of RhoA and therefore affect OEC morphology (see review by Baeryre and Schwab, 2003).

The cell survival assay revealed that the number of viable encapsulated OECs declined between initial encapsulation and four days *in vitro* after which the population number remained stable but did not increase. The decline in cell number could either represent cell death or a transition by these cells into a state of senescence or "arrested" proliferation. A clearer picture may be obtained by performing the same experiment with an equal number of free OECs for comparison with the encapsulated cells. If the population number of free OECs declined at the same rate as the encapsulated cells it could suggest that encapsulation does not affect survival/proliferation, whilst a less rapid decline in free OECs may indicate that encapsulation has a direct effect on cell survival/proliferation. However the effect of cell density per capsule on cell survival was

not investigated. It is possible that a higher density of OECs per capsule could improve survival rate since OECs produce growth/survival factors that act in an autocrine manner (Chuah and Teague, 1999; Chuah et al., 2000; Woodhall et al., 2001).

The proliferative state of encapsulated OECs compared with free OECs could be investigated further by western blot analsysis of cell cycle proteins involved in growth arrest. In a previous study it was found that astrocyte conditioned medium (ACM) although moderately mitogenic for OECs blocks their long-term proliferation (Alexander et al., 2002). This growth arrest response was accompanied by an upregulation of the cyclin dependent kinase inhibitors p16 and p27 known to be involved in triggering growth arrest in rodent cells (Alexander et al., 2002). Similarly switching OECs from ACM into serum- or growth factor-supplemented medium not only reversed proliferation arrest but also downregulated p16 and p27 expression. In light of their role in OEC proliferation *in vitro* these and other cell cycle proteins could potentially be involved in the cessation of growth in encapsulated OECs.

If encapsulation decreases OEC viability and/or proliferation these cells could benefit from the addition of mitogens and survival factors prior to implantation into the injured spinal cord. Candidate molecules for this application could include, members of the neuregulin family such as heregulin (HRG) and glial growth factor (GGF) or fibroblast growth factor 2 (FGF-2), platelet derived growth factor (PDGF), insulin-like growth factor 1 (IGF-1) and forskolin (FSK) which when used alone or in combination can enhance proliferation and survival of OECs *in vitro* (Chuah and Teague, 1999; Pollock et al., 1999; Chuah et al., 2000; Yan et al., 2001b; Alexander et al., 2002). In fact a previous study showed that growth arrested OECs could proliferate after addition of

FSK/FGF-2, FSK/HRG-β1, FSK/GGF-2 and HRG-β1/FGF-2 diluted in ACM (Alexander et al., 2002).

Although this study used a single technique to examine OEC morphology in the CNS injury environment the preliminary results are promising. The major limitation imposed by the use of SEM in this instance is that it cannot definitively characterise cell types. Hence the identity of OECs is based solely on their distinct morphological characteristics, which were sometimes difficult to define due to the heavy ECM deposits. This was further hampered by the fact that contaminating cells such as red blood cells were found within the capsules and the presence of others cannot be ruled out. Given this further investigation will be necessary to characterise the OECs, determine the identity of contaminating cells and to confirm the morphological changes observed. Immunohistochemistry for antigens such as $p75^{NTR}$, GFAP, N-CAM and S-100 could help to characterise the OECs. Similarly contaminating inflammatory cells such as B and T lymphocytes could be identified by immunostaining for specific antigens. Transmission electron microscopy (TEM) on pre-labelled capsule sections could also be used to gain a clearer picture of OEC morphology especially if sections could be cut on different planes.

Nevertheless the data presented in this study provide preliminary evidence indicating that morphological plasticity in OECs is facilitated by soluble factors within the injured spinal cord. The effect of morphological change on OEC function and what role it plays in the capacity of OECs to promote repair of the injured spinal cord is unknown. However it has been suggested that morphological plasticity in OECs may be an important factor in their ability to support the ongoing growth of olfactory axons and

that this could underlie their ability to initiate repair in the injured CNS (Van Den Pol, 2003).

CHAPTER FOUR

Optical PCR for Neuregulins in Olfactory Ensheathing Cells

4.1. Introduction

The neuregulins are a family of proteins initially discovered due to their involvement in neural and cardiac development (Meyer et al., 1997). There are four genes known to encode the neuregulins termed *nrg-1*, *nrg-2*, *nrg-3* and *nrg-4* (Orr-Urtreger et al., 1993; Carraway et al., 1997; Chang et al., 1997; Zhang et al., 1997; Harari et al., 1999). The *nrg-1* gene is well characterised and gives rise to multiple variants, classified as Type-I or NDF/HRG or ARIA, Type-II or GGF and Type-III or SMDF on the basis of their specific N-termini (Meyer et al., 1997). Diversity among products of this gene arises by the use of different promoters and alternative splicing. In general nrg-1 products are synthesised by splicing together different combinations of the same structural domains. These domains include an amino-terminus, an immunoglobulin-like domain, a glycosylation rich spacer, an EGF-like domain, a juxtamembrane domain, a transmembrane domain and a cytoplasmic domain (Wen et al., 1992). The EGF domain is common among all nrg-1 products and can be alternatively spliced to produce α- and β-variants. This domain is also thought to be responsible for receptor activation (Wen et al., 1994).

Nrg-1 isoforms influence many aspects of glial cell function including proliferation, differentiation and survival in SCs (Dong et al., 1995; Grinspan et al., 1996) OLGs (Canoll et al., 1996; Raabe, 1997; Vartanian et al., 1997), ASTs (Pinkas-Kramarski et al., 1994; Francis et al., 1999) and OECs (Pollock et al., 1999; Chuah et al., 2000; Yan et al.,

2001b; Alexander et al., 2002). Nrg-1 isoforms are also produced and secreted by glial cells such as SCs (Raabe et al., 1996; Rosenbaum et al., 1997; Cheng et al., 1998), ASTs (Pinkas-Kramarski et al., 1994; Francis et al., 1999), OLGs (Raabe, 1997; Raabe et al., 1998) and OECs (Boruch et al., 2001). Moreover AST-derived nrg-1 isoforms act as mitogens and survival factors for OECs *in vitro* (Pollock et al., 1999; Alexander et al., 2002).

Nrg-1 products bind to and activate members of the class I EGF receptor tyrosine kinase family, erbB2, erbB3 and erbB4. The different homo- and hetero-dimeric combinations of these receptors can elicit different cellular responses depending upon the isoform and cellular context (Riese et al., 1995; Pinkas-Kramarski et al., 1996; Sweeney et al., 2000). Glial cells such as SCs, OLGs (Vartanian et al., 1997), ASTs (Francis et al., 1999) and OECs (Pollock et al., 1999) are known to express members of the erbB receptor family. This suggests that these cell types not only respond to axonal-derived nrg-1 signals but may also use nrg-1 in an autocrine manner as has been shown for SCs (Rosenbaum et al., 1997).

It is well documented that OECs support axonal outgrowth throughout life (Doucette, 1990; Farbman, 1990) and that implantation of these cells into the injured spinal cord enhances outgrowth of injured axons and promotes functional recovery (Ramon-Cueto and Nieto-Sampedro, 1994; Li et al., 1998; Ramon-Cueto et al., 1998). Yet the properties of OECs after they are transplanted into injured spinal cord remain to be investigated. As OECs *in vitro* are known to be extremely heterogeneous in terms of both morphology and antigenic profile (Barber and Lindsay, 1982; Pixley, 1992; Ramon-Cueto and Nieto-Sampedro, 1992; Barnett et al., 1993; Franceschini and Barnett, 1996;

Vincent et al., 2003) it is possible that they may undergo a shift to a regeneration promoting phenotype when exposed to the injury environment.

In this study the nrg-1 gene was chosen as a candidate for analysis of the potential variation in OEC phenotype after implantation into the injured CNS for several reasons. First, specific isoforms of nrg-1 act as mitogens and survival factors for OECs *in vitro* (Pollock et al., 1999; Alexander et al., 2002). Second, it has been suggested that nrg-1 expression may promote olfactory axon outgrowth after injury (Salehi-Ashtiani and Farbman, 1996; Thompson et al., 2000; Williams et al., 2004). Third, preliminary RT-PCR analysis has demonstrated that cultured OECs express an array of nrg-1 isoforms (Thompson et al., 2000). Fourth, changes in nrg-1 expression in OECs have been observed after olfactory nerve injury (Thompson et al., 2000). Given these observations it is concievable that contact with soluble factors in the CNS injury environment may induce changes in nrg-1 expression in OECs and that such changes could be associated with their growth promoting behaviour. Especially since expression of nrg-1 and its receptors are known to be crucial for nervous system development (Kramer et al., 1996; Erickson et al., 1997; Meyer et al., 1997; Britsch et al., 1998) and potentially for regeneration. Therefore the focus of this study was to confirm the normal expression pattern of nrg-1 in OECs *in vivo* compared with other cell types and to quantitatively examine whether exposure to soluble factors in the injured spinal cord affects nrg-1 expression in encapsulated OECs. The results of this study will then provide a starting point for future analyses of the growth promoting properties of OECs at the injury site.

4.2. Materials and Methods

4.2.1. Cell Culture and Tissue Collection

Olfactory ensheathing cells, ASTs and fibroblasts (FBs) were cultured and characterised according to the methods described in sections 2.1.1. to 2.1.3. Olfactory ensheathing cells were encapsulated into polymer tubing and implanted into the lesioned spinal cord as described in the previous chapter. Neonatal rat brain tissue was collected as described in section 2.3.

4.2.2. Total RNA isolation and Quantitation

Total RNA was isolated from all cells and tissues using Trizol Reagent (Life Technologies) as described in section 2.4. Quantitation was performed as described in section 2.4.1.

4.2.3. Principle of TaqMan Real-Time PCR

During conventional PCR a DNA sample is heated to separate its complementary strands (denatured). Subsequent cooling allows specific primers added to the reaction mix to hybridise to their complementary target sequence in the DNA sample. Heat stable Taq polymerase then catalyses the synthesis of a new complementary DNA strand. During each cycle the amount of target DNA synthesised is doubled. The amplified target can then be separated on the basis of size by agarose gel electrophoresis and visualised by ethidium bromide staining.

Real-time (or optical) PCR is performed in a similar manner to conventional PCR. In addition to specific primers and Taq polymerase a flurogenic probe is added to the

reaction mix. These probes, referred to as TaqMan probes, are short strands of DNA whose sequence is complementary to that of the DNA target. The probes are dual-labelled with reporter and quencher dyes which are attached to the 5' and 3'ends respectively (Fig. 4.1). In the intact probe the close proximity of the quencher blocks (or quenches) the fluorescence of the reporter dye (by Forster Resonance Energy Transfer, or FRET). During each PCR cycle Taq polymerase cleaves the probe molecules from the target DNA allowing primer extension to continue to the end of the target DNA strand due to its exonuclease activity (Fig. 4.1). Cleavage also separates the reporter from the quencher dye thereby increasing the reporter dye signal. With each cycle more reporter dye molecules are cleaved from their respective probes increasing the fluorescence intensity in proportion to the amount of product generated.

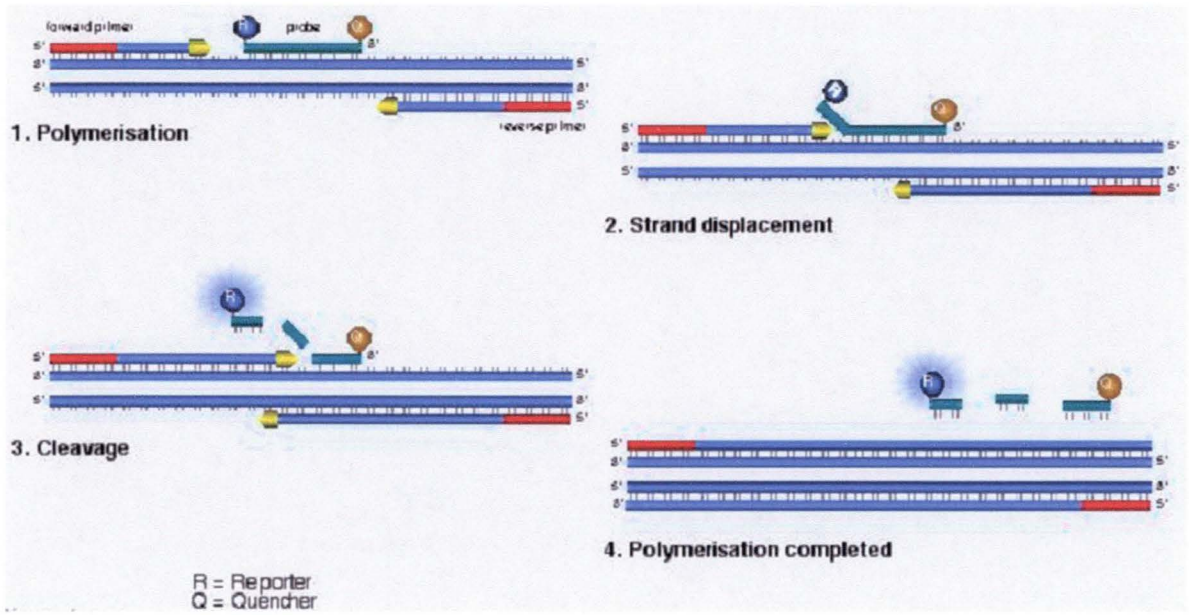

FIGURE 4.1. Schematic diagram showing the TaqMan® RT-PCR mechanism.

Two fluorescent dyes, a reporter (R) and a quencher (Q) are attached to the 5' and 3' ends of the TaqMan® probe respectively. When both dyes are attached to the probe reporter dye fluorescence is quenched. During the extension phase of each PCR cycle Taq polymerase displaces the probe allowing extension to continue to the end of the target DNA strand. This process also cleaves the reporter dye from the probe. Once the reporter and quencher dyes are spatially separated the fluorescence intensity of the reporter dye increases. With each PCR cycle the intensity of reporter dye fluorescence increases proportionally to the amount of specific product generated.

4.2.4. TaqMan Probe and Primer Design

TaqMan quantitative RT-PCR probes and primers were designed to selectively detect different subtypes of rat Nrg-1 transcripts, as defined by (Marchionni et al., 1993). It has been previously demonstrated that the domain structure observed in different variants encoded by the human nrg-1 gene is generated by alternate splicing of genomic exons. These variants can be classified into several subtypes (NDF/HRG, SMDF, GGF and ARIA), based on the presence or absence of the alternately spliced exons.

Since the genomic structure of the rat nrg-1 gene is currently unknown, a strategy was devised to delineate the exon-exon boundaries (and hence, domain boundaries) of rat nrg-1 by comparison of all known rat Nrg-1 cDNAs against the human genomic nrg-1 sequence. Thus, all known rat nrg-1 cDNA sequences from GenBank were aligned with the complete human gene sequence and putative exon-exon boundaries within the cDNAs were defined. These boundaries were consistent for all cDNAs examined (10), indicating that this approach is robust. Identification of exon-exon boundaries allowed design of RT-PCR primers (six forward, six reverse) targeted to specific rat nrg-1 exons (Table 4.1 and Fig. 4.2). Further specificity was given by design of three TaqMan probes, which specifically hybridised to the immunoglobulin domain common to NDF and GGF (probe 1; exon 3), EGF common domain (probe 2; exon 6) and to a separate region of the EGF common domain (probe 3; exon 6) (Fig. 4.2). In appropriate combinations as outlined in Table 4.2, it was possible to perform PCR specific for up to nine subtypes of rat nrg-1.

A probe and primer set for GAPDH was designed to amplify the region corresponding to nucleotides 1603-1669 of GenBank sequence accession number AF106860 producing a product with an expected size of 67bp. The probe sequence was located between nucleotides 1630-1647 of AF106860.

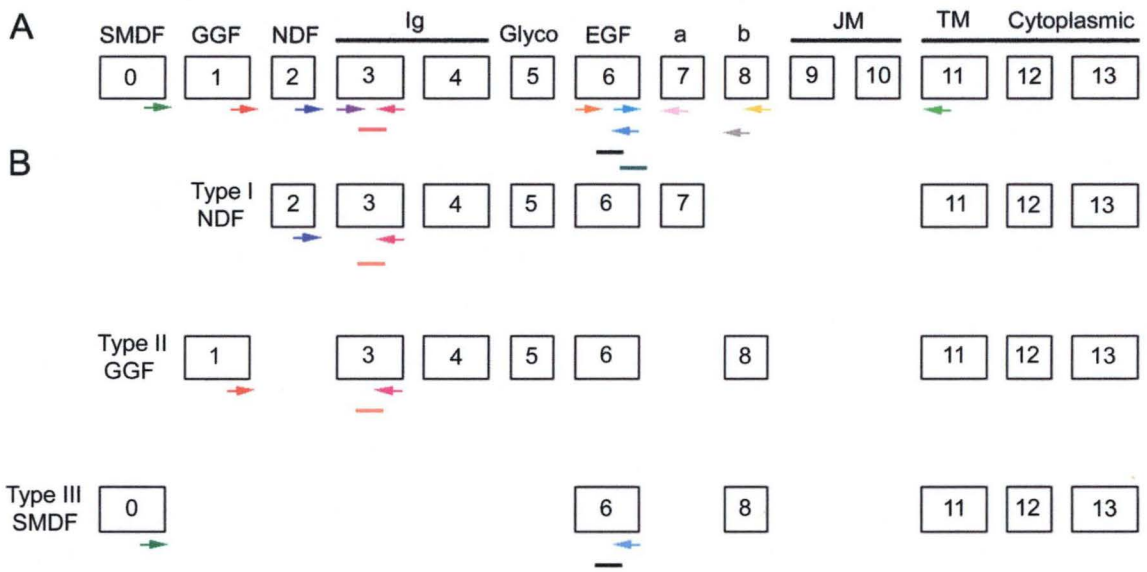

FIGURE 4.2. Putative representation of the rat *neuregulin-1* (*nrg-1*) gene including the locations of all primers and probes.

(A) The putative arrangement of exons includes, SMDF, GGF, NDF, immunoglobulin (Ig), glycoplasmic (Glyco), EGF, alpha (a), beta (b), juxtamembrane (JM), transmembrane (TM) and cytoplasmic. Right facing arrows represent forward primers including Nrg-F1, Nrg-F2, Nrg-F3, Nrg-F4, Nrg-F5, Nrg-F6. Left facing arrows represent reverse primers as follows, Nrg-R1, Nrg-R3, Nrg-R4, Nrg-R5, Nrg-R7, Nrg-R8. Lines represent probes, including Nrg-P1, Nrg-P2, Nrg-P3. (B) Shows one of the many possible cDNA isoforms for each major Nrg-1 subtype. The primer combinations shown are specific for each subtype although more than one isoform of each could be amplified using these primer sets.

TABLE 4.1. TaqMan® probe and primer sequences the *neuregulin-1 (nrg-1)* gene.

Probes and Primers	Sequences 5' - 3'
Forward Primers	
Nrg-F1	GAGGTCAGCCGGGTGTTGT
Nrg-F2	CGAGGGCGACCCGAG
Nrg-F3	GTGAGAACACCCAAGTCAGGAAC
Nrg-F4	TTCTTCATCCACATCAACATCCA
Nrg-F5	TGCCTCCCAGATTGAAAGAAA
Nrg-F6	GCGAGTGCTTCACGGTGAA
Reverse Primers	
Nrg-R1	TTTCGCACCGGAGCACTAG
Nrg-R3	CCCCCATTCACACAGAAAGTTT
Nrg-R4	GCATGCTCCTACTCAGGCAGA
Nrg-R5	TCTTCTGGTAGAGTTCCTCCGCT
Nrg-R7	TTGTCAGCACCCTCTTCTGGT
Nrg-R8	TCCAGTGAATCCAGGTTGGC
Probes	
Nrg-P1	CCAGGAGTCAGCTGCAGGCTCCAA
Nrg-P2	TGGGACCAGCCATCTCATAAAGTGTGC
Nrg-P3	CCTGTCAAACCCGTCAAGATACTTGTGCAA

[1] Probe and primer sequences were designed using primer express 1.0.

TABLE 4.2. Specific probe/primer combinations for the neuregulin-1 (nrg-1) subtypes.

		Target	Exons	Target Length
Probe 1				
Nrg-F1	Nrg-R1	GGF	1+3	106
Nrg-F2	Nrg-R1	NDF	2+3	95
Nrg-F5	Nrg-R1	NDF/GGF (Ig domain)	3	72
Probe 2				
Nrg-F4	Nrg-R3	EGF domain	6	87
Nrg-F4	Nrg-R4	Secreted	6+7/8+10	240
Nrg-F4	Nrg-R5	Transmembrane	6+8+9+11	221
Nrg-F3	Nrg-R3	SMDF	0+6	149
Probe 3				
Nrg-F6	Nrg-R7	β-types	6+8	147
Nrg-F6	Nrg-R8	α-types	6+7	174

[1] Nrg-1 transcript classes were identified by combining each specific probe with the forward (Nrg-F) and reverse primer (Nrg-R) combinations shown above.
[2] Amplicon length is given in base pairs.
[3] Target exons of the nrg-1 gene amplified by each primer set are shown.

4.2.5. RT-PCR Procedure

RT-PCR was performed using the one-step TaqMan® EZ RT-PCR Kit (Applied Biosystems, Cat. No. N808-0235) according to the manufacturer's protocol. Amplification reactions were performed in a final volume of 25µl containing ~50ng total RNA sample, 2-4mM MnOAc (depending on the isoform), 0.3mM dATP, dCTP, and dGTP, 0.6mM dUTP, 0.10U/µl rTth DNA polymerase and 0.01U/µl AmpErase UNG in 1× RT-PCR buffer. The final concentration of GAPDH forward and reverse primers was 500nM whilst the probe concentration was 250nM. The final concentration of the nrg primers was 900nM and the probes were 250nM. The concentration of each mRNA isoform was measured using the Rotorgene 2000 thermal cycler (Corbett Research). Amplification conditions included 2 minutes at 50°C, 30 minutes at 60°C, 5 minutes at 95°C and then run for 45 cycles at 94°C for 15 seconds and 60°C for 1 minute. Products were separated according to size by agarose gel electrophoresis on a 1.5% gel. Separated products were then stained with ethidium bromide and visualised under UV light to ensure they were the correct size (not shown).

4.2.6. Data Analysis (Relative Quantitation)

Relative quantitation is a method whereby a gene of interest (e.g. nrg-1) is compared to a housekeeping gene (e.g. GAPDH) in a test sample with the result being a ratio (Fig. 4.3). In real-time relative RT-PCR a standard curve is generated from a dilution series using a reference RNA sample. The reference sample used in this study was neonatal rat brain RNA (which is known to express each nrg-1 subtype). To generate the standard curves five different concentrations of neonatal rat brain RNA (e.g. 200, 20,

2.0, 0.2 and 0.02ng) were prepared. The units (ng or pg etc.) used to describe the dilution series were relative based on the dilution factor of the standard curve. Standard curves were generated for each nrg-1 subtype and GAPDH so as to compensate for their different amplification efficiencies. Test samples were always analysed at the same time as the standard curves to eliminate interference caused by run-run variations. The concentrations of each nrg-1 subtype and GAPDH in the test samples (e.g. OEC and ASTs) were then calculated by extrapolation of C_T values from the line of best fit on the corresponding standard curve (see Fig 4.1 and example calculation p. 101). C_T values are defined as the cycle number at which the sample fluorescence signal passes a fixed threshold above baseline. The concentration of the nrg-1 subtypes in each sample were then normalised to GAPDH by dividing each value by the corresponding GAPDH value. The results for each test sample were then averaged (see example Table 4.3). The statistical significance (student's t-test) was also calculated where appropriate. Data were considered statistically significant if the p value was less than 0.05. For each experimental sample target expression level was determined by dividing the normalised quantity of the specific target by the normalised quantity of that target in a calibrator sample. Thus the calibrator sample becomes the 1× sample and all other quantities are expressed as an n-fold difference relative to the calibrator. For example an appropriate calibrator sample for implanted encapsulated OECs would be unimplanted encapsulated OECs.

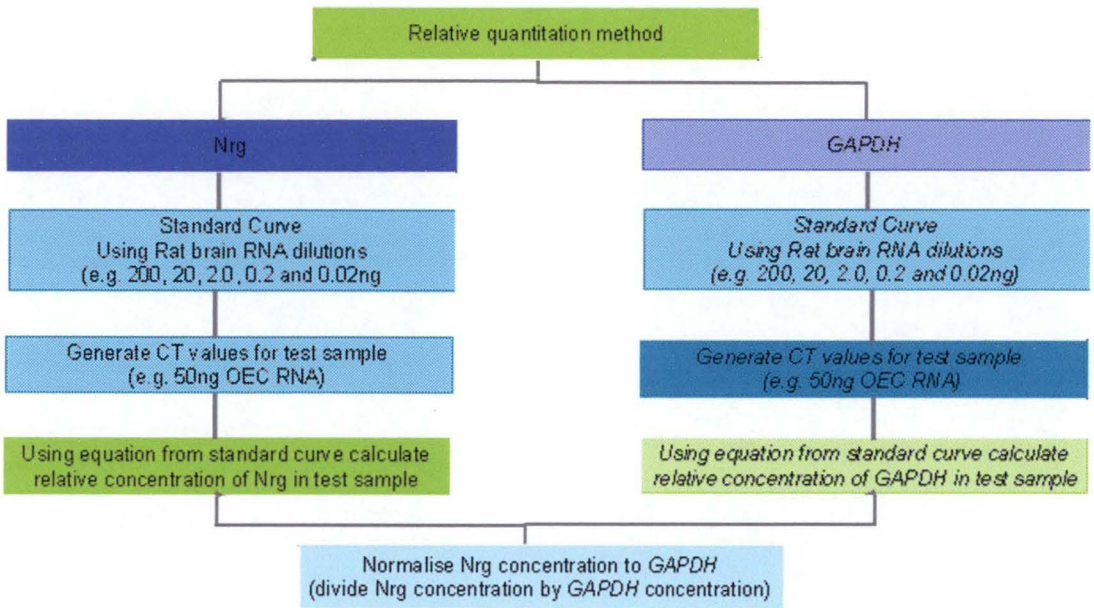

FIGURE 4.3. Flow chart showing an overview of the relative quantitation method.

For each test sample a standard curve for all Nrg-1 subtypes and GAPDH were generated using rat brain RNA as a reference sample. The test samples were run at the same time as the corresponding standard curves. The relative concentration of Nrg-1 subtypes and GAPDH were then calculated for the test samples by inserting the specific C_T values into the line of best fit equation for the corresponding standard curve. Values for each Nrg-1 subtype in all test samples were normalized to GAPDH by dividing the Nrg-1 values by the corresponding GAPDH values.

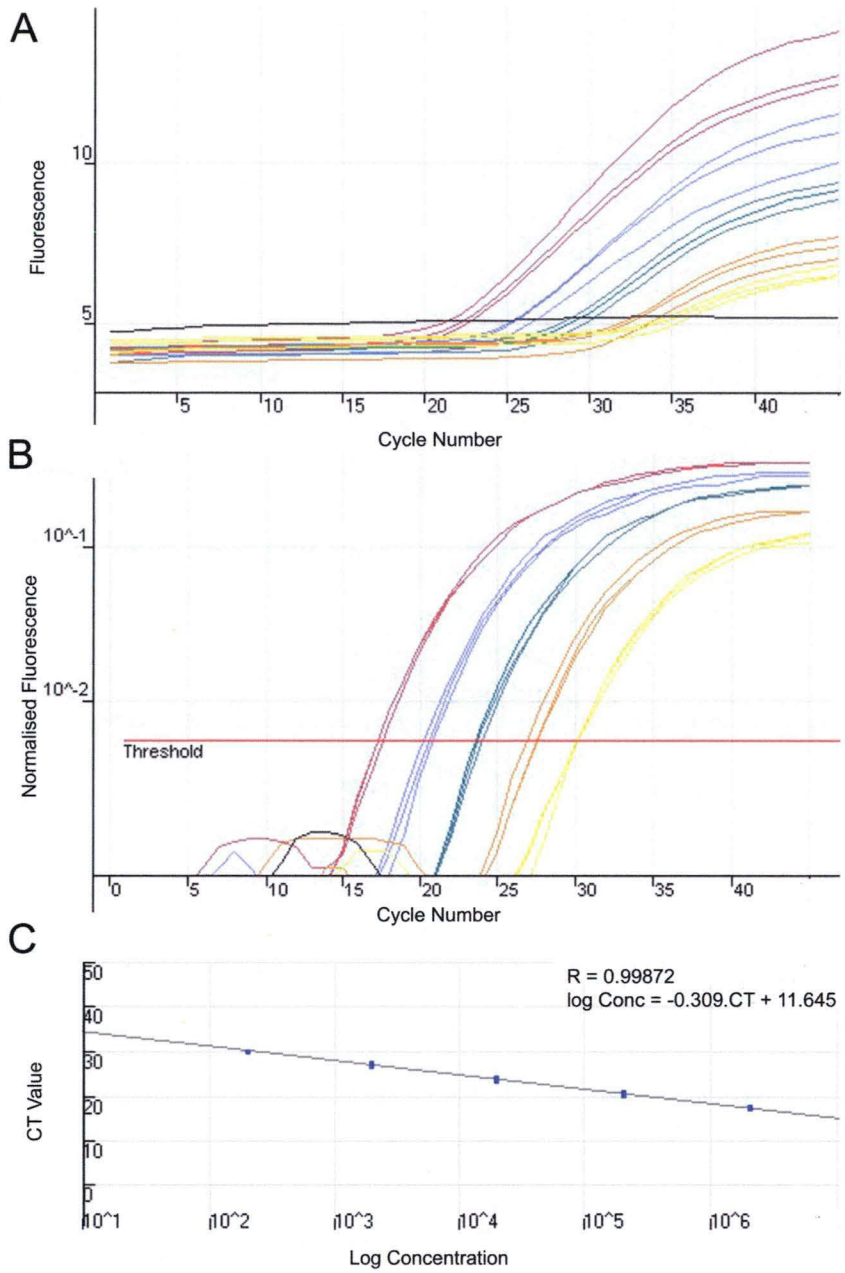

FIGURE 4.1. Example amplification plots and standard curve.

Real-time quantitative RT-PCR using the TaqMan® EZ RT-PCR kit (Applied Biosytems). (A) Rat brain RNA was amplified at concentrations of 200ng, 20ng, 2.0ng, 0.2ng, and 0.02ng respectively, test samples were run in parallel. (B) An amplification plot showing cycle number versus normalised fluorescence for each concentration of rat brain RNA. (C) Standard curve showing concentration versus threshold cycle (C_T). The concentration of the mRNA transcript in the unknown samples can then be calculated from their specific C_T values using the equation from the standard curve (calculation over page).

Example Calculation (using the equation to the line of best fit from a standard curve):

- Log relative concentration = $mC_T + b$

  (m = slope, C_T = test sample C_T value, b = y intercept)

If the sample then has a C_T value of 25

- Log relative concentration (pg) = $(-0.309 \times 25) + 11.645$
- Relative concentration (pg) = $10^{(\log \text{relative concentration})}$
- Relative concentration (pg) = $10^{(-0.309 \times 25) + 11.645}$

The final concentration of specific mRNA in the test sample is 8317pg (or 8.317ng.

It should be noted that the units for relative concentration (e.g. pg) are specified by the user when the standard curve is prepared and are therefore arbitrary.

TABLE 4.3. Calculation of normalised expression levels (NDF).

RNA Sample	Relative Concentration GAPDH (ng)	Relative Concentration NDF (ng)	Normalised NDF (NDF÷GAPDH)
OECs			
Replicate 1	35.012	157.925	4.51
Replicate 2	37.344	180.745	4.84
Replicate 3	39.598	181.685	4.59
Average (NDF÷GAPDH)			4.65
ASTs			
Replicate 1	66.326	73.250	1.10
Replicate 2	50.651	72.871	1.44
Replicate 3	58.302	67.063	1.15
Average (NDF÷GAPDH)			1.23
FBs			
Replicate 1	30.596	80.424	2.63
Replicate 2	30.063	79.593	2.65
Replicate 3	26.738	72.118	2.70
Average (NDF÷GAPDH)			2.66
OEC C			
Replicate 1	0.827	0.154	0.186
Replicate 2	2.067	0.427	0.207
Replicate 3	1.721	0.230	0.134
Average (NDF÷GAPDH)			0.176
OEC CI			
Replicate 1	2.286	2.684	1.16
Replicate 2	2.123	2.692	1.27
Replicate 3	2.113	2.321	1.10
Average (NDF÷GAPDH)			1.18

[1] Data for cultured cells is expressed as the amount of PCR product (ng) derived from a starting RNA quantity of 50ng per reaction. Capsule data is expressed as the amount (pg) of PCR product derived from a single capsule

[2] Normalised mRNA values are expressed as a ratio and are therefore unitless.

4.3. Results

4.3.1. Quantitation of Neuregulin-1 Expression in Encapsulated Olfactory Ensheathing Cells

To determine whether nrg-1 expression in OECs was affected by the *in vivo* environment of the injured spinal cord quantitative RT-PCR analysis was performed on cells that were encapsulated and implanted (OEC CI) into the injured spinal cord for one week. For comparison encapsulated cells were maintained for one week under the same culture conditions as the monolayered cells (OEC C). Samples were analysed in triplicate for each transcript and the results normalised to the houskeeping gene GAPDH (Table 4.4). The expression level of each subtype was examined in implanted OECs relative to OECs *in vitro* (Table 4.5). After implantation of OECs into the injured spinal cord only NDF (p <0.001) was found to significantly increase in expression level compared with encapsulated OECs *in vitro* (Fig. 4.5A). In fact implanted OECs contained 10 ± 1.3× as much NDF as OECs *in vitro* (Table 4.5). There was also an increase in expression of the secreted domain with 4.3 ± 2.7× as much detected in implanted compared with control encapsulated OECs (Fig. 4.5E and Table 4.5) yet this increase was not considered significant (p = 0.108) (Fig. 4.5E and Table 4.5). The expression levels of NDF/GGF (or Ig domain) (p = 0.026) and α-type (p = 0.007) transcripts decreased significantly after implantation (Fig. 4.5B and F). Only 0.07 ± 0.02× as much Ig and 0.3 ± 0.1× as much α-type mRNA was detected in implantated OECs compared with control OECs. SMDF (p = 0.193) and EGF (p = 0.051) transcripts also decreased in expression level, but the decrease was not significant (Fig. 4.5C and D). Both the transmembrane and β-type

isoforms were not detected in implanted encapsulated or control encapsulated OECs. No-template controls showed no contamination with genomic DNA.

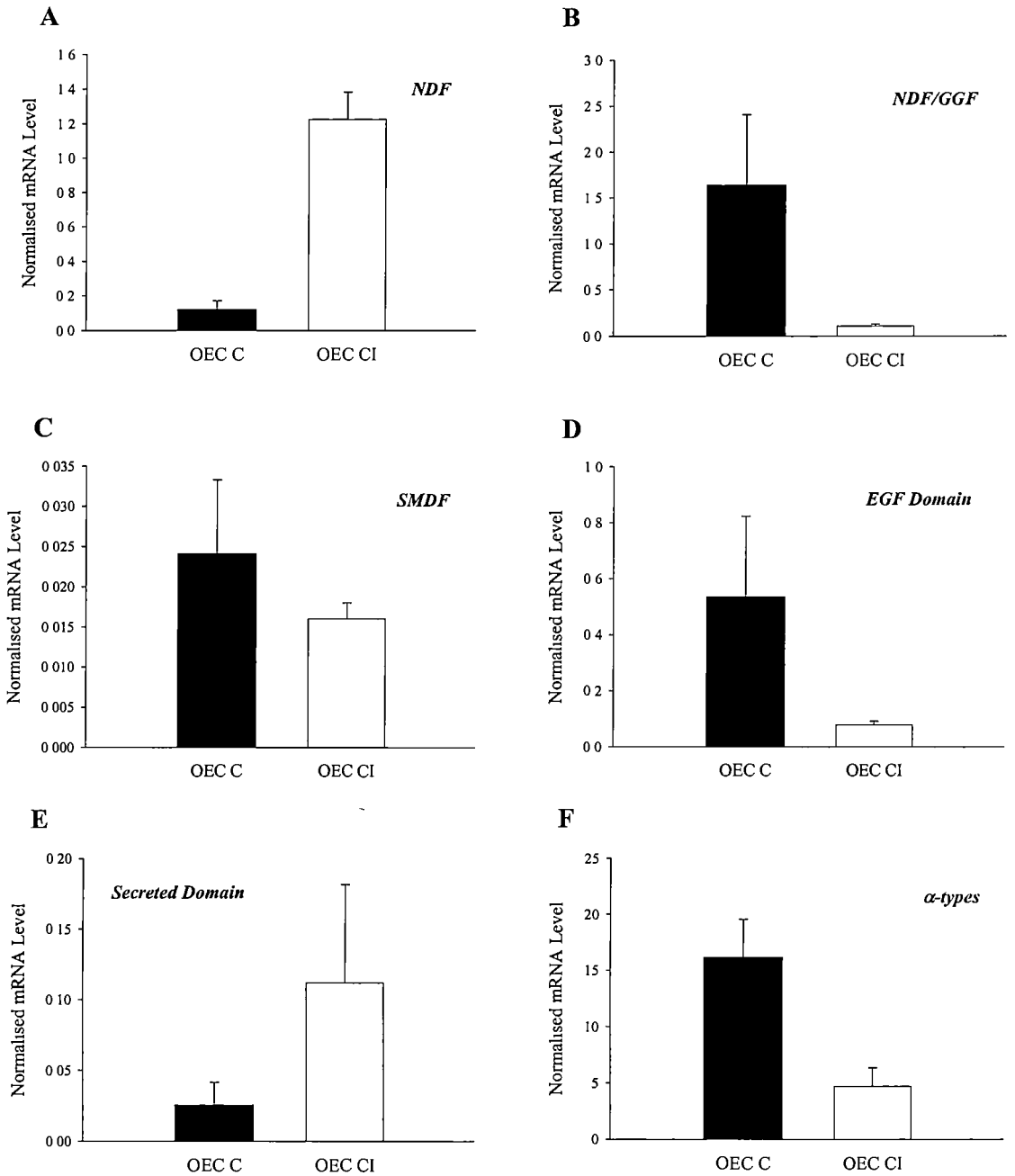

FIGURE 4.5. The effect of the injured rat spinal cord on neuregulin-1 (nrg-1) mRNA expression in olfactory ensheathing cells (OECs).

Cultured OECs were encapsulated into porous polymer tubes and implanted into the injured rat spinal cord for one week (OEC CI), or maintained in MEM D-valine supplemented with 10% dFCS at 37°C, 5%CO_2 for one week (OEC C). Error bars represent standard deviation.

4.3.2. Comparison of Neuregulin-1 Expression in Cultured Olfactory Ensheathing Cells with Astrocytes and Fibroblasts

To establish the normal nrg-1 expression profile in OECs quantitative RT-PCR was performed on primary cultures of OECs and compared with ASTs and FBs. Samples were analysed in triplicate as described above and the results normalised to GAPDH (Table 4.4). Expression levels in OECs were calculated relative to ASTs and FBs (Table 4.6 and 4.7). All cell types displayed a similar pattern of expression although the levels varied (Fig. 4.6). All transcripts with the exception of the transmembrane variant were expressed in cultured OECs. Astrocytes and FBs also lacked expression of the transmembrane variant while FBs also lacked GGF expression (Fig. 4.6D). Olfactory ensheathing cells expressed higher levels of the major subtypes NDF, SMDF and GGF than ASTs and FBs (Fig. 4.6A, B and D, Table 4.6 and 4.7). Similarly the minor subtypes including, EGF, secreted, α-type and β-type, nrg-1 were more highly expressed in OECs than ASTs (Fig. 4.6E, G, H and Table 4.6). One exception was the Ig subtype which was more highly expressed in FBs than OECs (Fig. 4.6C and Table 4.6). Compared with FBs, OECs expressed higher levels of the minor subtypes EGF, secreted and β-type (Table 4.7). Unlike the other subtypes expression of α-type was highest in FBs (Fig. 4.6G and Table 4.7). No-template controls showed no contamination with genomic

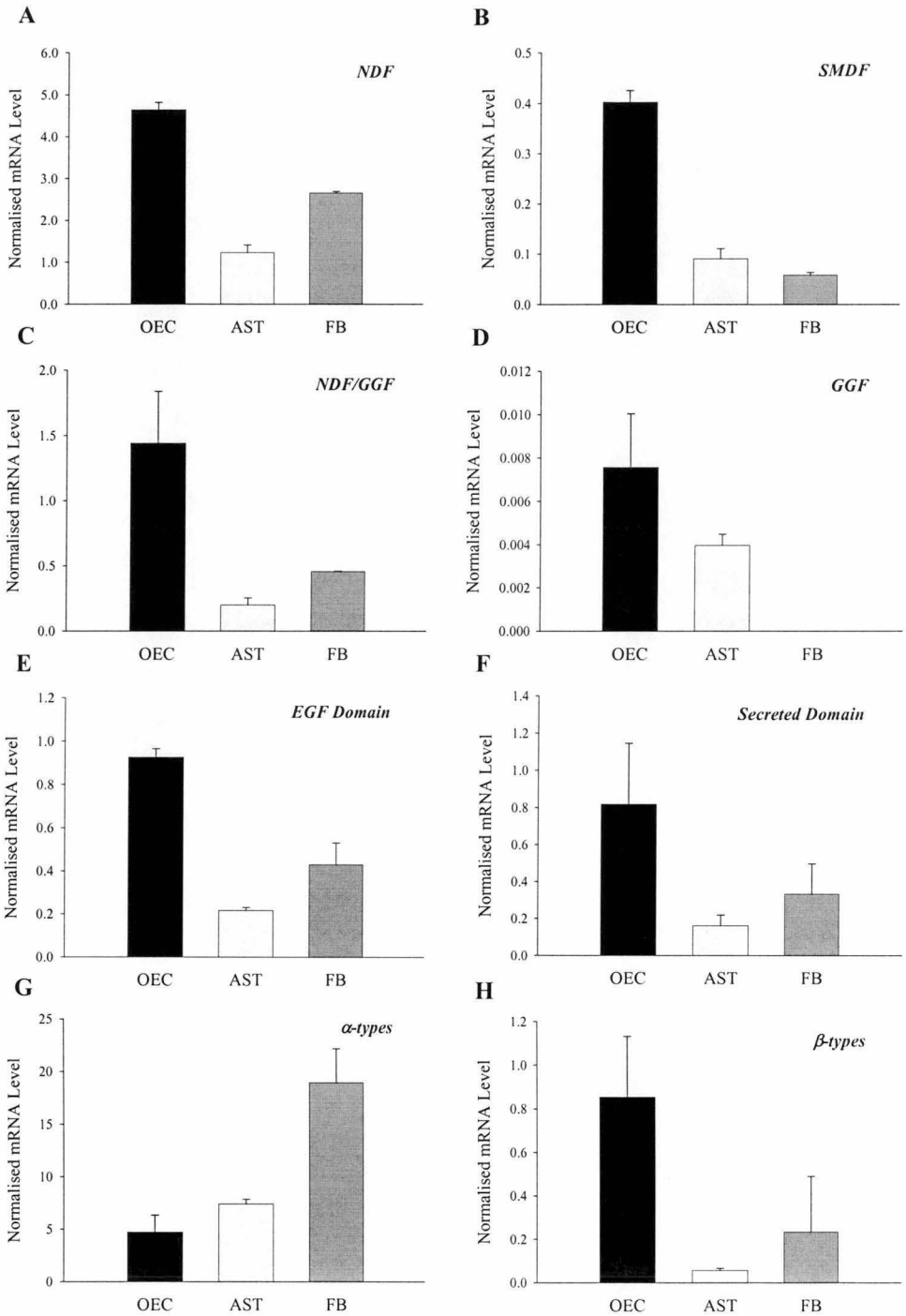

FIGURE 4.6. Expression levels of neuregulin-1 (nrg-1) mRNA in primary cultures of olfactory ensheathing cells (OECs) astrocytes (ASTs) and fibroblasts (FBs).

Primary cultures of OECs, ASTs and FBs were analysed for each nrg-1 mRNA subtype by real-time RT-PCR. Error bars represent standard deviation.

TABLE 4.4. Normalised expression levels of neuregulin-1 (nrg-1) mRNA in cultured and/or implanted encapsulated olfactory ensheathing cells (OECs), astrocytes (ASTs) and fibroblasts (FBs).

MAJOR SUBTYPES	OEC C	OEC CI	OEC	AST	FB
GGF	ND	ND	0.008 ± 0.0002	0.004 ± 0.0001	ND
NDF	0.123 ± 0.049	1.226 ± 0.158	4.646 ± 0.172	1.231 ± 0.182	2.658 ± 0.035
SMDF	0.024 ± 0.009	0.016 ± 0.002	0.403 ± 0.023	0.091 ± 0.020	0.058 ± 0.005

MINOR SUBTYPES	OEC C	OEC CI	OEC	AST	FB
NDF/GGF (Ig)	1.640 ± 0.768	0.108 ± 0.028	0.1442 ± 0.394	0.202 ± 0.054	0.459 ± 0.004
EGF	0.536 ± 0.287	0.079 ± 0.013	0.946 ± 0.040	0.212 ± 0.012	0.429 ± 0.101
Secreted	0.026 ± 0.016	0.112 ± 0.070	0.819 ± 0.327	0.162 ± 0.057	0.332 ± 0.165
β-Types	16.160 ± .0377	4.707 ± 1.643	15.440 ± 1.609	7.423 ± 0.427	18.970 ± 3.219
α-Types	ND	ND	0.854 ± 0.278	0.057 ± 0.010	0.110 ± 0.048
Transmembrane	ND	ND	ND	ND	ND

[1] ND indicates that the isoform was not detected.
[2] Normalised mRNA levels are given in arbitrary units ± standard deviation.
[3] Nrg-1 expression was compared in OEC capsules maintained *in vitro* (OEC C) and those implanted into the injured spinal cord (OEC CI).

TABLE 4.5. Expression levels of neuregulin-1 (nrg-1) in implanted encapsulated OECs relative to encapsulated OECs maintained *in vitro*.

MAJOR SUBTYPES	OEC CI
NDF	10 ± 1.3
SMDF	0.7 ± 0.08

MINOR SUBTYPES	OEC CI
NDF/GGF (Ig)	0.07 ± 0.02
EGF	0.2 ± 0.02
Secreted	4.3 ± 2.7
α-Type	0.3 ± 0.1

TABLE 4.6. Expression levels of neuregulin-1 (nrg-1) in olfactory ensheathing cells (OECs) relative to astrocytes.

MAJOR SUBTYPES	OEC
GGF	2.0 ± 0.05
NDF	3.8 ± 0.14
SMDF	4.4 ± 1.15

MINOR SUBTYPES	OEC
NDF/GGF (Ig)	0.7 ± 1.9
EGF	4.5 ± 0.2
Secreted	5.1 ± 2.0
α-Type	2.1 ± 0.2
β-Type	15.0 ± 4.9

[1]Relative expression levels were calculated by dividing the normalised expression values of the test samples by the normalised expression values of the calibrator sample.
[2] Assuming that the calibrator has an expression value of 1 the test samples have an *n*-fold change in target expression.

TABLE 4.7. Expression levels of neuregulin-1 (nrg-1) in olfactory ensheathing cells (OECs) relative to fibroblasts.

MAJOR SUBTYPES	OEC
NDF	1.7 ± 0.1
SMDF	6.9 ± 0.4

MINOR SUBTYPES	OEC
NDF/GGF (Ig)	0.3 ± 0.9
EGF	2.2 ± 0.1
Secreted	2.5 ± 1.0
α-Type	0.8 ± 0.1
β-Type	7.8 ± 2.5

4.4. Discussion

This study indicates that nrg-1 expression in OECs may be influenced by soluble factors within the CNS injury environment. One limitation of the real-time RT-PCR technique is that it relies on quantitation of nrg-1 expression normalised to the housekeeping gene GAPDH. Therefore the nrg-1 levels reported here are based on the assumption that GAPDH levels will remain constant in each cell type and in OECs whether implanted or not. To minimise GAPDH variation the same RNA pool was used for each cell type throughout the experiment, samples were not freeze-thawed multiple times and the same amount of RNA (ie. 50ng) was used per reaction for all cell types. To further improve the reliability of this technique other housekeeping genes could be used in addition to GAPDH or both nrg-1 and GAPDH reactions could be performed in the same tube (a technique known as multiplexing). However multiplex reactions require that the specific probes are labelled with different fluorophores whose fluorescent spectra do not overlap and that both primer sets use the same thermal cycling parameters.

Another limitation of the technique used in this study is that the quantitation is relative therefore the reported levels are given in arbitrary units. Hence relative levels cannot be correlated with cell number. This problem can be overcome by performing absolute quantitation. Here the absolute quantity of the RNA standard must be known and is determined by some independent means. Usually this is achieved by measuring the absorbance of the RNA standard at 260nm (A_{260}) and converting this to copy number using the molecular weight of the RNA. Once the absolute concentration is known the RNA can be used to generate the standard curve in the same manner as for the relative technique. Results can then be reported in absolute numbers and can therefore be related

to cell number. However two important factors to consider when using absolute quantitation are (1) the stability of the RNA standard and (2) the accuracy of the A_{260} measurement since these are crucial for absolute quantitation.

In this study the nrg-1 isoforms expressed by cultured OECs included NDF, SMDF, GGF, EGF and secreted nrg-1. Olfactory ensheathing cells expressed the highest levels of most subtypes relative to both ASTs and FBs. The expression profiles of ASTs and FBs were shown to be similar to that of OECs except that FBs lacked GGF. A similar range of isoforms in OECs, ASTs and SCs were reported previously (Thompson et al., 2000). After implantation into the injured spinal cord OECs were found to significantly increase expression of NDF. A previous study showed that both NDFα and β variants are survival factors for OECs, however only the NDFβ variant was mitogenic (Pollock et al., 1999). Hence it is plausible that encapsulated OECs increase expression of NDF after implantation to enhance their own survival and proliferation. This seems especially likely given that OECs are known to express functional erbB receptors including erbB2 and erbB4 suggesting that they have the capacity to use these factors in an autocrine manner (Pollock et al., 1999). Moreover the earlier finding (see chapter three) that OEC survival and proliferation are potentially limited after encapsulation may lend further support to this possibility.

Notably GGF expression was lacking in encapsulated OECs whether implanted or not. This would seem an unexpected result given that cultured OECs are known to express GGF (Chuah et al., 2000) and GGF transcripts were detected by real-time RT-PCR in normal cultured OECs in this study. Since GGF is known to induce proliferation in OECs its absence from the encapsulated cells could be directly related to the decline in

cell number seen in the cultured capsules in the previous chapter. The same could also be true of cells in the implanted capsules assuming that a lack of GGF affected their proliferation in a similar manner. However, further investigation will be required to establish whether the lack of proliferation in encapsulated OECs is directly linked to GGF downregulation.

The transmembrane nrg-1 transcript was not detected in normal cultured OECs, ASTs, FBs or encapsulated OECs (before or after implantation into the injured spinal cord). This observation did not support the findings of Thompson and colleagues (2000) who demonstrated the presence of the transmembrane variant in OECs. It is possible that this discrepancy may be related to differences in the age and strain of animals used and/or to the method of culture. For example cells used in this study were isolated from 2-3 day-old Hooded Wistar rat pups and purified by serial passage and use of mitotic inhibitors to produce a 91% $p75^{NTR}$ positive population. Cells in the previous study were prepared from 7 day-old Sprague-Dawley rat pups and purified by fluorescence-activated cell sorting (FACS) using the O4 antigen. These factors alone may have resulted in a slightly different population of OECs leading to the observed discrepancy. Another possibility is that the use of different primer sets in each study contributed to the apparently different result. The transmembrane primer set used here was designed to detect a single isoform. However the primer set used by Thompson and colleagues was reported to amplify both α- and β-transmembrane variants identified as two separate bands on the same gel. Furthermore they report that only the α-form is expressed by OECs, ASTs and SCs whilst the β-form is expressed in the cortex (Thompson et al., 2000). This may suggest that the isoform detected by our primer set was the β-form. Similarly this could explain the

absence of the transmembrane variant in OECs and its presence in rat whole brain total RNA used in this study to produce the standard curves.

The discrepancies between this study and the previous report by Thompson and colleagues highlight the fact that the nrg gene is very complex. The highly alternatively spliced nature of nrg-1 alone combined with the fact that its exonic structure is not well understood indicate that further investigation of this gene may be required.

Surprisingly little is known about how neuregulin expression is induced despite the fact that their bioactivity has been extensively studied. However nrg-1 expression in some neurons has been shown to be regulated by target interactions (Bermingham-McDonogh et al., 1997). For example axotomy of motor and sensory neurons reduces the expression of nrg-1 which is restored to normal levels after reinnervation of the target tissues (Bermingham-McDonogh et al., 1997).

The functional significance associated with down-regulation of GGF particularly in the context of nerve repair is not known. Given that GGF promotes OEC proliferation *in vitro*, a down-regulated level of GGF could indicate that OEC growth and survival are compromised. However the injured spinal cord contains elevated levels of PDGF, BDNF, NGF, TGFβ, FGF-2, IGF-I and IGF-II (Logan et al., 1992; Mocchetti et al., 1996; Lagord et al., 2002; Bareyre and Schwab, 2003) that could stimulate the proliferation of implanted OECs (Bianco et al., 2004). Future experiments could use protein arrays to analyse the spectrum of growth factors present in the injured spinal cord and each of the factors identified could then be tested for their effect on OECs *in vitro*.

Neuregulin-1 proteins are necessary for the proliferation, differentiation and survival of OLGs the myelin forming cells of the CNS (Canoll et al., 1996; Canoll et al.,

1999; Vartanian et al., 1999; Flores et al., 2000). Hence upregulation of nrg-1 by OECs could promote the survival of damaged OLGs and/or the proliferation and differentiation of OLG precursors after CNS injury. Studies of nrg-1 knockout mice have revealed that the nrg-1 proteins have multiple essential roles in nervous system development, see review by (Falls, 2003). Hence they not only promote the survival, proliferation and differentiation of glial cells (Dong et al., 1995; Canoll et al., 1996; Grinspan et al., 1996; Raabe, 1997; Vartanian et al., 1997; Flores et al., 2000) but also promote the survival and migration of several neuronal populations (Anton et al., 1997; Rio et al., 1997; Britsch et al., 1998; Wolpowitz et al., 2000). Hence nrg-1 expressed by OECs could have an overall protective effect on oligodendrocytes and neurons in the injured spinal cord.

CHAPTER FIVE

Nogo and Nogo-66 Receptor Expression in Olfactory Ensheathing Cells

5.1. Introduction

The insulating myelin sheath produced by OLGs that surrounds axons in the CNS has long been associated with inhibition of axonal regeneration. Myelin gives rise to a number of inhibitory molecules including; MAG, CSPG, arretin and NI-35/NI-250 (or Nogo). Interest in Nogo initially stemmed from the finding that a monoclonal antibody termed IN-1 could neutralise the inhibitory effects of NI-35/NI-250 thereby enhancing axonal regrowth of CST fibres and promoting functional recovery when applied to a lesion site *in vivo* (Schnell and Schwab, 1990; Brosamle et al., 2000).

The Nogo gene encodes three known protein products termed Nogo-A, -B and -C, which are thought to arise from alternative splicing and promoter usage (Chen et al., 2000; Oertle et al., 2003a). Nogo-A was classified as a Rtn protein, a family of ER-associated proteins of unknown function, due to the finding that the protein is concentrated largely in the ER with only small amounts reaching the surface of OLGs (GrandPre et al., 2000). This finding was thought to explain why OLGs contribute to axonal inhibition after injury as damaged cells could conceivably release intracellular stores of Nogo into the lesion environment, thereby inhibiting axonal regrowth (Goldberg and Barres, 2000).

The inhibitory characteristics of Nogo were later localized to a 66 amino acid C-terminal region referred to as Nogo-66 (found in all Nogo isoforms) and also to the N-

terminal domain of the protein (Fournier et al., 2001). A recent study of the Nogo-A protein also revealed the presence of a third inhibitory domain found in the Nogo-A specific exon three (Oertle et al., 2003b). The inhibitory Nogo-66 domain was found to interact with a GPI-linked receptor termed NgR, which is found on the axonal surfaces of many CNS neurons but is not expressed by OLGs. Cleavage of this receptor from the axonal surface renders neurons insensitive to Nogo-66 inhibition whilst induction of NgR expression is sufficient to impart Nogo-66 responsiveness to previously unresponsive neurons (Fournier et al., 2001). This suggested that the NgR plays a major role in Nogo-66 signaling. However because the NgR is GPI-linked to the cell surface, by analogy with other similarly linked proteins, it requires a transmembrane co-receptor for intracellular signaling. It is now known that the $p75^{NTR}$ can act as part of a signaling complex with NgR in MAG-associated neurite outgrowth inhibition (Wong et al., 2002).

The localization of Nogo to OLGs and the NgR to the surfaces of CNS neurons fits well with the notion that Nogo is an inhibitor of axon outgrowth in the CNS. Unfortunately in the injured CNS the presence of Nogo restricts neurite regrowth thereby preventing regeneration. Unlike OLGs, OECs are known to be permissive to axon outgrowth after injury and have been shown to promote the growth of injured axons after implantation into the lesioned spinal cord (Doucette, 1995; Franklin et al., 1996; Ramon-Cueto et al., 1998). In view of their growth promoting nature it would seem unlikely that OECs express Nogo and its receptor NgR. To the contrary the presence of Nogo and the NgR in the developing olfactory system along with the finding that $p75^{NTR}$ a widely accepted marker of OECs acts as part of a signaling complex with the NgR could suggest otherwise. Hence the aim of the present work was first to determine whether OECs

express Nogo and its receptor NgR compared with their glial counterparts It is hypothesised that OECs will express a low level of Nogo and its receptor NgR and that it will be altered when OECs are transplanted into the injured spinal cord.

5.2. Materials and Methods

5.2.1. Cell Cultures

Primary cultures of OECs, ASTs and OLGs were prepared according to the protocols described in section 2.1.1 and 2.2.2. Purity was determined by counting cells labeled with the appropriate markers. Schwann cells (a gift from Adele Vincent) were prepared from the sciatic nerves of neonatal rats and cultured by a modification of a previously described protocol (Brockes et al., 1979). Schwann cells were estimated to be 95-98% pure based on $p75^{NTR}$ staining. For the *in vivo* studies OECs were encapsulated into polymer tubes and implanted into the injured spinal cords of adult rats as described in sections 3.2.2. and 3.2.3.

5.2.2. RNA Synthesis and Quantitation

A full description of RNA synthesis and quantitation procedures can be found in section 2.4.1.

5.2.3. Principle of Real-time RT-PCR using SYBR Green

SYBR green is a fluorescent double-stranded DNA (dsDNA) intercalating dye (Fig. 5.1). SYBR green is incorporated into the PCR reaction mix in addition to the regular reaction components (e.g. primers and Taq polymerase). SYBR green binds non-specifically to all dsDNA and its fluorescence intensity increases when in its bound state. In its unbound state SYBR green emits very little fluorescence. After each amplification cycle the amount of dsDNA product increases and the SYBR green signal intensifies proportionally to the amount of product generated.

The fact that SYBR green binds to any dsDNA can be both an advantage, or disadvantage. On the positive side SYBR green allows detection of any dsDNA and therefore be used in any amplification reaction. However the disadvantage is that both specific and non-specific products can generate a signal. Thus any mis-priming events or primer-dimer formation can generate a false positive signal.

5.2.4. Probe and Primer Design

To design primers for real-time RT-PCR a Genbank search was performed to locate all known mRNA sequences for each Nogo isoform and the NgR. The sequences were subjected to Blast analysis to show regions of overlap between the isoforms. A common primer set termed Nogo-ABC was designed to lie in the C-terminal region of the sequence found in all Nogo isoforms (Fig. 5.2) (Chen et al., 2000). Nogo-A primers were designed to lie in exon 3, a region specific to the Nogo-A isoform (Fig. 5.2). Although no unique sequence was found in Nogo-B, primers were designed to overlap a splice site in the Nogo-A sequence that produces the truncated Nogo-B sequence (Fig. 5.2). No

primers were designed to analyse Nogo-C as no unique regions of sequence or splice sites were identified. Specific NgR primers were also designed. All Nogo primer sequences are given in (Table 5.1). The GAPDH primers used are described in section 4.2.4.

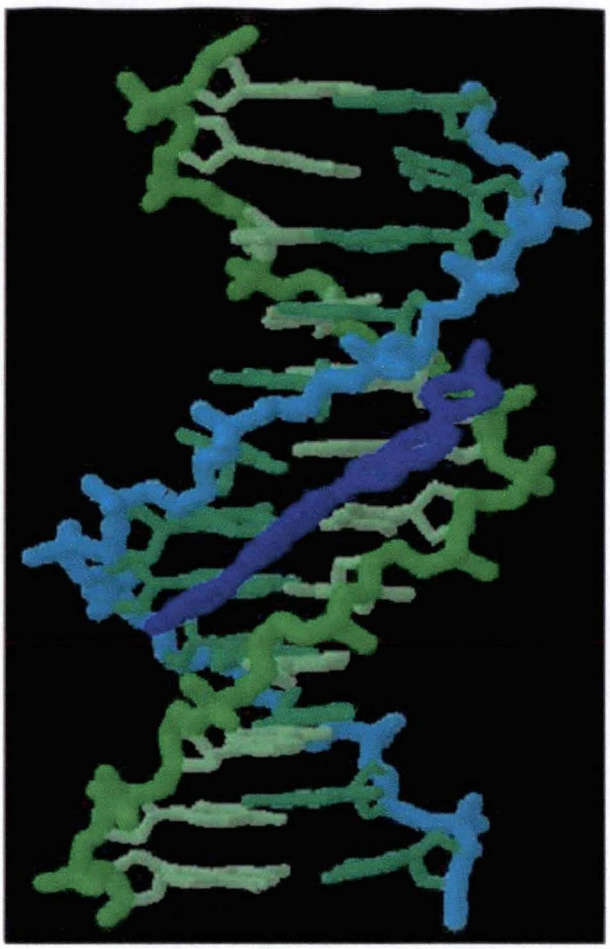

FIGURE 5.1. Schematic representation of the double-stranded DNA (dsDNA) intercalating dye, SYBR Green.

Shows SYBR Green (dark blue) incorporated into a dsDNA molecule (green and blue).

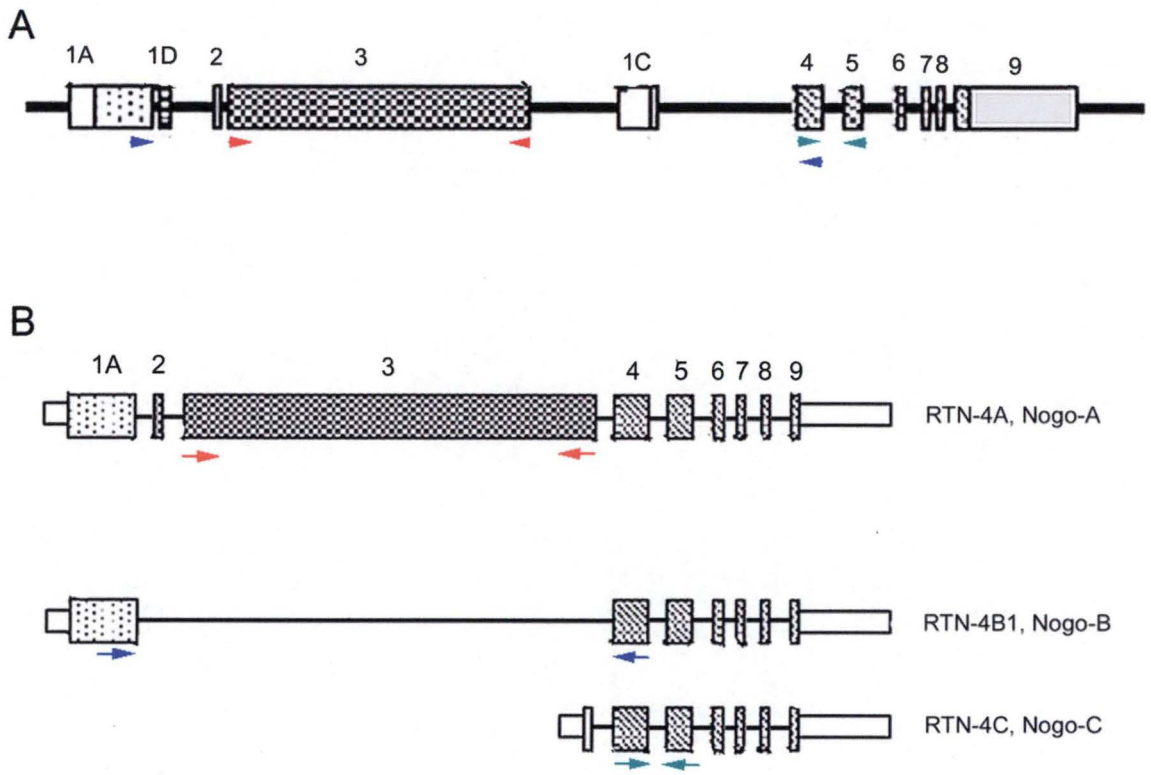

FIGURE 5.2. Schematic diagram of the mouse *nogo* gene showing primer locations.

(A) The locations of each primer set are shown as arrow heads. The Nogo-A primers are located in the Nogo-A specific exon 3, Nogo-B primers are located either side of the splice site that creates the truncated Nogo-B sequence, while the Nogo-ABC primers are located in the C-terminal region of the gene found in all Nogo isoforms. (B) Shows the three major isoforms of Nogo and the specific locations of the RT-PCR primers within each isoform. Modified from (Oertle et al., 2003a).

TABLE 5.1. Primer sequences for the Nogo isoforms.

Primers	Sequence (5'-3')	Target Length
Nogo-ABC forward	ATTGTAAGCTGCTGTGTATGGATCT	89
Nogo-ABC reverse	ACAGCTTTCCCCGAGTCCTT	
Nogo-A forward	TGTAGTGCAGCCCTTCACAG	199
Nogo-A reverse	GCACATCCCTACTTCCCTCA	
Nogo-B forward	GGCTCAGTGGTTGTTGACCT	208
Nogo-B reverse	GGCCTTCATCTGATTTCTGG	
NgR forward	ACAACACCTTCCGAGACCTG	194
NgR reverse	GGCAAAACGGGTAGAGGGTCA	

[1] Target length measured in base pairs.

5.2.5. RT-PCR Procedure

RT-PCR for Nogo and NgR was performed using the one-step QuantiTect™ SYBR® Green RT-PCR kit (Qiagen, Cat. No. 204243) according to the manufacturer's specifications. Each 25µl reaction contained ~50ng total RNA sample, 5mM $MgCl_2$, 1× RT-PCR master mix, 1× RT mix and 500nM primers (dependant on isoform). Reverse transcription was performed at 50°C for 30 minutes. Amplification reactions included an activation step of 15 minutes at 95°C to activate the Hot Start Taq Polymerase and were cycled at 94°C for 15 seconds and 60°C for 30 seconds for 30 cycles on a RotorGene 2000 thermal cycler (Corbett Research).

5.2.6. PCR Optimisation

Amplification of specific products and prevention of primer-dimer formation using SYBR green was found to be particularly dependent upon primer concentration. Excessive concentrations of primer inhibited the PCR amplification process and often resulted in a change in product melting temperature (T_m). SYBR green binds to any dsDNA hence the formation of primer-dimer products that occurs when excess primer concentrations are present can generate a signal and affect the quantitation process. Therefore to minimise primer-dimer formation an appropriate primer dilution series was used for each RNA concentration in the standard curves (for example see below).

RNA Concentration (ng)	200	20	2.0	0.2	0.02
Primer Concentration (nM)	500	400	300	200	100

5.2.7. Data Analysis

Relative quantitation of real-time RT-PCR data was performed as described in section 4.2.6. Statistical significance was determined where appropriate by student's t-test, where a p value of less than 0.05 was considered significant.

5.2.8. Product Characterisation

As SYBR green binds non-specifically to dsDNA molecules melt curve analysis was performed to ensure that the correct mRNAs were amplified. Melt curves were used to determine the specific T_m of the product and to ensure that there was little or no interference from primer-dimer formation. During melt curve analysis the temperature is raised slowly from a low temperature (ie. 65°C) to a high temperature (ie. 95°C). At low temperatures the RT-PCR products are double-stranded and SYBR Green binds to them emitting an intense fluorescent signal, hence at high temperatures RT-PCR products are denatured (or single-stranded) resulting in a rapid decrease in fluorescent signal. Fluorescence intensity is measured as the temperature increases and is plotted against temperature (Fig. 5.3). By plotting dF/dT of the fluorescence intensity against temperature a single peak is created which corresponds to the specific T_m of the product. The presence of other peaks would indicate the presence of non-specific products or primer-dimer formation.

To verify that there was no interference from primer-dimer formation or non-specific products all PCR products were separated on the basis of size by agarose gel electrophoresis on a 1.5% gel. The separated products were stained with ethidium bromide and visualised under UV light. The sizes of the products were determined by

comparing the products to a set of size standards separated on the same gel. If the product size correspondes to the known size, the correct product was amplified. Hence the presence of bands that were not the correct size could indicate the presence of non-specific products or primer-dimers.

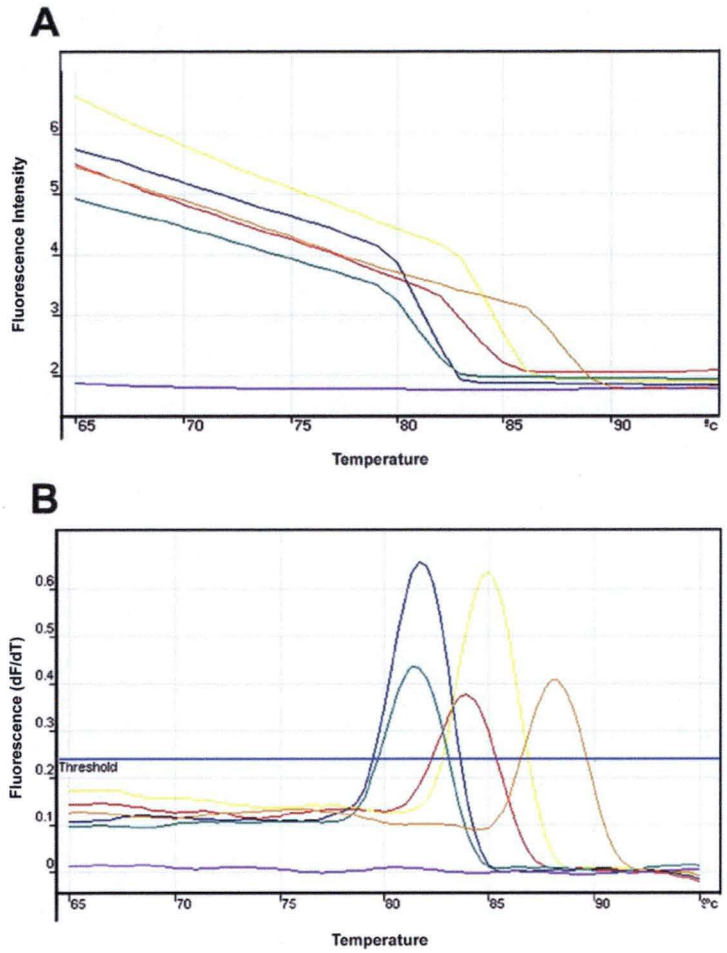

FIGURE 5.3. Melt curve analysis of the Nogo isoforms.

During melt curve analysis the fluorescence intensity of the product is measured at increasing temperatures. The fluorescence signal decreases dramatically at the temperature at which the product becomes denatured and is equivalent to the melting temperature (T_m) of that product (A). The dF/dT of fluorescence intensity is then plotted against temperature which shows a peak at the specific T_m of the product. Melt curve analysis of GAPDH 84°C, Nogo-A 81°C, Nogo-B 85°C, Nogo-ABC 81°C, NgR 88°C. The no template control (NTC) (B) shows a lack of primer-dimer and non-specific product formation.

5.2.9. Immunocytochemical Analysis of OECs for Nogo-A and NgR

For immunocytochemical analysis cultured OECs and OLGs were plated onto 13 mm diameter glass coverslips at a density of 1×10^4 per coverslip. Cells were fixed with phosphate buffered 4% paraformaldehyde for 15 minutes at room temperature. After washing three times in 0.1 M phosphate buffered saline (PBS; pH 7.4) the cells were incubated with DAKO® protein blocking solution. The cells were incubated with polyclonal goat anti-Nogo-A (S-19) or Nogo (I-20) (Santa Cruz) at a final concentration of 10μg/ml in PBS containing 0.3% triton-X 100 for 1 hour at room temperature. The negative controls were incubated with PBS containing 0.3% triton-X 100 without primary antibody. Cells were rinsed three times and incubated with a donkey anti-goat Alexa Fluor 594 conjugated secondary antibody diluted 1:2000 in PBS containing triton-X 100 for 45 minutes at room temperature. Cells were counterstained with 0.01% Nuclear Yellow and mounted with DAKO® Fluorescent Mounting Medium. They were then examined by fluorescent microscopy using an Olympus BX50 microscope with the appropriate filter for the dye conjugated to the secondary antibody. The cells were imaged with an Olympus DP50 digital camera.

For analysis of the NgR cultured OECs as described above were incubated with goat polyclonal anti-NgR (Santa Cruz) at a final concentration of 10μg/ml in PBS for 1 hour at 37°C. Controls were incubated in PBS without primary antibody. Cells were then post-fixed with phosphate buffered 4% paraformaldehyde for 15 minutes at room temperature. After three washes in PBS cells were incubated with a donkey anti-goat Alexa Fluor 594 (Molecular Probes) conjugated secondary antibody diluted 1:2000 in

PBS for 45 minutes at room temperature. Cells were counterstained with 0.01% Nuclear Yellow. Coverslips were mounted and examined as described above.

5.3. Results

5.3.1. Comparison of Nogo and NgR Expression in OECs and Other Glial Cell Types.

Expression of Nogo and its receptor NgR was examined by real-time RT-PCR analysis in cultured OECs, ASTs and SCs and normalised to GAPDH (Table 5.2). Nogo expression in OECs, ASTs and SCs was calculated relative to OLGs (Table 5.3). Oligodendrocytes were used as the calibrator cell type since they are known to express Nogo. Like OLGs, OECs, AST and SCs expressed Nogo mRNA (Fig. 5.4). These findings were in direct contrast to other reports suggesting that SCs and ASTs do not express Nogo (Josephson et al., 2001; Huber et al., 2002). Each cell type expressed Nogo-A, Nogo-B and Nogo-ABC mRNA. Unsurprisingly OECs, SCs and ASTs expressed 0.7 ± 0.1×, 0.5 ± 0.01× and 0.1 ± 0.01× lower levels of Nogo-A compared with OLGs (Fig. 5.4A and Table 5.3). Yet OECs expressed 2.9 ± 0.2× as much Nogo-B (Fig. 5.4B) and 1.6 ± 0.5× as much Nogo-ABC (Fig. 5.4C) levels than OLGs (Table 5.3). Similarly SCs expressed 1.1 ± 0.2× as much Nogo-B but less Nogo-ABC compared with OLGs while astrocytes expressed less Nogo-B and Nogo-ABC than OLGs (Table 5.3). Olfactory ensheathing cells, ASTs and SCs also expressed mRNA for the NgR (Fig. 5.4D), which was not detected in OLGs. This observation confirmed previous reports suggesting that OLGs lack the NgR (Josephson et al., 2002).

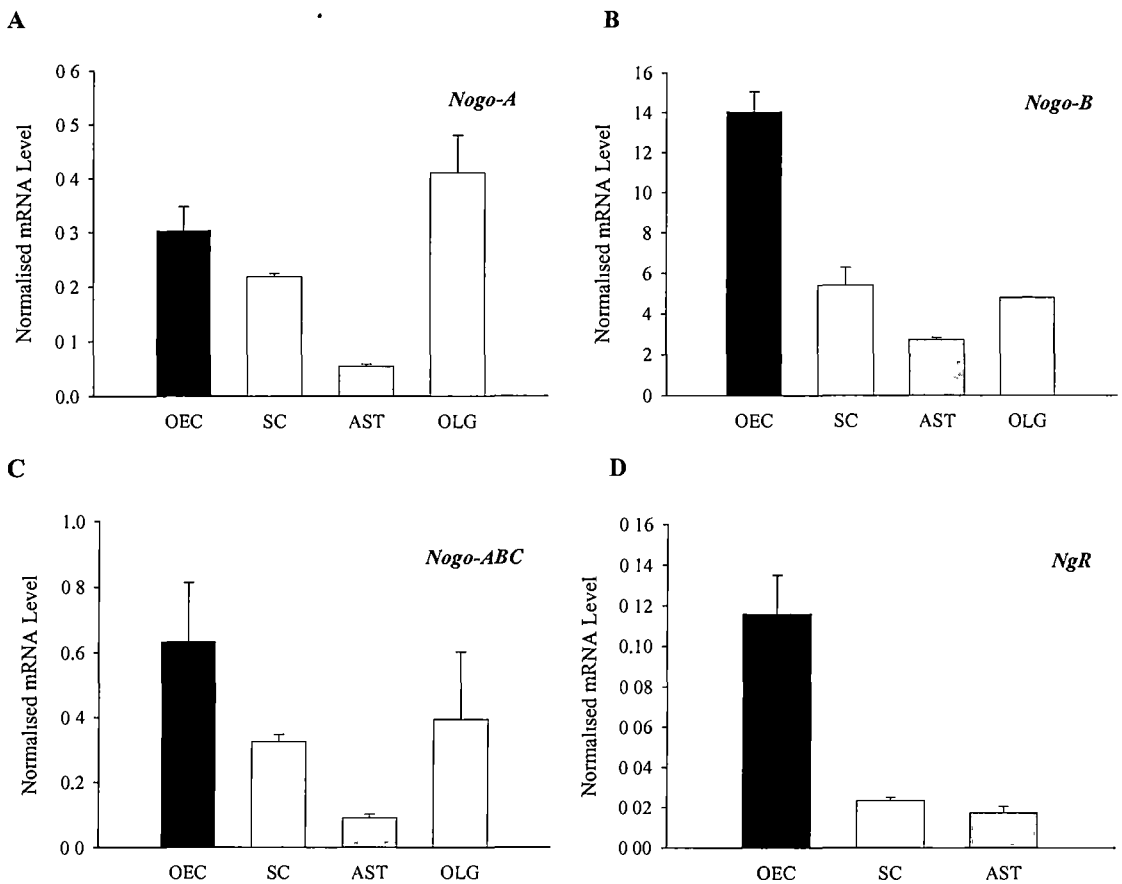

FIGURE 5.4. Nogo and NgR mRNA expression in primary cultures of olfactory ensheathing cells (OECs) and other glial cell types.

Primary cultures of OECs, ASTs, SCs and OLGs. Levels of Nogo-A (A), Nogo-B (B) Nogo-ABC (C) and NgR (D) were examined in each cell type by real-time RT-PCR using SYBR green. Error bars represent standard deviation.

5.3.2. Quantitation of Nogo Expression after Implantation into the Injured Spinal Cord.

To determine if Nogo expression in OECs was affected by implantation into the injured spinal cord OECs were encapsulated and maintained *in vitro* (OEC C) or implanted into the lesioned spinal cord for one week (OEC CI) (Table 5.2). Expression levels for implanted OECs were calculated relative to *in vitro* OECs (Table 5.4). After encapsulation OECs retained expression of Nogo-A, Nogo-B and Nogo-ABC mRNAs (Fig. 5.5). However implantation resulted in a significant increase in the expression level of Nogo-A (2.8 ± 0.7×) (p = 0.012) (Fig. 5.5A) and Nogo-B (p <0.001) (17.1 ± 2.9×) (Figure 5.5B and Table 5.4)) and a significant decrease in Nogo-ABC (p = 0.039) (0.2 ± 0.1×) (Fig. 5.5C and Table 5.4) compared with encapsulated cells maintained *in vitro*. Unlike normal cultured OECs, encapsulated OECs lacked NgR expression, which remained unchanged after implantation into the injured spinal cord.

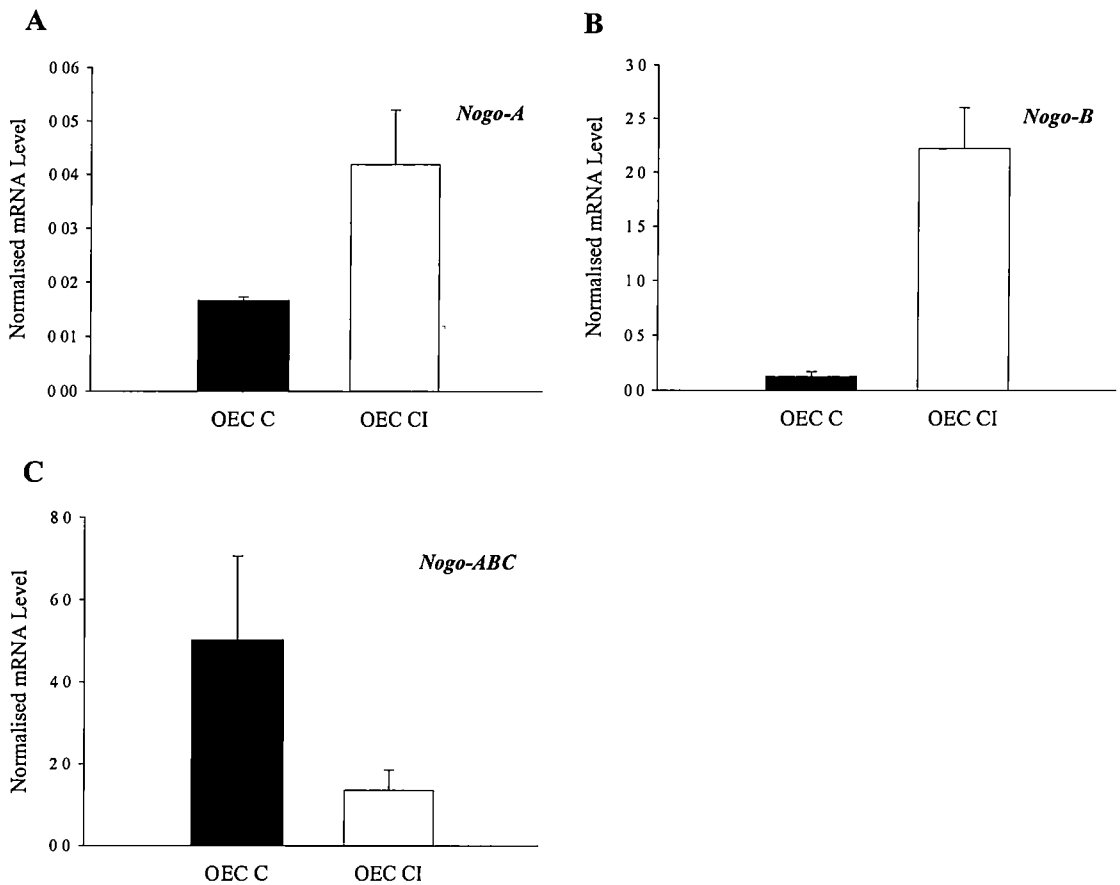

FIGURE 5.5. The effect of the injured rat spinal cord on Nogo mRNA expression in encapsulated olfactory ensheathing cells (OECs).

Encapsulated OECs were analysed for Nogo-A (A), Nogo-B (B), Nogo-ABC and NgR (C) by real-time RT-PCR after implantation into the spinal cord for one week (OEC CI). As a comparison un-implanted encapsulated OECs were analysed after one week in MEM D-valine supplemented with 10% dFCS at 37°C, 5%CO_2 (OEC C). Error bars represent standard deviation.

TABLE 5.2. Normalised expression levels of Nogo and NgR in encapsulated and/or cultured olfactory ensheathing cells (OECs), astrocytes (ASTs) and Schwann cells (SCs).

TARGET	OEC C	OEC CI	OEC	OLG	SC	AST
Nogo-A	0.015 ± 0.002	0.042 ± 0.010	0.303 ± 0.044	0.409 ± 0.070	0.218 ± 0.006	0.054 ± 0.004
Nogo-B	0.130 ± 0.041	2.219 ± 0.382	14.04 ± 1.018	4.79 ± 0.379	5.41 ± 0.875	2.74 ± 0.100
Nogo-ABC	5.016 ± 2.040	1.355 ± 0.496	0.633 ± 0.180	0.394 ± 0.207	0.325 ± 0.022	0.091 ± 0.011
NgR	ND	ND	0.116 ± 0.019	ND	0.023 ± 0.002	0.017 ± 0.003

[1] The presence of ND indicates that the isoform was not detected.
[2] Normalised mRNA levels are given in arbitrary units ± standard deviation.
[3] Encapsulated OECs maintained *in vitro* (OEC C) were compared with encapsulated cells implanted into the injured spinal cord (OEC CI).

TABLE 5.3. Expression levels of Nogo in olfactory ensheathing cells (OECs), astrocytes (ASTs) and Schwann cells (SCs) relative to oligodendrocytes (OLGs).

TARGET	OEC	SC	AST
Nogo-A	0.7 ± 0.1	0.5 ± 0.01	0.1 ± 0.01
Nogo-B	2.9 ± 0.2	1.1 ± 0.2	0.6 ± 0.02
Nogo-ABC	1.6 ± 0.5	0.8 ± 0.06	0.2 ± 0.03

TABLE 5.4. Expression levels of Nogo in implanted encapsulated OECs (OEC CI) relative to encapsulated OECs maintained *in vitro*.

TARGET	OEC CI
Nogo-A	2.8 ± 0.7
Nogo-B	17.1 ± 2.9
Nogo-ABC	0.2 ± 0.1

[1]Relative expression levels were calculated by dividing the normalised expression values of the test samples by the normalised expression values of the calibrator sample.
[2] Assuming that the calibrator has an expression value of 1 the test samples have an *n*-fold change (see above) in target expression.

5.3.3. Cultured OECs Express Nogo-A Protein

RT-PCR analysis demonstrated that cultured OECs, regardless of whether they are encapsulated and implanted in the spinal cord or not, consistently express Nogo (Table 5.2). In contrast, NgR mRNA was only present in unencapsulated OECs (Fig. 5.4). Immunocytochemical analysis of cultured OECs from flasks revealed that the cells were positive for Nogo-A (Fig. 5.6) and negative for NgR. Similarly cultured OLGs were immunopositive for Nogo-A (Fig. 5.6) and negative for NgR. Interestingly Nogo-A in cultured OECs could only be detected after the cells were permeabilised, suggesting that Nogo-A was intracellular (Fig. 5.7). However in OLGs Nogo-A was detected with or without permeabilising the cells, indicating that the protein was probably both intra- and extracellular. This finding confirms previous reports suggesting that Nogo-A protein is largely intracellular in OLGs with small amounts reaching the extracellular surface (GrandPre et al., 2000).

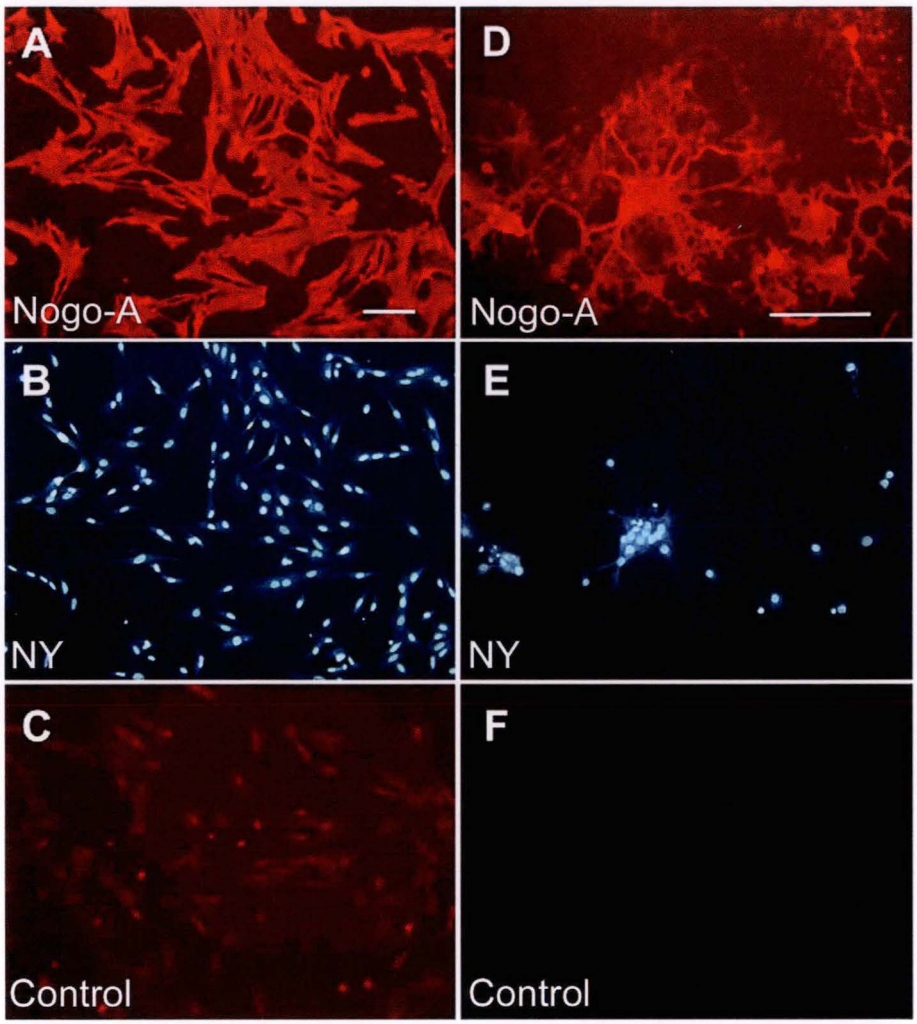

FIGURE 5.6. Nogo-A protein expression in cultured olfactory ensheathing cells (OECs) and oligodendrocytes (OLGs) permeabilised with Triton X-100.

Immunofluorescence staining for Nogo-A protein in OECs (A) and OLGs (D). Nogo-A was detected in OECs only after permeabilisation with Triton X-100. Both cells types were counterstained with Nuclear Yellow (B and E). Controls in which the primary antibody was omitted were negative for both cell types (C and F). Scale bar, 100μm.

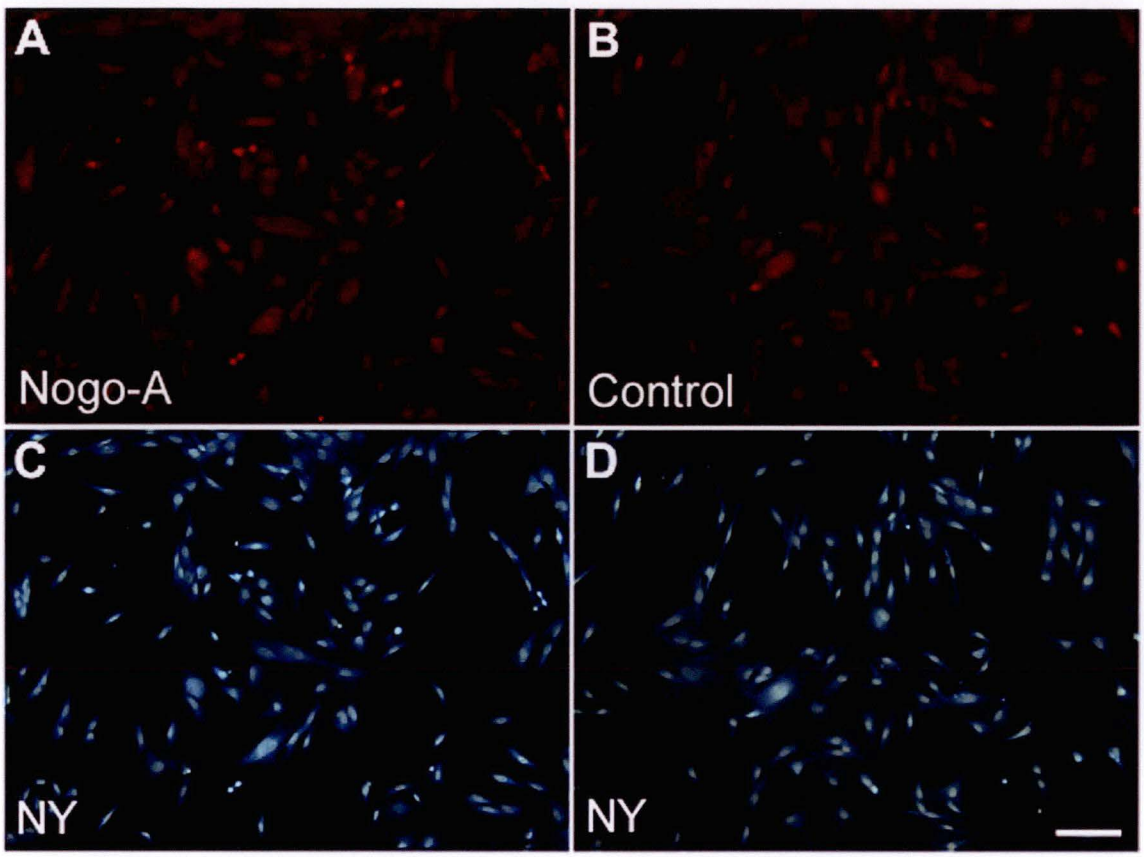

FIGURE 5.7. Lack of Nogo-A protein expression in unpermeabilised Olfactory Ensheathing Cells (OECs).

Unpermeabilised OECs showed negative staining for Nogo-A (A) when compared with controls in which the primary antibody was omitted (B). Cells were double labeled with Nuclear Yellow (C and D). Scale bar, 100μm

5.4. Discussion

The results of this study indicate that OECs express the inhibitory molecule Nogo and its receptor NgR. The expression pattern of Nogo transcripts appears to alter when OECs are implanted into the injured spinal cord. This provides further support for the theory that OEC phenotype is influenced by soluble factors intrinsic to the injured spinal cord and reflects their capacity for antigenic plasticity.

Cultured OECs, OLGs, SCs and ASTs were found to express Nogo-A, -B and -ABC mRNA transcripts. However one puzzling observation was that the sum of Nogo-ABC did not equal the sum of Nogo-A, Nogo-B (measured) and any Nogo-C (not measured) in each cell type (see Table 5.2). There are two possibilities that could account for this observation. First, each primer set amplified a separate region of the *nogo* gene hence their amplification efficiencies could vary. As a result of this Nogo-A, -B and -ABC levels were not compared within the same cell type. Second, because Nogo-C expression was not measured it is possible that any fluctuations in Nogo-C could be reflected in the Nogo-ABC level.

Cultured OECs, SCs and ASTs also expressed mRNA for the NgR, which was not detected in OLGs. The finding that SCs and ASTs express the NgR is in contrast to previous reports (Josephson et al., 2001; Huber et al., 2002; Josephson et al., 2002). This apparent discrepancy could be due to the different techniques used in the previous studies. To confirm these findings immunocytochemical analysis of Nogo-A and NgR was performed on OECs *in vitro*. Olfactory ensheathing cells were positive for the Nogo-A protein (which was found to be intracellular), but negative for the NgR protein.

Implantation of encapsulated OECs into the injured spinal cord resulted in a significant increase in Nogo-A, and Nogo-B and a decrease in Nogo-ABC mRNA expression when compared with encapsulated OECs maintained *in vitro*. These changes may have been due to up- or down-regulation of Nogo in response to unknown injury associated factors. Because the effects of very few lesion-induced factors have been described for OECs it is not known which of these specifically influenced Nogo expression.

It was notable that NgR mRNA was present in cultured OECs in flasks but was not detected when the cells were encapsulated, either *in vitro* or when implanted. The underlying reasons for this are unclear, but observations from light and scanning electron microscopy suggest that there were distinct differences in the morphology between OECs cultured in flasks and those encapsulated. When cultured in flasks OECs flatten and elaborate processes (Vincent et al., 2003), but when placed in capsules many of them assume a round morphology (see chapter three). The difference in morphology could reflect a physiological difference possibly in the expression of cell membrane associated molecules such as the NgR.

Previous reports have shown that Nogo and its receptor NgR are present within the olfactory system (Josephson et al., 2001; Josephson et al., 2002; Tozaki et al., 2002). Nogo-A and Nogo-ABC were detected in the OB of fetal rats although no data regarding expression in neonatal or adult animals have been reported (Josephson et al., 2001). The NgR is expressed in the OB during embryonic development and in the adult mouse where it was localised to neurons of the mitral cell layer (Josephson et al., 2002). This may

suggest that Nogo plays an important role in restricting growth and plasticity in the developing olfactory system.

Schwann cells like OECs promote axonal growth and until now were thought not to express Nogo (Josephson et al., 2001). However an early report showed that IN-1 antibody staining (against Nogo) produced a similar distribution pattern to that of MBP and MAG, which are known to be expressed by SCs (Rubin et al., 1994). Furthermore it was demonstrated that MBP, MAG and IN-1 stained the sciatic nerve in which SCs reside. However IN-1 staining was observed only after pre-fixation of sciatic nerve tissue with formaldehyde (Rubin et al., 1994). Since then several studies have confirmed that Nogo-A, Nogo-B and Nogo-C are present within the sciatic nerve (Chen et al., 2000; GrandPre et al., 2002; Huber et al., 2002). Given that Nogo is present in SCs its expression in the sciatic nerve could be attributed at least in part to the presence of SCs.

The predicted topology of the Nogo protein suggests that there are two hypothetical means by which neurite inhibition could occur. Firstly the neurite growth inhibitory Nogo-66 domain was thought to be exposed to the extracellular surface (GrandPre et al., 2000) and secondly an inhibitory region in the N-terminus could potentially be located extracellularly (Chen et al., 2000). Recent studies of the Nogo-A protein have revealed a third possible inhibitory domain within the Nogo-A specific exon 3 (Oertle et al., 2003b). However there have been several studies suggesting that Nogo is primarily located intracellularly (Josephson et al., 2001; Taketomi et al., 2002; Jin et al., 2003). This is consistent with the finding that Nogo-A in OECs was detected only after permeabilisation of the cell membrane suggesting that it is intracellular. However in OLGs Nogo-A could be detected with or without permeabilisation of the cell membrane suggesting that the

protein is both intra- and extracellular. In contrast another study has shown that OLGs express Nogo in their cytoplasm but not on their plasma membrane or in the myelin sheath they produce (Taketomi et al., 2002).

At the present time we cannot rule out the possiblility that OEC-derived Nogo is inhibitory to axonal growth. It could be that these cells simply produce or secrete levels of Nogo that are well below that required to exert an inhibitory effect. Hence Nogo function could be dose-dependant whereby high levels inhibit growth and low levels restrict plasticity or alternatively have no noticeable effect. Similarly the inhibitory effects of OEC Nogo may be dependant upon its release into the extracellular environment as suggested for OLGs (Goldberg and Barres, 2000; GrandPre et al., 2000).

Many studies of Nogo function have focused on the inhibitory activity of Nogo-A expressed by OLGs and how this can be neutralized by application of the antibody IN-1 (Bregman et al., 1995; Brosamle et al., 2000). Recent studies suggest that Nogo expressed by OECs could have functional roles unrelated to those already identified.

CHAPTER SIX

Summary and Future Directions

6.1. Summary and Future Directions

In summary this study provides evidence that the injured spinal cord influences the morphology and gene expression of transplanted OECs. This study provides further support for the notion that OECs are an extremely plastic cell type and that this may underlie their ability to promote the growth of injured axons. In this section future experiments are proposed to address some of the uncertainties raised by these experiments well as new projects that can be initiated to investigate other areas.

In addition to the experiments proposed in chapter three, a more complete picture of OEC plasticity after implantation may be gained by including more control groups in the scanning electron microscopy (SEM) and real-time RT-PCR analyses. By implanting OEC-filled capsules near the uninjured as well as injured spinal cord the effect of both injury-associated factors and factors intrinsic to the spinal cord itself on OEC phenotype could be examined. Any differences between OECs in these two groups would be attributable to the presence of injury-associated factors.

By implanting empty capsules into the injured and uninjured spinal cord the influx of contaminating cells could be investigated. Comparison of empty capsules with the corresponding OEC-filled capsules from injured and uninjured spinal cord may have assisted with the identification and morphological analysis of OECs. Similarly any contribution by cellular contaminants to the gene expression profile of OECs from the

injured and uninjured spinal cord could be accounted for by subtracting the empty capsule values from the OEC-filled capsule values. In effect the resultant expression values may then be a better reflection of the presence of OECs not of contaminating cells.

Due to the growth promoting nature of OECs it was not expected that they would express Nogo and its receptor NgR. In contrast the presence of Nogo and the NgR in the developing olfactory system (Josephson et al., 2001; Josephson et al., 2002; Jin et al., 2003) along with the finding that $p75^{NTR}$ acts as part of a signaling complex with the NgR (Wang et al., 2002a) may indicate a role for expression of Nogo and NgR in OECs. In this study cultured OECs, SCs and ASTs were shown to express mRNA for Nogo and its receptor NgR. Moreover implantation into the injured spinal cord significantly increased the levels of Nogo-A and -B in OECs. The Nogo-A protein was also located intracellularly in OECs, although the NgR protein could not be detected.

Future studies will be necessary to investigate the presence of NgR protein in OECs *in vitro*. This could be assesed using different culture media and/or supplements to induce expression of the NgR. For example in a previous study morphological change was induced in OECs by addition of the membrane permeant cAMP analogue dibutyryl cAMP (dBcAMP) to serum-containing medium (Vincent et al., 2003). Similarly the effects of some growth factors on OECs in serum-containing medium can be potentiated by addition of the intracellular cAMP raising agent forskolin (FSK) (Yan et al., 2001b). Both dBcAMP and FSK are thought to exert their effects via activation of Rho-A and its downstream signalling cascade. Furthermore cultured SCs have been shown to proliferate in reponse to PDGF only when cultured in the presence of intracellular cAMP raising agents a response that has been attributed to a cAMP-mediated PDGF receptor

upregulation (Weinmaster and Lemke, 1990). Since the effects of Nogo are mediated by activation of Rho-A (Niederost et al., 2002; Fournier et al., 2003) which in turn is regulated by cAMP, addition of dBcAMP or FSK to OECs *in vitro* could potentially induce expression of the NgR.

If the presence of the NgR in OECs could be confirmed the effect of Nogo proteins on OECs and perhaps also SCs could be assessed by a series of *in vitro* assays. Cell morphology could be examined by light and scanning electron microscopic analysis of cells treated with different concentrations of Nogo-A, -B or -C protein compared with untreated cells. Similarly antigenic phenotype after treatment with Nogo-A, -B or -C proteins could be examined by immunofluorescence staining of treated and untreated cells for common OEC and SC markers (such as S-100, $p75^{NTR}$, N-CAM, P_0 and GFAP) and/or growth factor proteins (including GGF, BDNF, GDNF, NDF and CNTF). Proliferation could also be investigated by measuring bromodeoxyuridine uptake (BrdU) in Nogo-A, -B and -C treated cells compared with untreated cells. Such experiments would provide a starting point for a more intensive analysis of the role of Nogo in OECs and SCs.

The presence of Nogo in OECs opens up a new avenue of research. The function of Nogo in the olfactory system could be examined using Nogo deficient knockout (KO) mice. If Nogo plays a role in olfactory axon outgrowth any abnormalities could be identified by histology and/or immunohistochemistry of tissue sections from the olfactory systems of both adult and embryonic KO mice. Similarly the effects of the different isoforms on olfactory system development could be examined in mice deficient in a

single Nogo isoform. The olfactory system of Nogo KO mice would also provide a unique environment for investigating the role of Nogo in axonal growth after injury.

Because Nogo is inhibitory to axonal growth and plasticity its role in growth promoting cell types, such as OECs and SCs is unclear. Yet its location in OECs could be indicative of an unknown intracellular role. In fact a recent study has proposed a novel function for Nogo in vascular remodelling in particular for the enhanced migration of endothelial cells (Acevedo et al., 2004). Similarly another study reported that neurons of the sciatic nerve and spinal cord express Nogo-A mRNA and protein both before and after injury (Hunt et al., 2003) suggesting that Nogo-A expression does not necessarily correlate with a lack of regenerative potential.

REFERENCES

Acevedo L, Yu J, Erdjument-Bromage H, Miao RQ, Kim JE, Fulton D, Tempst P, Strittmatter SM, Sessa WC (2004) A new role for Nogo as a regulator of vascular remodeling. Nat Med 10:382-388.

Airaksinen MS, Titievsky A, Saarma M (1999) GDNF family neurotrophic factor signaling: four masters, one servant? Mol Cell Neurosci 13:313-325.

Alexander CL, Fitzgerald UF, Barnett SC (2002) Identification of growth factors that promote long-term proliferation of olfactory ensheathing cells and modulate their antigenic phenotype. Glia 37:349-364.

Andres R, Forgie A, Wyatt S, Chen Q, de Sauvage FJ, Davies AM (2001) Multiple effects of artemin on sympathetic neurone generation, survival and growth. Development 128:3685-3695.

Anton ES, Marchionni MA, Lee KF, Rakic P (1997) Role of GGF/neuregulin signaling in interactions between migrating neurons and radial glia in the developing cerebral cortex. Development 124:3501-3510.

Arquint M, Roder J, Chia LS, Down J, Wilkinson D, Bayley H, Braun P, Dunn R (1987) Molecular cloning and primary structure of myelin-associated glycoprotein. Proc Natl Acad Sci U S A 84:600-604.

Asher RA, Morgenstern DA, Fidler PS, Adcock KH, Oohira A, Braistead JE, Levine JM, Margolis RU, Rogers JH, Fawcett JW (2000) Neurocan is upregulated in injured brain and in cytokine-treated astrocytes. J Neurosci 20:2427-2438.

Au WW, Treloar HB, Greer CA (2002) Sublaminar organization of the mouse olfactory bulb nerve layer. J Comp Neurol 446:68-80.

Bahr M, Przyrembel C, Bastmeyer M (1995) Astrocytes from adult rat optic nerves are nonpermissive for regenerating retinal ganglion cell axons. Exp Neurol 131:211-220.

Baird A (1994) Fibroblast growth factors: activities and significance of non-neurotrophin neurotrophic growth factors. Curr Opin Neurobiol 4:78-86.

Baloh RH, Tansey MG, Lampe PA, Fahrner TJ, Enomoto H, Simburger KS, Leitner ML, Araki T, Johnson EM, Jr., Milbrandt J (1998) Artemin, a novel member of the GDNF ligand family, supports peripheral and central neurons and signals through the GFRalpha3-RET receptor complex. Neuron 21:1291-1302.

Bandtlow C, Zachleder T, Schwab ME (1990) Oligodendrocytes arrest neurite growth by contact inhibition. J Neurosci 10:3837-3848.

Barber PC, Lindsay RM (1982) Schwann cells of the olfactory nerves contain glial fibrillary acidic protein and resemble astrocytes. Neuroscience 7:3077-3090.

Bareyre FM, Schwab ME (2003) Inflammation, degeneration and regeneration in the injured spinal cord: insights from DNA microarrays. Trends Neurosci 26:555-563.

Bareyre FM, Haudenschild B, Schwab ME (2002) Long-lasting sprouting and gene expression changes induced by the monoclonal antibody IN-1 in the adult spinal cord. J Neurosci 22:7097-7110.

Barnett SC, Hutchins AM, Noble M (1993) Purification of olfactory nerve ensheathing cells from the olfactory bulb. Dev Biol 155:337-350.

Barnett SC, Alexander CL, Iwashita Y, Gilson JM, Crowther J, Clark L, Dunn LT, Papanastassiou V, Kennedy PG, Franklin RJ (2000) Identification of a human

olfactory ensheathing cell that can effect transplant-mediated remyelination of demyelinated CNS axons. Brain 123:1581-1588.

Bauer S, Rasika S, Han J, Mauduit C, Raccurt M, Morel G, Jourdan F, Benahmed M, Moyse E, Patterson PH (2003) Leukemia inhibitory factor is a key signal for injury-induced neurogenesis in the adult mouse olfactory epithelium. J Neurosci 23:1792-1803.

Bermingham-McDonogh O, Xu YT, Marchionni MA, Scherer SS (1997) Neuregulin Expression in PNS Neurons: Isoforms and Regulation by Target Interactions. Mol Cell Neurosci 10:184-195.

Bianco JI, Perry C, Harkin DG, Mackay-Sim A, Feron F (2004) Neurotrophin 3 promotes purification and proliferation of olfactory ensheathing cells from human nose. Glia 45:111-123.

Blochlinger S, Weinmann O, Schwab ME, Thallmair M (2001) Neuronal plasticity and formation of new synaptic contacts follow pyramidal lesions and neutralization of Nogo-A: a light and electron microscopic study in the pontine nuclei of adult rats. J Comp Neurol 433:426-436.

Boruch AV, Conners JJ, Pipitone M, Deadwyler G, Storer PD, Devries GH, Jones KJ (2001) Neurotrophic and migratory properties of an olfactory ensheathing cell line. Glia 33:225-229.

Bregman BS, Kunkel-Bagden E, Schnell L, Dai HN, Gao D, Schwab ME (1995) Recovery from spinal cord injury mediated by antibodies to neurite growth inhibitors. Nature 378:498-501.

Britsch S, Li L, Kirchhoff S, Theuring F, Brinkmann V, Birchmeier C, Riethmacher D (1998) The ErbB2 and ErbB3 receptors and their ligand, neuregulin-1, are essential for development of the sympathetic nervous system. Genes Dev 12:1825-1836.

Brockes JP, Fields KL, Raff MC (1979) Studies on cultured rat Schwann cells. I. Establishment of purified populations from cultures of peripheral nerve. Brain Res 165:105-118.

Brosamle C, Huber AB, Fiedler M, Skerra A, Schwab ME (2000) Regeneration of lesioned corticospinal tract fibers in the adult rat induced by a recombinant, humanized IN-1 antibody fragment. J Neurosci 20:8061-8068.

Buffo A, Zagrebelsky M, Huber AB, Skerra A, Schwab ME, Strata P, Rossi F (2000) Application of neutralizing antibodies against NI-35/250 myelin-associated neurite growth inhibitory proteins to the adult rat cerebellum induces sprouting of uninjured purkinje cell axons. J Neurosci 20:2275-2286.

Caggiano M, Kauer JS, Hunter DD (1994) Globose basal cells are neuronal progenitors in the olfactory epithelium: a lineage analysis using a replication-incompetent retrovirus. Neuron 13:339-352.

Cai D, Qiu J, Cao Z, McAtee M, Bregman BS, Filbin MT (2001) Neuronal cyclic AMP controls the developmental loss in ability of axons to regenerate. J Neurosci 21:4731-4739.

Calof AL, Chikaraishi DM (1989) Analysis of neurogenesis in a mammalian neuroepithelium: proliferation and differentiation of an olfactory neuron precursor in vitro. Neuron 3:115-127.

Calof AL, Lander AD (1991) Relationship between neuronal migration and cell-substratum adhesion: laminin and merosin promote olfactory neuronal migration but are anti- adhesive. J Cell Biol 115:779-794.

Canoll PD, Kraemer R, Teng KK, Marchionni MA, Salzer JL (1999) GGF/neuregulin induces a phenotypic reversion of oligodendrocytes. Mol Cell Neurosci 13:79-94.

Canoll PD, Musacchio JM, Hardy R, Reynolds R, Marchionni MA, Salzer JL (1996) GGF/neuregulin is a neuronal signal that promotes the proliferation and survival and inhibits the differentiation of oligodendrocyte progenitors. Neuron 17:229-243.

Caroni P, Schwab ME (1988a) Antibody against myelin-associated inhibitor of neurite growth neutralizes nonpermissive substrate properties of CNS white matter. Neuron 1:85-96.

Caroni P, Schwab ME (1988b) Two membrane protein fractions from rat central myelin with inhibitory properties for neurite growth and fibroblast spreading. J Cell Biol 106:1281-1288.

Carraway KL, 3rd, Weber JL, Unger MJ, Ledesma J, Yu N, Gassmann M, Lai C (1997) Neuregulin-2, a new ligand of ErbB3/ErbB4-receptor tyrosine kinases. Nature 387:512-516.

Chang H, Riese DJ, 2nd, Gilbert W, Stern DF, McMahan UJ (1997) Ligands for ErbB-family receptors encoded by a neuregulin-like gene. Nature 387:509-512.

Chao MV (1994) The p75 neurotrophin receptor. J Neurobiol 25:1373-1385.

Chen MS, Huber AB, van der Haar ME, Frank M, Schnell L, Spillmann AA, Christ F, Schwab ME (2000) Nogo-A is a myelin-associated neurite outgrowth inhibitor and an antigen for monoclonal antibody IN-1. Nature 403:434-439.

Cheng L, Esch FS, Marchionni MA, Mudge AW (1998) Control of Schwann cell survival and proliferation: autocrine factors and neuregulins. Mol Cell Neurosci 12:141-156.

Chuah MI, Au C (1991) Olfactory Schwann cells are derived from precursor cells in the olfactory epithelium. J Neurosci Res 29:172-180.

Chuah MI, Teague R (1999) Basic fibroblast growth factor in the primary olfactory pathway: mitogenic effect on ensheathing cells. Neuroscience 88:1043-1050.

Chuah MI, West AK (2002) Cellular and molecular biology of ensheathing cells. Microsc Res Tech 58:216-227.

Chuah MI, Cossins J, Woodhall E, Tennent R, Nash G, West AK (2000) Glial growth factor 2 induces proliferation and structural changes in ensheathing cells. Brain Res 857:265-274.

Chuah MI, Choi-Lundberg D, Weston S, Vincent AJ, Chung RS, Vickers JC, West AK (2004) Olfactory ensheathing cells promote collateral axonal branching in the injured adult rat spinal cord. Exp Neurol 185:15-25.

David S, Aguayo AJ (1981) Axonal elongation into peripheral nervous system "bridges" after central nervous system injury in adult rats. Science 214:931-933.

Davies SJ, Field PM, Raisman G (1996) Regeneration of cut adult axons fails even in the presence of continuous aligned glial pathways. Exp Neurol 142:203-216.

Davis S, Aldrich TH, Valenzuela DM, Wong VV, Furth ME, Squinto SP, Yancopoulos GD (1991) The receptor for ciliary neurotrophic factor. Science 253:59-63.

DeBellard ME, Tang S, Mukhopadhyay G, Shen YJ, Filbin MT (1996) Myelin-associated glycoprotein inhibits axonal regeneration from a variety of neurons via interaction with a sialoglycoprotein. Mol Cell Neurosci 7:89-101.

Dechant G, Barde YA (1997) Signalling through the neurotrophin receptor p75NTR. Curr Opin Neurobiol 7:413-418.

Dechant G, Tsoulfas P, Parada LF, Barde YA (1997) The neurotrophin receptor p75 binds neurotrophin-3 on sympathetic neurons with high affinity and specificity. J Neurosci 17:5281-5287.

Del Pozo MA, Kiosses WB, Alderson NB, Meller N, Hahn KM, Schwartz MA (2002) Integrins regulate GTP-Rac localized effector interactions through dissociation of Rho-GDI. Nat Cell Biol 4:232-239.

Devon R, Doucette R (1992) Olfactory ensheathing cells myelinate dorsal root ganglion neurites. Brain Res 589:175-179.

Domeniconi M, Cao Z, Spencer T, Sivasankaran R, Wang K, Nikulina E, Kimura N, Cai H, Deng K, Gao Y, He Z, Filbin M (2002) Myelin-associated glycoprotein interacts with the Nogo66 receptor to inhibit neurite outgrowth. Neuron 35:283-290.

Dong Z, Brennan A, Liu N, Yarden Y, Lefkowitz G, Mirsky R, Jessen KR (1995) Neu differentiation factor is a neuron-glia signal and regulates survival, proliferation, and maturation of rat Schwann cell precursors. Neuron 15:585-596.

Doucette JR, Kiernan JA, Flumerfelt BA (1983) The re-innervation of olfactory glomeruli following transection of primary olfactory axons in the central or peripheral nervous system. J Anat 137:1-19.

Doucette R (1990) Glial influences on axonal growth in the primary olfactory system. Glia 3:433-449.

Doucette R (1991) PNS-CNS transitional zone of the first cranial nerve. J Comp Neurol 312:451-466.

Doucette R (1993) Glial cells in the nerve fiber layer of the main olfactory bulb of embryonic and adult mammals. Microsc Res Tech 24:113-130.

Doucette R (1995) Olfactory ensheathing cells: potential for glial cell transplantation into areas of CNS injury. Histol Histopathol 10:503-507.

Doucette R (1996) Immunohistochemical localization of laminin, fibronectin and collagen type IV in the nerve fiber layer of the olfactory bulb. Int J Dev Neurosci 14:945-959.

Doucette R, Devon R (1994) Media that support the growth and differentiation of oligodendrocytes do not induce olfactory ensheathing cells to express a myelinating phenotype. Glia 10:296-310.

Doucette R, Devon R (1995) Elevated intracellular levels of cAMP induce olfactory ensheathing cells to express GAL-C and GFAP but not MBP. Glia 13:130-140.

Emerick AJ, Neafsey EJ, Schwab ME, Kartje GL (2003) Functional reorganization of the motor cortex in adult rats after cortical lesion and treatment with monoclonal antibody IN-1. J Neurosci 23:4826-4830.

Erickson SL, O'Shea KS, Ghaboosi N, Loverro L, Frantz G, Bauer M, Lu LH, Moore MW (1997) ErbB3 is required for normal cerebellar and cardiac development: a comparison with ErbB2-and heregulin-deficient mice. Development 124:4999-5011.

Ernfors P, Wetmore C, Olson L, Persson H (1990) Identification of cells in rat brain and peripheral tissues expressing mRNA for members of the nerve growth factor family. Neuron 5:511-526.

Falls DL (2003) Neuregulins: functions, forms, and signaling strategies. Exp Cell Res 284:14-30.

Falls DL, Rosen KM, Corfas G, Lane WS, Fischbach GD (1993) ARIA, a protein that stimulates acetylcholine receptor synthesis, is a member of the neu ligand family. Cell 72:801-815.

Farbman AI (1990) Olfactory neurogenesis: genetic or environmental controls? Trends Neurosci 13:362-365.

Flores AI, Mallon BS, Matsui T, Ogawa W, Rosenzweig A, Okamoto T, Macklin WB (2000) Akt-mediated survival of oligodendrocytes induced by neuregulins. J Neurosci 20:7622-7630.

Fournier AE, GrandPre T, Strittmatter SM (2001) Identification of a receptor mediating Nogo-66 inhibition of axonal regeneration. Nature 409:341-346.

Fournier AE, Takizawa BT, Strittmatter SM (2003) Rho kinase inhibition enhances axonal regeneration in the injured CNS. J Neurosci 23:1416-1423.

Fournier AE, Gould GC, Liu BP, Strittmatter SM (2002) Truncated soluble Nogo receptor binds Nogo-66 and blocks inhibition of axon growth by myelin. J Neurosci 22:8876-8883.

Franceschini IA, Barnett SC (1996) Low-affinity NGF-receptor and E-N-CAM expression define two types of olfactory nerve ensheathing cells that share a common lineage. Dev Biol 173:327-343.

Francis A, Raabe TD, Wen D, DeVries GH (1999) Neuregulins and ErbB receptors in cultured neonatal astrocytes. J Neurosci Res 57:487-494.

Franklin RJ, Gilson JM, Franceschini IA, Barnett SC (1996) Schwann cell-like myelination following transplantation of an olfactory bulb-ensheathing cell line into areas of demyelination in the adult CNS. Glia 17:217-224.

Gage FH, Armstrong DM, Williams LR, Varon S (1988) Morphological response of axotomized septal neurons to nerve growth factor. J Comp Neurol 269:147-155.

Gall CM, Berschauer R, Isackson PJ (1994) Seizures increase basic fibroblast growth factor mRNA in adult rat forebrain neurons and glia. Brain Res Mol Brain Res 21:190-205.

Gassmann M, Lemke G (1997) Neuregulins and neuregulin receptors in neural development. Curr Opin Neurobiol 7:87-92.

Gassmann M, Casagranda F, Orioli D, Simon H, Lai C, Klein R, Lemke G (1995) Aberrant neural and cardiac development in mice lacking the ErbB4 neuregulin receptor. Nature 378:390-394.

Gearing DP, Bruce AG (1992) Oncostatin M binds the high-affinity leukemia inhibitory factor receptor. New Biol 4:61-65.

Gearing DP, Thut CJ, VandeBos T, Gimpel SD, Delaney PB, King J, Price V, Cosman D, Beckmann MP (1991) Leukemia inhibitory factor receptor is structurally related to the IL-6 signal transducer, gp130. Embo J 10:2839-2848.

Gearing DP, Comeau MR, Friend DJ, Gimpel SD, Thut CJ, McGourty J, Brasher KK, King JA, Gillis S, Mosley B, et al. (1992) The IL-6 signal transducer, gp130: an oncostatin M receptor and affinity converter for the LIF receptor. Science 255:1434-1437.

Getchell TV, Shah DS, Partin JV, Subhedar NK, Getchell ML (2002) Leukemia inhibitory factor mRNA expression is upregulated in macrophages and olfactory receptor neurons after target ablation. J Neurosci Res 67:246-254.

Gilbert M, Smith J, Roskams AJ, Auld VJ (2001) Neuroligin 3 is a vertebrate gliotactin expressed in the olfactory ensheathing glia, a growth-promoting class of macroglia. Glia 34:151-164.

Goldberg JL, Barres BA (2000) Nogo in nerve regeneration. Nature 403:369-370.

Gomez-Pinilla F, Cotman CW (1993) Distribution of fibroblast growth factor 5 mRNA in the rat brain: an in situ hybridization study. Brain Res 606:79-86.

Gong Q, Shipley MT (1996) Expression of extracellular matrix molecules and cell surface molecules in the olfactory nerve pathway during early development. J Comp Neurol 366:1-14.

GrandPre T, Li S, Strittmatter SM (2002) Nogo-66 receptor antagonist peptide promotes axonal regeneration. Nature 417:547-551.

GrandPre T, Nakamura F, Vartanian T, Strittmatter SM (2000) Identification of the Nogo inhibitor of axon regeneration as a Reticulon protein. Nature 403:439-444.

Graziadei PP, Graziadei GA (1979) Neurogenesis and neuron regeneration in the olfactory system of mammals. I. Morphological aspects of differentiation and structural organization of the olfactory sensory neurons. J Neurocytol 8:1-18.

Grinspan JB, Marchionni MA, Reeves M, Coulaloglou M, Scherer SS (1996) Axonal interactions regulate Schwann cell apoptosis in developing peripheral nerve: neuregulin receptors and the role of neuregulins. J Neurosci 16:6107-6118.

Gudino-Cabrera G, Nieto-Sampedro M (1996) Ensheathing cells: Large scale purification from adult olfactory bulb, freeze-preparation and migration of transplanted cells in adult brain. Restorative Neurology and Neuroscience 10:25-34.

Gudino-Cabrera G, Pastor AM, de la Cruz RR, Delgado-Garcia JM, Nieto-Sampedro M (2000) Limits to the capacity of transplants of olfactory glia to promote axonal regrowth in the CNS. Neuroreport 11:467-471.

Guth L (1974) Axonal regeneration and functional plasticity in the central nervous system. Exp Neurol 45:606-654.

Hall A (1994) Small GTP-binding proteins and the regulation of the actin cytoskeleton. Annu Rev Cell Biol 10:31-54.

Harari D, Tzahar E, Romano J, Shelly M, Pierce JH, Andrews GC, Yarden Y (1999) Neuregulin-4: a novel growth factor that acts through the ErbB-4 receptor tyrosine kinase. Oncogene 18:2681-2689.

Hartikka J, Hefti F (1988) Development of septal cholinergic neurons in culture: plating density and glial cells modulate effects of NGF on survival, fiber growth, and expression of transmitter-specific enzymes. J Neurosci 8:2967-2985.

Hatanaka H, Tsukui H, Nihonmatsu I (1988) Developmental change in the nerve growth factor action from induction of choline acetyltransferase to promotion of cell survival in cultured basal forebrain cholinergic neurons from postnatal rats. Brain Res 467:85-95.

Hefti F (1986) Nerve growth factor promotes survival of septal cholinergic neurons after fimbrial transections. J Neurosci 6:2155-2162.

Hilton DJ, Hilton AA, Raicevic A, Rakar S, Harrison-Smith M, Gough NM, Begley CG, Metcalf D, Nicola NA, Willson TA (1994) Cloning of a murine IL-11 receptor alpha-chain; requirement for gp130 for high affinity binding and signal transduction. Embo J 13:4765-4775.

Hisaoka T, Morikawa Y, Kitamura T, Senba E (2004) Expression of a member of tumor necrosis factor receptor superfamily, TROY, in the developing olfactory system. Glia 45:313-324.

Ho WH, Armanini MP, Nuijens A, Phillips HS, Osheroff PL (1995) Sensory and motor neuron-derived factor. A novel heregulin variant highly expressed in sensory and motor neurons. J Biol Chem 270:14523-14532.

Hoffman GR, Nassar N, Cerione RA (2000) Structure of the Rho family GTP-binding protein Cdc42 in complex with the multifunctional regulator RhoGDI. Cell 100:345-356.

Honma Y, Araki T, Gianino S, Bruce A, Heuckeroth R, Johnson E, Milbrandt J (2002) Artemin is a vascular-derived neurotropic factor for developing sympathetic neurons. Neuron 35:267-282.

Horger BA, Nishimura MC, Armanini MP, Wang LC, Poulsen KT, Rosenblad C, Kirik D, Moffat B, Simmons L, Johnson E, Jr., Milbrandt J, Rosenthal A, Bjorklund A, Vandlen RA, Hynes MA, Phillips HS (1998) Neurturin exerts potent actions on survival and function of midbrain dopaminergic neurons. J Neurosci 18:4929-4937.

Huber AB, Weinmann O, Brosamle C, Oertle T, Schwab ME (2002) Patterns of Nogo mRNA and protein expression in the developing and adult rat and after CNS lesions. J Neurosci 22:3553-3567.

Hunt D, Mason MR, Campbell G, Coffin R, Anderson PN (2002) Nogo receptor mRNA expression in intact and regenerating CNS neurons. Mol Cell Neurosci 20:537-552.

Hunt D, Coffin RS, Prinjha RK, Campbell G, Anderson PN (2003) Nogo-A expression in the intact and injured nervous system. Mol Cell Neurosci 24:1083-1102.

Imaizumi T, Lankford KL, Waxman SG, Greer CA, Kocsis JD (1998) Transplanted olfactory ensheathing cells remyelinate and enhance axonal conduction in the demyelinated dorsal columns of the rat spinal cord. J Neurosci 18:6176-6185.

Ip NY, Yancopoulos GD (1996) The neurotrophins and CNTF: two families of collaborative neurotrophic factors. Annu Rev Neurosci 19:491-515.

Iwashita Y, Fawcett JW, Crang AJ, Franklin RJ, Blakemore WF (2000) Schwann cells transplanted into normal and X-irradiated adult white matter do not migrate extensively and show poor long-term survival. Exp Neurol 164:292-302.

Jin WL, Liu YY, Liu HL, Yang H, Wang Y, Jiao XY, Ju G (2003) Intraneuronal localization of Nogo-A in the rat. J Comp Neurol 458:1-10.

Jones LL, Yamaguchi Y, Stallcup WB, Tuszynski MH (2002) NG2 is a major chondroitin sulfate proteoglycan produced after spinal cord injury and is expressed by macrophages and oligodendrocyte progenitors. J Neurosci 22:2792-2803.

Josephson A, Widenfalk J, Widmer HW, Olson L, Spenger C (2001) NOGO mRNA expression in adult and fetal human and rat nervous tissue and in weight drop injury. Exp Neurol 169:319-328.

Josephson A, Trifunovski A, Widmer HR, Widenfalk J, Olson L, Spenger C (2002) Nogo-receptor gene activity: cellular localization and developmental regulation of mRNA in mice and humans. J Comp Neurol 453:292-304.

Kafitz KW, Greer CA (1999) Olfactory ensheathing cells promote neurite extension from embryonic olfactory receptor cells in vitro. Glia 25:99-110.

Kato T, Honmou O, Uede T, Hashi K, Kocsis JD (2000) Transplantation of human olfactory ensheathing cells elicits remyelination of demyelinated rat spinal cord. Glia 30:209-218.

Kelm S, Pelz A, Schauer R, Filbin MT, Tang S, de Bellard ME, Schnaar RL, Mahoney JA, Hartnell A, Bradfield P, et al. (1994) Sialoadhesin, myelin-associated glycoprotein and CD22 define a new family of sialic acid-dependent adhesion molecules of the immunoglobulin superfamily. Curr Biol 4:965-972.

Key B, Treloar HB, Wangerek L, Ford MD, Nurcombe V (1996) Expression and localization of FGF-1 in the developing rat olfactory system. J Comp Neurol 366:197-206.

Kingsley DM (1994) The TGF-beta superfamily: new members, new receptors, and new genetic tests of function in different organisms. Genes Dev 8:133-146.

Klein R, Lamballe F, Bryant S, Barbacid M (1992) The trkB tyrosine protein kinase is a receptor for neurotrophin-4. Neuron 8:947-956.

Klein R, Jing SQ, Nanduri V, O'Rourke E, Barbacid M (1991a) The trk proto-oncogene encodes a receptor for nerve growth factor. Cell 65:189-197.

Klein R, Nanduri V, Jing SA, Lamballe F, Tapley P, Bryant S, Cordon-Cardo C, Jones KR, Reichardt LF, Barbacid M (1991b) The trkB tyrosine protein kinase is a receptor for brain-derived neurotrophic factor and neurotrophin-3. Cell 66:395-403.

Kotzbauer PT, Lampe PA, Heuckeroth RO, Golden JP, Creedon DJ, Johnson EM, Jr., Milbrandt J (1996) Neurturin, a relative of glial-cell-line-derived neurotrophic factor. Nature 384:467-470.

Kozma R, Sarner S, Ahmed S, Lim L (1997) Rho family GTPases and neuronal growth cone remodelling: relationship between increased complexity induced by Cdc42Hs, Rac1, and acetylcholine and collapse induced by RhoA and lysophosphatidic acid. Mol Cell Biol 17:1201-1211.

Kramer R, Bucay N, Kane DJ, Martin LE, Tarpley JE, Theill LE (1996) Neuregulins with an Ig-like domain are essential for mouse myocardial and neuronal development. Proc Natl Acad Sci U S A 93:4833-4838.

Kranenburg O, Poland M, van Horck FP, Drechsel D, Hall A, Moolenaar WH (1999) Activation of RhoA by lysophosphatidic acid and Galpha12/13 subunits in neuronal cells: induction of neurite retraction. Mol Biol Cell 10:1851-1857.

Kromer LF (1987) Nerve growth factor treatment after brain injury prevents neuronal death. Science 235:214-216.

Lagord C, Berry M, Logan A (2002) Expression of TGFbeta2 but not TGFbeta1 correlates with the deposition of scar tissue in the lesioned spinal cord. Mol Cell Neurosci 20:69-92.

Lakatos A, Franklin RJ, Barnett SC (2000) Olfactory ensheathing cells and Schwann cells differ in their in vitro interactions with astrocytes. Glia 32:214-225.

Lakatos A, Smith PM, Barnett SC, Franklin RJ (2003) Meningeal cells enhance limited CNS remyelination by transplanted olfactory ensheathing cells. Brain 126:598-609.

Lamballe F, Klein R, Barbacid M (1991) trkC, a new member of the trk family of tyrosine protein kinases, is a receptor for neurotrophin-3. Cell 66:967-979.

Latov N, Nilaver G, Zimmerman EA, Johnson WG, Silverman AJ, Defendini R, Cote L (1979) Fibrillary astrocytes proliferate in response to brain injury: a study combining immunoperoxidase technique for glial fibrillary acidic protein and radioautography of tritiated thymidine. Dev Biol 72:381-384.

Lee KF, Simon H, Chen H, Bates B, Hung MC, Hauser C (1995) Requirement for neuregulin receptor erbB2 in neural and cardiac development. Nature 378:394-398.

Lee MJ, Calle E, Brennan A, Ahmed S, Sviderskaya E, Jessen KR, Mirsky R (2001) In early development of the rat mRNA for the major myelin protein P(0) is expressed in nonsensory areas of the embryonic inner ear, notochord, enteric nervous system, and olfactory ensheathing cells. Dev Dyn 222:40-51.

Lehmann M, Fournier A, Selles-Navarro I, Dergham P, Sebok A, Leclerc N, Tigyi G, McKerracher L (1999) Inactivation of Rho signaling pathway promotes CNS axon regeneration. J Neurosci 19:7537-7547.

Levine JM (1994) Increased expression of the NG2 chondroitin-sulfate proteoglycan after brain injury. J Neurosci 14:4716-4730.

Li Q, Qi B, Oka K, Shimakage M, Yoshioka N, Inoue H, Hakura A, Kodama K, Stanbridge EJ, Yutsudo M (2001) Link of a new type of apoptosis-inducing gene ASY/Nogo-B to human cancer. Oncogene 20:3929-3936.

Li Y, Field PM, Raisman G (1997) Repair of adult rat corticospinal tract by transplants of olfactory ensheathing cells. Science 277:2000-2002.

Li Y, Field PM, Raisman G (1998) Regeneration of adult rat corticospinal axons induced by transplanted olfactory ensheathing cells. J Neurosci 18:10514-10524.

Li Y, Decherchi P, Raisman G (2003) Transplantation of olfactory ensheathing cells into spinal cord lesions restores breathing and climbing. J Neurosci 23:727-731.

Liesi P (1985) Laminin-immunoreactive glia distinguish regenerative adult CNS systems from non-regenerative ones. Embo J 4:2505-2511.

Lin LF, Zhang TJ, Collins F, Armes LG (1994) Purification and initial characterization of rat B49 glial cell line-derived neurotrophic factor. J Neurochem 63:758-768.

Lin LF, Doherty DH, Lile JD, Bektesh S, Collins F (1993) GDNF: a glial cell line-derived neurotrophic factor for midbrain dopaminergic neurons. Science 260:1130-1132.

Lipson AC, Widenfalk J, Lindqvist E, Ebendal T, Olson L (2003) Neurotrophic properties of olfactory ensheathing glia. Exp Neurol 180:167-171.

Liu BP, Fournier A, GrandPre T, Strittmatter SM (2002a) Myelin-associated glycoprotein as a functional ligand for the Nogo-66 receptor. Science 297:1190-1193.

Liu H, Ng CE, Tang BL (2002b) Nogo-A expression in mouse central nervous system neurons. Neurosci Lett 328:257-260.

Logan A, Frautschy SA, Gonzalez AM, Baird A (1992) A time course for the focal elevation of synthesis of basic fibroblast growth factor and one of its high-affinity receptors (flg) following a localized cortical brain injury. J Neurosci 12:3828-3837.

Lu J, Feron F, Mackay-Sim A, Waite PM (2002) Olfactory ensheathing cells promote locomotor recovery after delayed transplantation into transected spinal cord. Brain 125:14-21.

Marchionni MA, Goodearl AD, Chen MS, Bermingham-McDonogh O, Kirk C, Hendricks M, Danehy F, Misumi D, Sudhalter J, Kobayashi K, et al. (1993) Glial growth factors are alternatively spliced erbB2 ligands expressed in the nervous system. Nature 362:312-318.

Mathewson AJ, Berry M (1985) Observations on the astrocyte response to a cerebral stab wound in adult rats. Brain Res 327:61-69.

Matsuyama A, Iwata H, Okumura N, Yoshida S, Imaizumi K, Lee Y, Shiraishi S, Shiosaka S (1992) Localization of basic fibroblast growth factor-like immunoreactivity in the rat brain. Brain Res 587:49-65.

McCarthy KD, De Vellis J (1980) Preparation of separate astroglial and oligodendroglial cell cultures from rat cerebral tissue. J Cell Biol 85:890-902.

McKeon RJ, Hoke A, Silver J (1995) Injury-induced proteoglycans inhibit the potential for laminin-mediated axon growth on astrocytic scars. Exp Neurol 136:32-43.

McKeon RJ, Schreiber RC, Rudge JS, Silver J (1991) Reduction of neurite outgrowth in a model of glial scarring following CNS injury is correlated with the expression of inhibitory molecules on reactive astrocytes. J Neurosci 11:3398-3411.

McKerracher L, David S, Jackson DL, Kottis V, Dunn RJ, Braun PE (1994) Identification of myelin-associated glycoprotein as a major myelin-derived inhibitor of neurite growth. Neuron 13:805-811.

Merkler D, Metz GA, Raineteau O, Dietz V, Schwab ME, Fouad K (2001) Locomotor recovery in spinal cord-injured rats treated with an antibody neutralizing the myelin-associated neurite growth inhibitor Nogo-A. J Neurosci 21:3665-3673.

Meyer D, Birchmeier C (1995) Multiple essential functions of neuregulin in development. Nature 378:386-390.

Meyer D, Yamaai T, Garratt A, Riethmacher-Sonnenberg E, Kane D, Theill LE, Birchmeier C (1997) Isoform-specific expression and function of neuregulin. Development 124:3575-3586.

Meyer M, Johansen J, Gramsbergen JB, Johansen TE, Zimmer J (2000) Improved survival of embryonic porcine dopaminergic neurons in coculture with a conditionally immortalized GDNF-producing hippocampal cell line. Exp Neurol 164:82-93.

Milbrandt J, de Sauvage FJ, Fahrner TJ, Baloh RH, Leitner ML, Tansey MG, Lampe PA, Heuckeroth RO, Kotzbauer PT, Simburger KS, Golden JP, Davies JA, Vejsada R, Kato AC, Hynes M, Sherman D, Nishimura M, Wang LC, Vandlen R, Moffat B,

Klein RD, Poulsen K, Gray C, Garces A, Johnson EM, Jr., et al. (1998) Persephin, a novel neurotrophic factor related to GDNF and neurturin. Neuron 20:245-253.

Miragall F, Kadmon G, Schachner M (1989) Expression of L1 and N-CAM cell adhesion molecules during development of the mouse olfactory system. Dev Biol 135:272-286.

Miragall F, Kadmon G, Husmann M, Schachner M (1988) Expression of cell adhesion molecules in the olfactory system of the adult mouse: presence of the embryonic form of N-CAM. Dev Biol 129:516-531.

Mizuno K, Carnahan J, Nawa H (1994) Brain-derived neurotrophic factor promotes differentiation of striatal GABAergic neurons. Dev Biol 165:243-256.

Mocchetti I, Rabin SJ, Colangelo AM, Whittemore SR, Wrathall JR (1996) Increased basic fibroblast growth factor expression following contusive spinal cord injury. Exp Neurol 141:154-164.

Moon LD, Asher RA, Rhodes KE, Fawcett JW (2002) Relationship between sprouting axons, proteoglycans and glial cells following unilateral nigrostriatal axotomy in the adult rat. Neuroscience 109:101-117.

Mukhopadhyay G, Doherty P, Walsh FS, Crocker PR, Filbin MT (1994) A novel role for myelin-associated glycoprotein as an inhibitor of axonal regeneration. Neuron 13:757-767.

Murakami M, Hibi M, Nakagawa N, Nakagawa T, Yasukawa K, Yamanishi K, Taga T, Kishimoto T (1993) IL-6-induced homodimerization of gp130 and associated activation of a tyrosine kinase. Science 260:1808-1810.

Murphy M, Dutton R, Koblar S, Cheema S, Bartlett P (1997) Cytokines which signal through the LIF receptor and their actions in the nervous system. Prog Neurobiol 52:355-378.

Muthuswamy SK, Gilman M, Brugge JS (1999) Controlled dimerization of ErbB receptors provides evidence for differential signaling by homo- and heterodimers. Mol Cell Biol 19:6845-6857.

Nan B, Getchell ML, Partin JV, Getchell TV (2001) Leukemia inhibitory factor, interleukin-6, and their receptors are expressed transiently in the olfactory mucosa after target ablation. J Comp Neurol 435:60-77.

Nash HH, Borke RC, Anders JJ (2002a) Ensheathing cells and methylprednisolone promote axonal regeneration and functional recovery in the lesioned adult rat spinal cord. J Neurosci 22:7111-7120.

Nash HH, Anders JJ, Borke RC (2002b) Ensheathing cells and methylprednisolone promote axonal regeneration and functional recovery in the lesioned adult rat spinal cord. J Neurosci 22(16) , p. 7111-20.

Navarro X, Valero A, Gudino G, Fores J, Rodriguez FJ, Verdu E, Pascual R, Cuadras J, Nieto-Sampedro M (1999) Ensheathing glia transplants promote dorsal root regeneration and spinal reflex restitution after multiple lumbar rhizotomy. Ann Neurol 45:207-215.

Niederost B, Oertle T, Fritsche J, McKinney RA, Bandtlow CE (2002) Nogo-A and myelin-associated glycoprotein mediate neurite growth inhibition by antagonistic regulation of RhoA and Rac1. J Neurosci 22:10368-10376.

Norgren RB, Jr., Ratner N, Brackenbury R (1992) Development of olfactory nerve glia defined by a monoclonal antibody specific for Schwann cells. Dev Dyn 194:231-238.

Oertle T, Huber C, van der Putten H, Schwab ME (2003a) Genomic structure and functional characterisation of the promoters of human and mouse nogo/rtn4. J Mol Biol 325:299-323.

Oertle T, Van Der Haar ME, Bandtlow CE, Robeva A, Burfeind P, Buss A, Huber AB, Simonen M, Schnell L, Brosamle C, Kaupmann K, Vallon R, Schwab ME (2003b) Nogo-A Inhibits Neurite Outgrowth and Cell Spreading with Three Discrete Regions. J Neurosci 23:5393-5406.

Ohbayashi N, Hoshikawa M, Kimura S, Yamasaki M, Fukui S, Itoh N (1998) Structure and expression of the mRNA encoding a novel fibroblast growth factor, FGF-18. J Biol Chem 273:18161-18164.

Olayioye MA, Beuvink I, Horsch K, Daly JM, Hynes NE (1999) ErbB receptor-induced activation of stat transcription factors is mediated by Src tyrosine kinases. J Biol Chem 274:17209-17218.

Olofsson B (1999) Rho guanine dissociation inhibitors: pivotal molecules in cellular signalling. Cell Signal 11:545-554.

Ornitz DM, Xu J, Colvin JS, McEwen DG, MacArthur CA, Coulier F, Gao G, Goldfarb M (1996) Receptor specificity of the fibroblast growth factor family. J Biol Chem 271:15292-15297.

Orr-Urtreger A, Trakhtenbrot L, Ben-Levy R, Wen D, Rechavi G, Lonai P, Yarden Y (1993) Neural expression and chromosomal mapping of Neu differentiation factor to 8p12-p21. Proc Natl Acad Sci U S A 90:1867-1871.

Oudega M, Rosano C, Sadi D, Wood PM, Schwab ME, Hagg T (2000) Neutralizing antibodies against neurite growth inhibitor NI-35/250 do not promote regeneration of sensory axons in the adult rat spinal cord. Neuroscience 100:873-883.

Papadopoulos CM, Tsai SY, Alsbiei T, O'Brien TE, Schwab ME, Kartje GL (2002) Functional recovery and neuroanatomical plasticity following middle cerebral artery occlusion and IN-1 antibody treatment in the adult rat. Ann Neurol 51:433-441.

Patterson PH (1992) The emerging neuropoietic cytokine family: first CDF/LIF, CNTF and IL-6; next ONC, MGF, GCSF? Curr Opin Neurobiol 2:94-97.

Perez-Navarro E, Alberch J, Neveu I, Arenas E (1999) Brain-derived neurotrophic factor, neurotrophin-3 and neurotrophin-4/5 differentially regulate the phenotype and prevent degenerative changes in striatal projection neurons after excitotoxicity in vivo. Neuroscience 91:1257-1264.

Perroteau I, Oberto M, Ieraci A, Bovolin P, Fasolo A (1998) ErbB-3 and ErbB-4 expression in the mouse olfactory system. Ann N Y Acad Sci 855:255-259.

Pignot V, Hein AE, Barske C, Wiessner C, Walmsley AR, Kaupmann K, Mayeur H, Sommer B, Mir AK, Frentzel S (2003) Characterization of two novel proteins, NgRH1 and NgRH2, structurally and biochemically homologous to the Nogo-66 receptor. J Neurochem 85:717-728.

Pinkas-Kramarski R, Eilam R, Spiegler O, Lavi S, Liu N, Chang D, Wen D, Schwartz M, Yarden Y (1994) Brain neurons and glial cells express Neu differentiation factor/heregulin: a survival factor for astrocytes. Proc Natl Acad Sci U S A 91:9387-9391.

Pinkas-Kramarski R, Soussan L, Waterman H, Levkowitz G, Alroy I, Klapper L, Lavi S, Seger R, Ratzkin BJ, Sela M, Yarden Y (1996) Diversification of Neu differentiation factor and epidermal growth factor signaling by combinatorial receptor interactions. Embo J 15:2452-2467.

Pixley SK (1992) The olfactory nerve contains two populations of glia, identified both in vivo and in vitro. Glia 5:269-284.

Pollock GS, Franceschini IA, Graham G, Marchionni MA, Barnett SC (1999) Neuregulin is a mitogen and survival factor for olfactory bulb ensheathing cells and an isoform is produced by astrocytes. Eur J Neurosci 11:769-780.

Prinjha R, Moore SE, Vinson M, Blake S, Morrow R, Christie G, Michalovich D, Simmons DL, Walsh FS (2000) Inhibitor of neurite outgrowth in humans. Nature 403:383-384.

Raabe TD, Francis A, DeVries GH (1998) Neuregulins in glial cells. Neurochem Res 23:311-318.

Raabe TD, Clive DR, Neuberger TJ, Wen D, DeVries GH (1996) Cultured neonatal Schwann cells contain and secrete neuregulins. J Neurosci Res 46:263-270.

Raabe TDC, D.R. Wen, D. DeVries, G.H. (1997) Neonatal oligodendrocytes contain and secrete neuregulins in vitro. J Neurochem 69:1859-1863.

Raineteau O, Schwab ME (2001) Plasticity of motor systems after incomplete spinal cord injury. Nat Rev Neurosci 2:263-273.

Raineteau O, Z'Graggen WJ, Thallmair M, Schwab ME (1999) Sprouting and regeneration after pyramidotomy and blockade of the myelin-associated neurite growth inhibitors NI 35/250 in adult rats. Eur J Neurosci 11:1486-1490.

Raineteau O, Fouad K, Bareyre FM, Schwab ME (2002) Reorganization of descending motor tracts in the rat spinal cord. Eur J Neurosci 16:1761-1771.

Raineteau O, Fouad K, Noth P, Thallmair M, Schwab ME (2001) Functional switch between motor tracts in the presence of the mAb IN-1 in the adult rat. Proc Natl Acad Sci U S A 98:6929-6934.

Ramon-Cueto A, Nieto-Sampedro M (1992) Glial cells from adult rat olfactory bulb: immunocytochemical properties of pure cultures of ensheathing cells. Neuroscience 47:213-220.

Ramon-Cueto A, Nieto-Sampedro M (1994) Regeneration into the spinal cord of transected dorsal root axons is promoted by ensheathing glia transplants. Exp Neurol 127:232-244.

Ramon-Cueto A, Avila J (1998) Olfactory ensheathing glia: properties and function. Brain Res Bull 46:175-187.

Ramon-Cueto A, Plant GW, Avila J, Bunge MB (1998) Long-distance axonal regeneration in the transected adult rat spinal cord is promoted by olfactory ensheathing glia transplants. J Neurosci 18:3803-3815.

Ramon-Cueto A, Cordero MI, Santos-Benito FF, Avila J (2000) Functional recovery of paraplegic rats and motor axon regeneration in their spinal cords by olfactory ensheathing glia. Neuron 25:425-435.

Reier PJ, Houle JD (1988) The glial scar: its bearing on axonal elongation and transplantation approaches to CNS repair. Adv Neurol 47:87-138.

Reilly JF, Maher PA, Kumari VG (1998) Regulation of astrocyte GFAP expression by TGF-beta1 and FGF-2. Glia 22:202-210.

Richardson PM, McGuinness UM, Aguayo AJ (1980) Axons from CNS neurons regenerate into PNS grafts. Nature 284:264-265.

Riese DJ, 2nd, van Raaij TM, Plowman GD, Andrews GC, Stern DF (1995) The cellular response to neuregulins is governed by complex interactions of the erbB receptor family. Mol Cell Biol 15:5770-5776.

Rio C, Rieff HI, Qi P, Khurana TS, Corfas G (1997) Neuregulin and erbB receptors play a critical role in neuronal migration. Neuron 19:39-50.

Rodriguez-Tebar A, Dechant G, Barde YA (1990) Binding of brain-derived neurotrophic factor to the nerve growth factor receptor. Neuron 4:487-492.

Rosenbaum C, Karyala S, Marchionni MA, Kim HA, Krasnoselsky AL, Happel B, Isaacs I, Brackenbury R, Ratner N (1997) Schwann cells express NDF and SMDF/n-ARIA mRNAs, secrete neuregulin, and show constitutive activation of erbB3 receptors: evidence for a neuregulin autocrine loop. Exp Neurol 148:604-615.

Rubin BP, Dusart I, Schwab ME (1994) A monoclonal antibody (IN-1) which neutralizes neurite growth inhibitory proteins in the rat CNS recognizes antigens localized in CNS myelin. J Neurocytol 23:209-217.

Ruitenberg MJ, Plant GW, Christensen CL, Blits B, Niclou SP, Harvey AR, Boer GJ, Verhaagen J (2002) Viral vector-mediated gene expression in olfactory ensheathing glia implants in the lesioned rat spinal cord. Gene Ther 9:135-146.

Ruitenberg MJ, Plant GW, Hamers FP, Wortel J, Blits B, Dijkhuizen PA, Gispen WH, Boer GJ, Verhaagen J (2003) Ex vivo adenoviral vector-mediated neurotrophin gene transfer to olfactory ensheathing glia: effects on rubrospinal tract regeneration, lesion size, and functional recovery after implantation in the injured rat spinal cord. J Neurosci 23:7045-7058.

Safavi-Abbasi S, Wolff JR, Missler M (2001) Rapid morphological changes in astrocytes are accompanied by redistribution but not by quantitative changes of cytoskeletal proteins. Glia 36:102-115.

Salehi-Ashtiani K, Farbman AI (1996) Expression of neu and Neu differentiation factor in the olfactory mucosa of rat. Int J Dev Neurosci 14:801-811.

Santos-Silva A, Cavalcante LA (2001) Expression of the non-compact myelin protein 2',3'-cyclic nucleotide 3'- phosphodiesterase (CNPase) in olfactory bulb ensheathing glia from explant cultures. Neurosci Res 40:189-193.

Schnell L, Schwab ME (1990) Axonal regeneration in the rat spinal cord produced by an antibody against myelin-associated neurite growth inhibitors. Nature 343:269-272.

Schulz MK, Schnell L, Castro AJ, Schwab ME, Kartje GL (1998) Cholinergic innervation of fetal neocortical transplants is increased after neutralization of myelin-associated neurite growth inhibitors. Exp Neurol 149:390-397.

Schuster N, Bender H, Philippi A, Subramaniam S, Strelau J, Wang Z, Krieglstein K (2002) TGF-beta induces cell death in the oligodendroglial cell line OLI-neu. Glia 40:95-108.

Schwab ME, Caroni P (1988) Oligodendrocytes and CNS myelin are nonpermissive substrates for neurite growth and fibroblast spreading in vitro. J Neurosci 8:2381-2393.

Schwarting GA, Kostek C, Ahmad N, Dibble C, Pays L, Puschel AW (2000) Semaphorin 3A is required for guidance of olfactory axons in mice. J Neurosci 20:7691-7697.

Smale KA, Doucette R, Kawaja MD (1996) Implantation of olfactory ensheathing cells in the adult rat brain following fimbria-fornix transection. Exp Neurol 137:225-233.

Smith PM, Sim FJ, Barnett SC, Franklin RJ (2001) SCIP/Oct-6, Krox-20, and desert hedgehog mRNA expression during CNS remyelination by transplanted olfactory ensheathing cells. Glia 36:342-353.

Sonigra RJ, Brighton PC, Jacoby J, Hall S, Wigley CB (1999) Adult rat olfactory nerve ensheathing cells are effective promoters of adult central nervous system neurite outgrowth in coculture. Glia 25:256-269.

Spillmann AA, Bandtlow CE, Lottspeich F, Keller F, Schwab ME (1998) Identification and characterization of a bovine neurite growth inhibitor (bNI-220). J Biol Chem 273:19283-19293.

St John JA, Key B (1999) Expression of galectin-1 in the olfactory nerve pathway of rat. Brain Res Dev Brain Res 117:171-178.

Stichel CC, Muller HW (1998) Experimental strategies to promote axonal regeneration after traumatic central nervous system injury. Prog Neurobiol 56:119-148.

Suidan HS, Nobes CD, Hall A, Monard D (1997) Astrocyte spreading in response to thrombin and lysophosphatidic acid is dependent on the Rho GTPase. Glia 21:244-252.

Sweeney C, Lai C, Riese DJ, 2nd, Diamonti AJ, Cantley LC, Carraway KL, 3rd (2000) Ligand discrimination in signaling through an ErbB4 receptor homodimer. J Biol Chem 275:19803-19807.

Tagashira S, Ozaki K, Ohta M, Itoh N (1995) Localization of fibroblast growth factor-9 mRNA in the rat brain. Brain Res Mol Brain Res 30:233-241.

Taketomi M, Kinoshita N, Kimura K, Kitada M, Noda T, Asou H, Nakamura T, Ide C (2002) Nogo-A expression in mature oligodendrocytes of rat spinal cord in association with specific molecules. Neurosci Lett 332:37-40.

Tang S, Shen YJ, DeBellard ME, Mukhopadhyay G, Salzer JL, Crocker PR, Filbin MT (1997) Myelin-associated glycoprotein interacts with neurons via a sialic acid binding site at ARG118 and a distinct neurite inhibition site. J Cell Biol 138:1355-1366.

Tennent R, Chuah MI (1996) Ultrastructural study of ensheathing cells in early development of olfactory axons. Brain Res Dev Brain Res 95:135-139.

Thallmair M, Metz GA, Z'Graggen WJ, Raineteau O, Kartje GL, Schwab ME (1998) Neurite growth inhibitors restrict plasticity and functional recovery following corticospinal tract lesions. Nat Neurosci 1:124-131.

Thompson RJ, Roberts B, Alexander CL, Williams SK, Barnett SC (2000) Comparison of neuregulin-1 expression in olfactory ensheathing cells, Schwann cells and astrocytes. J Neurosci Res 61:172-185.

Tisay KT, Key B (1999) The extracellular matrix modulates olfactory neurite outgrowth on ensheathing cells. J Neurosci 19:9890-9899.

Tozaki H, Kawasaki T, Takagi Y, Hirata T (2002) Expression of Nogo protein by growing axons in the developing nervous system. Brain Res Mol Brain Res 104:111-119.

Treloar HB, Nurcombe V, Key B (1996) Expression of extracellular matrix molecules in the embryonic rat olfactory pathway. J Neurobiol 31:41-55.

Trupp M, Arenas E, Fainzilber M, Nilsson AS, Sieber BA, Grigoriou M, Kilkenny C, Salazar-Grueso E, Pachnis V, Arumae U (1996) Functional receptor for GDNF encoded by the c-ret proto-oncogene. Nature 381:785-789.

Van Den Pol ANS, J.G. (2003) Olfactory ensheathing cells: time lapse imaging of cellular interactions, axonal support, rapid morphological shifts, and mitosis. J Comp Neurol 458:175-194.

Vartanian T, Fischbach G, Miller R (1999) Failure of spinal cord oligodendrocyte development in mice lacking neuregulin. Proc Natl Acad Sci U S A 96:731-735.

Vartanian T, Goodearl A, Viehover A, Fischbach G (1997) Axonal neuregulin signals cells of the oligodendrocyte lineage through activation of HER4 and Schwann cells through HER2 and HER3. J Cell Biol 137:211-220.

Vartanian T, Corfas G, Li Y, Fischbach GD, Stefansson K (1994) A role for the acetylcholine receptor-inducing protein ARIA in oligodendrocyte development. Proc Natl Acad Sci U S A 91:11626-11630.

Ventimiglia R, Mather PE, Jones BE, Lindsay RM (1995) The neurotrophins BDNF, NT-3 and NT-4/5 promote survival and morphological and biochemical differentiation of striatal neurons in vitro. Eur J Neurosci 7:213-222.

Verdu E, Garcia-Alias G, Fores J, Lopez-Vales R, Navarro X (2003) Olfactory ensheathing cells transplanted in lesioned spinal cord prevent loss of spinal cord parenchyma and promote functional recovery. Glia 42:275-286.

Verdu E, Navarro X, Gudino-Cabrera G, Rodriguez FJ, Ceballos D, Valero A, Nieto-Sampedro M (1999) Olfactory bulb ensheathing cells enhance peripheral nerve regeneration. Neuroreport 10:1097-1101.

Verdu E, Garcia-Alias G, Fores J, Gudino-Cabrera G, Muneton VC, Nieto-Sampedro M, Navarro X (2001) Effects of ensheathing cells transplanted into photochemically damaged spinal cord. Neuroreport 12:2303-2309.

Vijayan VK, Lee YL, Eng LF (1990) Increase in glial fibrillary acidic protein following neural trauma. Mol Chem Neuropathol 13:107-118.

Vincent AJ, West AK, Chuah MI (2003) Morphological plasticity of olfactory ensheathing cells is regulated by cAMP and endothelin-1. Glia 41:393-403.

Vinson M, van der Merwe PA, Kelm S, May A, Jones EY, Crocker PR (1996) Characterization of the sialic acid-binding site in sialoadhesin by site-directed mutagenesis. J Biol Chem 271:9267-9272.

Vinson M, Strijbos PJ, Rowles A, Facci L, Moore SE, Simmons DL, Walsh FS (2001) Myelin-associated glycoprotein interacts with ganglioside GT1b. A mechanism for neurite outgrowth inhibition. J Biol Chem 276:20280-20285.

Vinson M, Rausch O, Maycox PR, Prinjha RK, Chapman D, Morrow R, Harper AJ, Dingwall C, Walsh FS, Burbidge SA, Riddell DR (2003) Lipid rafts mediate the interaction between myelin-associated glycoprotein (MAG) on myelin and MAG-receptors on neurons. Mol Cell Neurosci 22:344-352.

von Meyenburg J, Brosamle C, Metz GA, Schwab ME (1998) Regeneration and sprouting of chronically injured corticospinal tract fibers in adult rats promoted by NT-3 and the mAb IN-1, which neutralizes myelin-associated neurite growth inhibitors. Exp Neurol 154:583-594.

Vyas AA, Patel HV, Fromholt SE, Heffer-Lauc M, Vyas KA, Dang J, Schachner M, Schnaar RL (2002) Gangliosides are functional nerve cell ligands for myelin-associated glycoprotein (MAG), an inhibitor of nerve regeneration. Proc Natl Acad Sci U S A 99:8412-8417.

Wang KC, Kim JA, Sivasankaran R, Segal R, He Z (2002a) P75 interacts with the Nogo receptor as a co-receptor for Nogo, MAG and OMgp. Nature 420:74-78.

Wang KC, Koprivica V, Kim JA, Sivasankaran R, Guo Y, Neve RL, He Z (2002b) Oligodendrocyte-myelin glycoprotein is a Nogo receptor ligand that inhibits neurite outgrowth. Nature 417:941-944.

Watabe K, Fukuda T, Tanaka J, Toyohara K, Sakai O (1994) Mitogenic effects of platelet-derived growth factor, fibroblast growth factor, transforming growth factor-beta, and heparin-binding serum factor for adult mouse Schwann cells. J Neurosci Res 39:525-534.

Weinmaster G, Lemke G (1990) Cell-specific cyclic AMP-mediated induction of the PDGF receptor. Embo J 9:915-920.

Wen D, Peles E, Cupples R, Suggs SV, Bacus SS, Luo Y, Trail G, Hu S, Silbiger SM, Levy RB, et al. (1992) Neu differentiation factor: a transmembrane glycoprotein containing an EGF domain and an immunoglobulin homology unit. Cell 69:559-572.

Wen D, Suggs SV, Karunagaran D, Liu N, Cupples RL, Luo Y, Janssen AM, Ben-Baruch N, Trollinger DB, Jacobsen VL, et al. (1994) Structural and functional aspects of the multiplicity of Neu differentiation factors. Mol Cell Biol 14:1909-1919.

Wenk CA, Thallmair M, Kartje GL, Schwab ME (1999) Increased corticofugal plasticity after unilateral cortical lesions combined with neutralization of the IN-1 antigen in adult rats. J Comp Neurol 410:143-157.

Wewetzer K, Grothe C, Claus P (2001) In vitro expression and regulation of ciliary neurotrophic factor and its alpha receptor subunit in neonatal rat olfactory ensheathing cells. Neurosci Lett 306:165-168.

Widenfalk J, Tomac A, Lindqvist E, Hoffer B, Olson L (1998) GFRalpha-3, a protein related to GFRalpha-1, is expressed in developing peripheral neurons and ensheathing cells. Eur J Neurosci 10:1508-1517.

Williams LR, Varon S, Peterson GM, Wictorin K, Fischer W, Bjorklund A, Gage FH (1986) Continuous infusion of nerve growth factor prevents basal forebrain neuronal death after fimbria fornix transection. Proc Natl Acad Sci U S A 83:9231-9235.

Williams SK, Franklin RJ, Barnett SC (2004) Response of olfactory ensheathing cells to the degeneration and regeneration of the peripheral olfactory system and the involvement of the neuregulins. J Comp Neurol 470:50-62.

Wolpowitz D, Mason TB, Dietrich P, Mendelsohn M, Talmage DA, Role LW (2000) Cysteine-rich domain isoforms of the neuregulin-1 gene are required for maintenance of peripheral synapses. Neuron 25:79-91.

Wong ST, Henley JR, Kanning KC, Huang KH, Bothwell M, Poo MM (2002) A p75(NTR) and Nogo receptor complex mediates repulsive signaling by myelin-associated glycoprotein. Nat Neurosci 5:1302-1308.

Woodhall E, West AK, Chuah MI (2001) Cultured olfactory ensheathing cells express nerve growth factor, brain- derived neurotrophic factor, glia cell line-derived neurotrophic factor and their receptors. Brain Res Mol Brain Res 88:203-213.

Xu XM, Chen A, Guenard V, Kleitman N, Bunge MB (1997) Bridging Schwann cell transplants promote axonal regeneration from both the rostral and caudal stumps of transected adult rat spinal cord. J Neurocytol 26:1-16.

Yamada H, Fredette B, Shitara K, Hagihara K, Miura R, Ranscht B, Stallcup WB, Yamaguchi Y (1997) The brain chondroitin sulfate proteoglycan brevican associates with astrocytes ensheathing cerebellar glomeruli and inhibits neurite outgrowth from granule neurons. J Neurosci 17:7784-7795.

Yamasaki K, Taga T, Hirata Y, Yawata H, Kawanishi Y, Seed B, Taniguchi T, Hirano T, Kishimoto T (1988) Cloning and expression of the human interleukin-6 (BSF-2/IFN beta 2) receptor. Science 241:825-828.

Yamasaki M, Yamada K, Furuya S, Mitoma J, Hirabayashi Y, Watanabe M (2001) 3-Phosphoglycerate dehydrogenase, a key enzyme for l-serine biosynthesis, is preferentially expressed in the radial glia/astrocyte lineage and olfactory ensheathing glia in the mouse brain. J Neurosci 21:7691-7704.

Yamashita T, Tohyama M (2003) The p75 receptor acts as a displacement factor that releases Rho from Rho-GDI. Nat Neurosci 6:461-467.

Yamashita T, Higuchi H, Tohyama M (2002) The p75 receptor transduces the signal from myelin-associated glycoprotein to Rho. J Cell Biol 157:565-570.

Yan H, Nie X, Kocsis JD (2001a) Hepatocyte growth factor is a mitogen for olfactory ensheathing cells. J Neurosci Res 66:698-704.

Yan H, Lu D, Rivkees SA (2003) Lysophosphatidic acid regulates the proliferation and migration of olfactory ensheathing cells in vitro. Glia 44:26-36.

Yan H, Bunge MB, Wood PM, Plant GW (2001b) Mitogenic response of adult rat olfactory ensheathing glia to four growth factors. Glia 33:334-342.

Yan P, Li Q, Kim GM, Xu J, Hsu CY, Xu XM (2001c) Cellular localization of tumor necrosis factor-alpha following acute spinal cord injury in adult rats. J Neurotrauma 18:563-568.

Yayon A, Klagsbrun M, Esko JD, Leder P, Ornitz DM (1991) Cell surface, heparin-like molecules are required for binding of basic fibroblast growth factor to its high affinity receptor. Cell 64:841-848.

Yazaki N, Hosoi Y, Kawabata K, Miyake A, Minami M, Satoh M, Ohta M, Kawasaki T, Itoh N (1994) Differential expression patterns of mRNAs for members of the fibroblast growth factor receptor family, FGFR-1-FGFR-4, in rat brain. J Neurosci Res 37:445-452.

Yong VW, Moumdjian R, Yong FP, Ruijs TC, Freedman MS, Cashman N, Antel JP (1991) Gamma-interferon promotes proliferation of adult human astrocytes in

vitro and reactive gliosis in the adult mouse brain in vivo. Proc Natl Acad Sci U S A 88:7016-7020.

Z'Graggen WJ, Metz GA, Kartje GL, Thallmair M, Schwab ME (1998) Functional recovery and enhanced corticofugal plasticity after unilateral pyramidal tract lesion and blockade of myelin-associated neurite growth inhibitors in adult rats. J Neurosci 18:4744-4757.

Zhang D, Sliwkowski MX, Mark M, Frantz G, Akita R, Sun Y, Hillan K, Crowley C, Brush J, Godowski PJ (1997) Neuregulin-3 (NRG3): a novel neural tissue-enriched protein that binds and activates ErbB4. Proc Natl Acad Sci U S A 94:9562-9567.